MINERAL NUTRIENTS IN *LOW PHYTIC ACID*1-1 CORN GRAINS

THE CONCENTRATIONS AND DISTRIBUTION OF MINERAL NUTRIENTS AND PHYTIC ACID-PHOSPHORUS IN WILD-TYPE AND *LOW PHYTIC ACID* 1-1 (*LPA*1-1) CORN (*ZEA MAYS L.*) GRAINS AND GRAIN PARTS

By

LAN LIN, B.Sc.

A Thesis

Submitted to the School of Graduate Studies

in Partial Fulfilment of the Requirements

for the Degree

Master of Science

McMaster University

MASTER OF SCIENCE (2004) McMaster University
(Biology) Hamilton, Ontario

TITLE: The concentrations and distribution of mineral nutrients and phytic acid -phosphorus in wild-type and *low phytic acid* 1-1 (*lpa*1-1) corn (*Zea mays* L.) grains and grain parts

AUTHOR: Lan Lin, B. Sc. (Wuhan University, P. R. China)

SUPERVISOR: Professor John N. A. Lott

NUMBER OF PAGES: x, 128

ABSTRACT

Mature grains of wild-type (WT) and *low phytic acid*1-1 (*lpa*1-1) mutant from corn (*Zea mays* L.) were studied for total phosphorus (total P), phytic acid-phosphorus (PA-P), and mineral cations. Whole grain PA-P in *lpa*1-1 was reduced 61.6% compared to WT whereas whole grain total P remained constant. Scutellum and root-shoot axis PA-P was 91.6% and 3.6% of WT whole-grain amounts respectively, compared to 89.3% and 4.0% in *lpa*1-1. Relative partitioning of PA-P between the scutellum and root-shoot axis was not altered in *lpa*1-1 mutant embryos as compared to WT. In *lpa*1-1 the total P was slightly decreased in the scutella and increased in both root-shoot axes and rest-of-grain fractions. Whole grain Mg, Fe, and Mn amounts were higher in *lpa*1-1 grains than in WT grains; K and Zn were similar, and Ca was lower. The *lpa*1-1 whole grains and embryos contained 1/3 higher Fe than WT. For both grain types all measured metallic elements, except Ca, were more concentrated in embryos than the rest-of-grain fractions.

Studies showed that WT grains contained larger globoids than *lpa*1-1 grains in both scutellum and aleurone layer cells. This globoid size reduction reflected the PA-P decrease. Most *lpa*1-1 aleurone globoids were non-spherical and *lpa*1-1 scutellum globoids were clusters of spheres while both scutellum and aleurone globoids of WT were discrete spheres. The *lpa*1-1 mutation had an impact on the globoid formation. X-ray analyses of scutellum and aleurone layer globoids from both grain types revealed major amounts of P, K, and Mg and traces of Ca, Fe, and Zn. Analysis demonstrated lower P, K and Mg and higher Ca, Fe and Zn in aleurone globoids than scutellum

globoids. Both grain types contained almost no mineral nutrient stores in the starchy endosperm, whereas the scutellum was the major site of PA-P and mineral nutrient deposition.

ACKNOWLEDGEMENTS

I wish to thank my supervisor, Dr. J. N. A. Lott, for providing me with an opportunity to pursue M. Sc. in his lab, and for his excellent academic instruction, illuminative discussion and continual encouragement throughout my studies. I would like to express my appreciation to Dr. I. Ockenden for her kind help in both the academic area and daily life, and for her patience to answer my countless questions. I would like to thank Dr. E. Weretilnyk for her invaluable and helpful advice in my supervisory committee. My thanks also go to Mrs. M. Reid and Mr. K. Schultes for their technical assistance in the field of electron microscopic studies.

Special thanks to my husband, who always understood and encouraged me under the stressful condition and has gone through many difficulties with me. I am indebted to my parents for their support whatever I chose and for their help when I was in need.

TABLE OF CONTENTS

LIST OF FIGURES

LIST OF TABLES

Chapter 1
Introduction

Corn as a cereal crop

Corn (*Zea mays* L.) is a popular cereal crop in the Americas, Asia, Africa and elsewhere in the world. In the pre-Columbian New World, it was the principal food crop cultivated by the native Americans. The earliest evidence of the domestication of corn came from the archaeological sites in south-central Mexico. Corn, with squash, chili pepper and avocado were found in the same sites dated at about 6000 BC (Eubanks, 2001; Heiser, 1973). After Columbus and his crew visited the New World around 1500 AD, they brought the grains of corn, which the inhabitants of the America called maize, back to Spain (National Research Council, 1988). In a short period of time usage of corn spread throughout Europe, Asia and Africa.

Corn is an important source of human food and animal feed (O'Dell *et al.*, 1972). Today, corn is one of several plants that supply much of the world's food. In tonnage produced it ranks as the second major cereal in the world, after wheat. According to data from 1996 to 1998 presented by the FAO (Food and Agriculture Organization) of the United Nations, the average annual global production of wheat, corn and rice was 594,637,000, 592,221,000 and 570,875,000 metric tonnes respectively (FAO yearbook on production 1998, 1999). Corn is adaptable to a variety of environmental conditions, being grown from latitude 40°S in Argentina to latitude 58°N in Canada and the Soviet Union (National Research Council, 1988). In many areas of the developing world, corn is a vital

staple, particularly for the rural poor. It is prepared and consumed in various ways, mainly being ground and pounded and then cooked (National Research Council, 1988). Corn is also the world's chief animal feed grain. Industrialized countries, such as the United States, use corn mainly as a feed grain and they depend on it to produce meat, milk and eggs (National Research Council, 1988). A significant part of this consumption is by non-ruminant animals, such as poultry, swine and fish (Raboy *et al.*, 1997). Besides serving as a human staple food and livestock feed, corn is also an important raw ingredient for hundreds of processed foods and industrial materials, i.e. starch, glucose, alcohol, sweetener, cooking oil, margarine, salad dressing and shortening (ADM Foods).

Anatomical structure of the corn grain

Corn is one of the cereals, which are the major cultivated members of the grass family (*Gramineae*). Members of this family produce dry, single-seeded fruits, which are commonly called kernels or grains (Hoseney, 1986). In this case, the dispersal unit is a fruit, not a seed (Bewley and Black, 1985). There are several types of tissue within the corn grain. The structure of a corn grain is shown in Figure 1 (adapted from Duffus and Slaughter, 1980). The outermost shell of the grain is the pericarp (fruit coat), which is fused with a seed coat. The seed consists of a seed coat for protection, an endosperm for nutrient storage, and an embryo which gives rise to a new plant. Most of the endosperm is starchy endosperm, which, in the mature dry grain, consists of large dead cells. The outer layer of the endosperm, called the aleurone layer, consists of living cells at maturity. The aleurone layer in the mature corn grain is a single layer of rectangular, thick-walled cells

which surround the starchy endosperm, while other cereals such as rice, barley and oats, have aleurone layers that are several cells thick (Rooney *et al.*, 1983). However, the aleurone layer thickness in maize can be genetically modified. Recent studies reported that transgenic maize grains could contain up to seven layers of aleurone layer cells (Shen *et al.*, 2003). The embryo consists of scutellum and root-shoot axis. Within the cereals, the corn grain has a relatively large embryo, forming 10-14% of the grain on a dry weight basis (Hoseney, 1986).

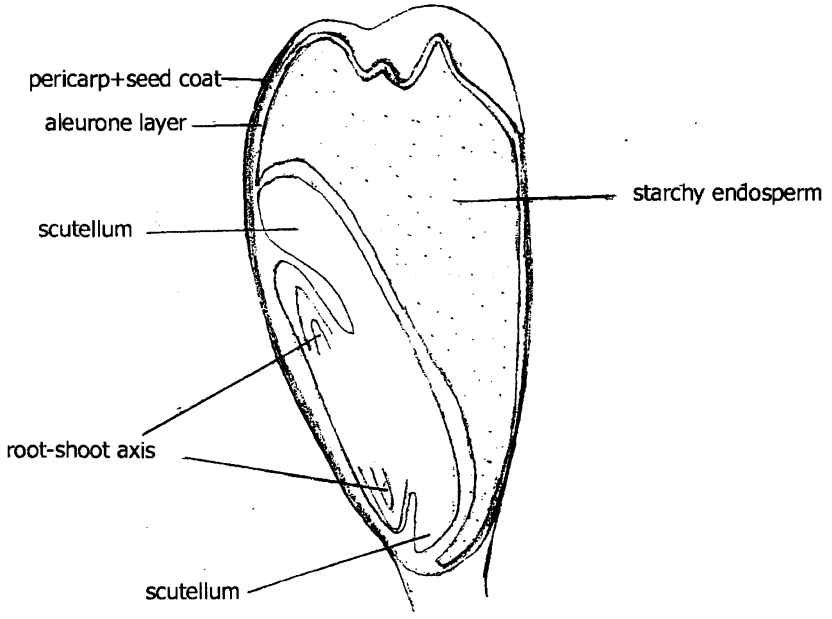

Scale: ~ 8 times enlargement

Figure 1. The structure of corn grain (Adapted from Duffus and Slaughter, 1980)

Protein bodies in plant seeds

Protein bodies, also called protein storage vacuoles or aleurone grains, are considered to be the main subcellular location of protein and phytate storage in plant seeds. They are single membrane-bounded, approximately round in shape, with sizes varying from 0.1 to 22 μm in diameter (Lott, 1980). Protein bodies are the specialized form of the plant cell's vacuoles. During seed germination and seedling development, storage protein and phytate are degraded and mobilized to support growing seedlings (Lott, 1984). As the contents of protein bodies are consumed, the protein bodies become aqueous vacuoles and fuse to form the large central vacuole of the cell (Lott, 1980).

Phytate, phytic acid and globoids

Phytate is a mixed cation salt of *myo*-inositol hexaphosphoric acid, which is commonly called phytic acid (Lott *et al.*, 2000; IUPAC and IUPAC-IUB, 1968). Phytic acid, whose molecular structure is shown below, is found widely in eukaryotic cells (Graf, 1986). As shown in Figure 2, phytic acid is a six carbon ring with a phosphate group attached to each carbon via a hydroxyl group. It thus has 12 possible negatively charged sites. In seeds these sites bind mainly K^+ and Mg^{++}, but also other cations, such as Ca^{++}, Mn^{++}, Zn^{++}, Ba^{++} or Fe^{+++}, to form salts named phytate (Lott *et al.*, 2000). Thus phytate in seed tissues mainly contains the plant mineral nutrients P, K, Mg with trace amounts of Ca, Mn, Zn, Ba, and Fe (Lott, 1980). Phytate is concentrated in the globoids (globoid crystals) within protein bodies, as found in the seeds of most species including cereals (Lott, 1980). In the seeds of some legumes like pea, and soybean, phytate often

occurs as protein-phytate complexes or water-soluble potassium phytate in the proteinaceous matrix of protein bodies (Lott, 1980).

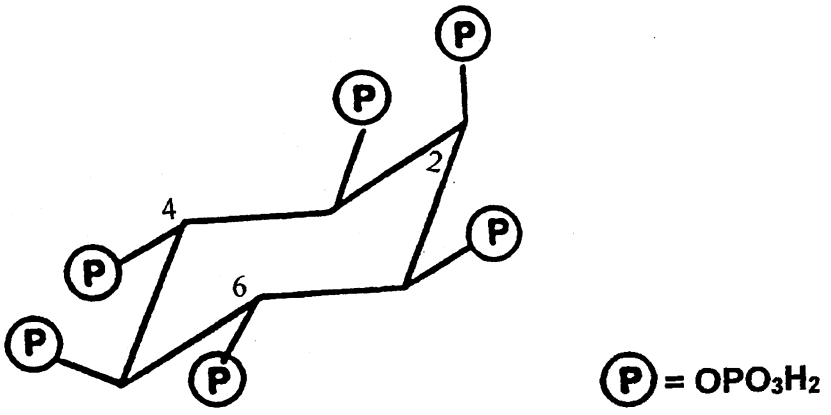

Figure 2. The structure of a phytic acid molecule (Adapted from Graf, 1986)

Phytic acid typically represents 75% to 80% of the total phosphorus in maize grains. More than 80% of the phytic acid is found in the embryo (germ) and the remainder is in the aleurone layer (O'Dell *et al.*, 1972).

Phytate clearly has two physiological roles in plants (Lott *et al.*, 1995). The first role is as a reserve compound for phosphate, various mineral cations and inositol. Upon seed imbibition and germination, phytate is broken down by the enzyme phytase to release phosphate, mineral cations and inositol needed for the growth of seedlings (Chen and Lott, 1992; Chen and Pan, 1977; Wada and Lott, 1997). The second role of phytate is to maintain inorganic phosphate homeostasis in developing seeds and seedlings (Matheson and Strother, 1969; Strother, 1980). As described by Matheson and Strother (1969), during wheat seedling growth, phytate was degraded to release *myo*-inositol and

inorganic phosphate (Pi) and the Pi content per g fresh weight remained constant for up to 14 days. Later, Strother's studies (1980) showed that a similar Pi homeostasis was present in barley, broad bean, pea and lettuce during seedling growth. He suggested that the mechanism by which the homeostasis is maintained could involve a feedback loop where increased inorganic phosphate inhibits phytase production or its activity on phytate.

Many studies have focused on the phytic acid biosynthetic pathway. Using rice cell suspension culture, Yoshida and his coworkers demonstrated that formation of $Ins(3)P_1$ is probably the first step in phytic acid biosynthesis (Yoshida *et al.*, 1999). $Ins(3)P_1$ is formed from D-glucose-6-P or free *myo*-inositol, catalyzed by $Ins(3)P_1$ synthase or *myo*-inositol kinase, respectively. Stephens and Irvine (1990) put forward the hypothesis of stepwise phosphorylation of $Ins(3)P_1$ to $InsP_6$ (phytic acid) in *Dictyostelium* (slime mold). Brearley and Hanke's studies with *Spirodela polyrrhiza* (duckweed), provided evidence for such a stepwise phosphorylation process, though the sequence of addition of individual phosphate esters in this pathway is somewhat different from that in *Dictyostelium* (Brearley and Hanke, 1996). In both pathways, phosphorylation of position 2 was the final step to $InsP_6$ (Loewus and Murthy, 2000). Phytic acid synthesis may also proceed in part by way of free inositol through phosphatidyl-inositol intermediates (York *et al.*, 1999). Recently, Shi *et al.* (2003) proposed multiple pathways of $Ins(3)P_1$ phosphorylation leading to PA synthesis in developing maize seeds.

Phytic acid synthesis appears to occur only in the tissue in which it will be stored (Lott, 1984). Greenwood and Bewley (1984), by using developing castor bean endosperm, proposed that phytic acid was synthesized in the cytoplasm, probably in the

endoplasmic reticulum cisternae, and then moved to the developing protein bodies. Vesicles containing phytic acid and protein fused with the tonoplast of developing protein bodies, and phytic acid was then deposited into the protein bodies, where it formed the globoids. It seemed that the phytate-containing particles in the cytoplasm were the precursors of globoids. As the globoids within the protein bodies increased in size, the number of these cytoplasmic particles was reduced (Greenwood and Bewley, 1984).

Problems related to phytate and phytic acid

A global estimate of the phytate produced by crop seeds/fruits is around 50 million metric tonnes each year (Lott *et al.*, 2002). With this amount of phytate production, more than 6.4, 8.1 and 2.5 million tonnes of P, K and Mg respectively, are sequestered annually in phytate in crop seeds/fruits (Lott *et al.*, 2000). Global synthesis of PA by corn grains is 4,764,125 tonnes, where around 1,606,507 tonnes of P is sequestered (Lott *et al.*, 2000).

Phytic acid has negative charges that can bind with different mineral elements and the insoluble complexes thus formed render them less available for uptake in the small intestine (Lopez *et al.*, 2002; Thompson, 1993). This decreases the bioavailability of some essential mineral elements, including Ca, Fe and Zn, in humans and many monogastric animals (Lonnerdal, 2002; Marie Minihane and Rimbach, 2002; Sandstead, 1992). The insoluble phytate that is sequestered in grains/seeds/fruits cannot be digested by monogastric farm animals and thus is excreted to the environment as animal wastes. Livestock waste P contributes to the eutrophication of lakes and rivers in many developed

countries (Lee *et al.*, 1996). This is one part of the global "phytic acid problem"(Lott *et al.*, 2000).

After nitrogen, phosphorus and potassium are the fertilizers most widely used to improve crop yields (Batten, 1992). A significant amount of P from soil is taken up by plants, sequestered in the form of insoluble phytate and removed with the harvested seeds/fruits (Lott *et al.*, 2000). This removal of P from the soil may lead to the increasing need for P fertilizer application, which adds to the cost to the crop production (Lott *et al.*, 2000).

There is some evidence that phytic acid has beneficial effects on human health by acting as an anti-oxidant and anti-cancer agent *in vivo* (Graf, 1986; Thompson and Zhang, 1991). Due to its ability of chelating mineral elements, phytic acid may inactivate some oxidoreductases, whose cofactors are these mineral elements (Fe, Zn, Mg, Cu, etc.). Thus, PA has been proposed to play a role in anti-oxidant activity *in vivo* (Graf and Eaten, 1990; Graf *et al.*, 1987).

Some mineral elements essential for plants

Although mineral nutrients make up less than one percent of the corn grain dry weight, they play significant physiological roles in plant growth and development (Hoseney, 1986; Taiz and Zeiger, 1998). Absence or inadequate supply of these mineral elements causes metabolic and functional disorders in plants, such as death, stunted growth or inability to complete the life cycle (Kochian, 2000). The biological functions of seven mineral elements, which are under investigation in this study, are described in this

section. This information was adapted from Taiz and Zeiger (1998) unless otherwise cited.

Phosphorus, present within plants as phosphate (PO_4^{3-}), is a vital constituent of many important compounds of plant cells, including sugar-phosphates in respiration and photosynthesis, phospholipids that are part of plant cell membranes, and nucleotides which participate in plant energy metabolism and make up DNA and RNA. It is also a structural component of phytic acid, which is an important storage compound in mature seeds of plants (Lott, 1980; Lott *et al.*, 1995; Raboy *et al.*, 2000).

Potassium ions (K^+) play a key role in establishing cell turgor and maintaining cell electroneutrality. Potassium ions also act as cofactors for many enzymes involved in key metabolic processes such as respiration and photosynthesis.

Magnesium (Mg) is an integral component of the ring structure of the chlorophyll molecule. Magnesium ions (Mg^{++}) also activate many enzymes involved in phosphate transfer in respiration, photosynthesis and the synthesis of DNA and RNA.

Calcium (Ca) is a structural constituent of the middle lamella of cell walls. It is also a cofactor for some enzymes in the hydrolysis of ATP and is required for the normal functioning of plant membranes and the mitotic spindle. It acts as a second messenger which, when bound to calmodulin, regulates many metabolic processes.

Zinc ions (Zn^{++}) are cofactors of some enzymes, including alcohol dehydrogenase, glutamic dehydrogenase and carbonic anhydrase. Zinc may be involved in chlorophyll biosynthesis in some plants. Recent studies have proposed that Zn is a structural

component of some transcription factors, such as Zn finger, Zn cluster and RING finger domains, which play important roles in protein synthesis (Kochian, 2000).

Iron (Fe) is a key component of cytochromes and nonheme iron proteins in photosynthesis, nitrogen fixation and respiration. The reversible conversion from Fe^{2+} to Fe^{3+} plays a role in the transfer of electrons.

Manganese ions (Mn^{++}) play an important role in activation of some enzymes in plant cells, such as dehydrogenases and decarboxylases involved in the tricarboxylic acid (TCA) cycle. Manganese is also required in the water-splitting process to produce O_2 during photosynthesis.

***Low phytic acid* (*lpa*) mutants**

An approach to solving the dietary and environmental problems associated with phytic acid is to reduce its content in seeds. Dr. Victor Raboy and his colleagues from the United States Department of Agriculture-Agricultural Research Service (USDA-ARS) and other institutions successfully isolated *low phytic acid* (*lpa*) mutants from mutagenized materials in several cereals, including corn (Raboy *et al.*, 2000), barley (Larson *et al.*, 1998; Dorsch *et al.*, 2003), wheat (Souza *et al.*, 2003) and rice (Larson *et al.*, 2000) and the legume soybean (Wilcox *et al.*, 2000). Scientists from other countries have isolated *lpa* mutants in barley (Rasmussen and Hatzack, 1998) and corn (Pilu *et al.*, 2003) as well. For corn, there are two types of *lpa* mutants: *lpa*1-1 and *lpa*2-1. Dr. Raboy and his colleagues used the "pollen-treatment" method to produce high rates of mutation in corn (Raboy *et al.*, 2002). A population of ethyl methanesulfonate (EMS)-induced

mutants was generated as described below (Raboy *et al.*, 2000). Mature maize pollen was placed in paraffin oil containing EMS for 45 minutes, and then applied to the silks of 54 plants to produce M_1 kernels heterozygous for any induced mutations. M_1 kernels were planted in a field nursery, and the plants obtained were self-pollinated, producing 872 M_2 ears each of which consisted of sibling seeds. They screened the M_2 progenies segregating for induced mutations in P status by using a high-voltage paper electrophoresis (HVPE) assay. Five or more grains that appeared wild-type to the naked eye were sampled from each of 872 M_2 ears. They were individually ground and then assayed using HVPE for those containing either reduced phytic acid P (PA-P), increased "lower" Ins phosphates or increased inorganic P (Pi) (Raboy *et al.*, 2000). The remaining grains from M_2 ears containing putative mutants were planted in a field nursery. The plants obtained were self-pollinated to produce M_3 ears. In this way, two kinds of *lpa* mutants were isolated and they were termed *lpa*1-1 and *lpa*2-1 (Raboy *et al.*, 2000).

The *lpa*1-1 and *lpa*2-1 corn grains are, to the naked eye phenotypically wild-type but contain 55%-65% and 50% reduced PA-P respectively, compared to wild-type grains (Raboy, 2000). Both *lpa* mutants have approximately normal levels of total grain P. In *lpa*1-1 mutants, the reduced levels of grain PA-P are accompanied by "molar-equivalent"(in terms of P) increases in grain Pi, while in *lpa*2-1 mutants, the reduced levels of PA-P are accompanied by increases in both grain Pi and "lower" Ins phosphates (Raboy *et al.*, 2002).

In the context of plant biology, *lpa* mutants are of great value in understanding the phytic acid synthetic pathway(s). *Lpa* mutant grains contain reduced PA-P levels that are

paired by an increase of Pi and/or lower inositol phosphates. Obviously, the phytic acid accumulation is disrupted in these mutant grains. The perturbed functions may be in the synthetic pathway itself, or in the genes which regulate the expression of this pathway (Raboy *et al.*, 2002). Thus, *lpa* mutants provide us valuable tools for dissecting the phytic acid synthetic pathways in plants such as maize, barley, rice and soybean, as well as enhancing our knowledge regarding how phytic acid and/or phytate function in the mineral nutrient storage and homeostasis processes in plants (Raboy, 1997).

In this study, only one kind of *lpa* corn mutant, *lpa*1-1, was compared to wild-type corn grains since an adequate supply of grains was only available for the *lpa*1-1 mutant. In addition, the *lpa*1-1 mutant provides a better and more distinct test system than the *lpa*2-1 mutant in that the *lpa*1-1 mutant contains only an increased Pi level to compensate for the decreased PA-P level, while the *lpa*2-1 mutant contains both increased Pi and lower inositol phosphates to match the reduced PA-P.

Hypothesis tested

Null hypothesis (abbreviated H_0) means that no difference was found between the two subjects. In this study, the null hypotheses are as follows: 1) I hypothesize that the globoids in wild-type and *lpa*1-1 grains will be identical in structure and element composition. 2) I hypothesize that *lpa*1-1 and wild type will have a similar distribution of total P and/or PA-P among different grain parts. 3) I hypothesize that the concentration of other mineral nutrient elements (K, Mg, Ca, Zn, Fe and Mn) will be unchanged in *lpa*1-1 mutant grains and grain parts as compared to wild type.

If the experimental results show that the H_0's are false, then alternate hypotheses (H_A's) will be assumed to be true. Here, H_A's would include: 1) I hypothesize that the globoids in wild-type and *lpa*1-1 mutant grains will differ both in terms of structure (size, shape and/or frequency) and element composition. 2) I hypothesize that *lpa*1-1 grains will have an altered distribution of total P and/or PA-P among different grain parts as compared to wild type. 3) I hypothesize that the concentrations of other mineral nutrient elements such as K, Mg, Ca, Zn, Fe, and Mn will be different in *lpa*1-1 mutant grains and grain parts compared to wild type.

Objectives

The objectives of this study are described as follows:

(1) To examine the ultrastructure and element composition within scutellum, starchy endosperm and aleurone layer cells, by using Environmental Scanning Electron Microscopy (ESEM) and Energy Dispersive X-ray (EDX) analysis, to determine the possible differences between wild type and *lpa*1-1 mutant grains.

(2) To determine the possible element composition and structural differences between globoids within the scutellum and aleurone layer cells of the wild-type and *lpa*1-1 mutant corn grains, by using EDX analysis under the Scanning Transmission Electron Microscopy (STEM) mode and Transmission Electron Microscopy (TEM).

(3) To examine the total P concentrations of whole grain and grain parts (scutella, root-shoot axes and rest-of-grain fractions) to see if the distribution of total P in *lpa*1-1 mutant grains was different from that in the wild type.

(4) To examine the PA-P concentrations of whole corn grain and grain parts (as previously described) to investigate if *lpa*1-1 mutant grains had an altered distribution of PA-P compared to wild type.

(5) To examine mineral nutrient concentrations of K, Mg, Ca, Zn, Fe and Mn within embryos, rest-of-grain fractions and whole grains from both wild-type and *lpa*1-1 corn to see if the distribution of any or all of these mineral nutrients was affected by the *lpa*1-1 mutation. Data will be presented both as element concentrations and as the amounts of element per grain or grain part.

Chapter 2
Measurements of total phosphorus, phytic acid phosphorus, K, Mg, Ca, Zn, Fe and Mn

Introduction

Phosphorus in plant seeds is stored primarily in the form of phytic acid (*myo*-inositol hexa*kis*phophate, $InsP_6$) (Cosgrove, 1980; IUPAC and IUPAC-IUB, 1968). Corn grains, which are mainly consumed as human food and farm-animal feed, contain substantial amounts of phosphorus (Abelson, 1999). Total phosphorus (total P) includes inorganic phosphorus (Pi) and organic phosphorus. Phosphorus in many physiologically active macromolecules such as DNA, RNA, ATP, phospholipids, sugar-phosphates and phytic acid (PA), is classified as organic phosphorus (Schachtman *et al.*, 1998). PA-P will be used throughout this study when referring to phytic acid-phosphorus.

The molybdenum blue colorimetric procedure was employed to measure total P in corn grain tissues in this study. The quantitation of phosphorus is based on the fact that phosphate in solution reacts with molybdate to form phospho-molybdate that is easily reduced to a blue compound (Oberleas and Harland, 1986). Briggs (1924) used hydroquinone and sulfite as the reducing mixture. There have been a number of modifications since then. The molybdenum blue colorimetric assay in this study was carried out as described in the official method for P measurement in cereal foods (AOAC, 1990). It involves the addition of ammonium molybdate, hydroquinone and sodium sulfite,

which react with phosphate to produce a blue-colored compound, the intensity of which is proportional to the phosphate concentration in the sample.

Ammonium molybdate is added to the sample first and reacts with phosphate to form phospho-molybdate, which has a yellow color. It is subsequently converted to a blue compound due to reduction by hydroquinone. Sodium sulfite is added to stabilize the color reaction. The blue color develops only in the presence of phosphate and the intensity of blue-color compound can be measured at 650nm via spectrophotometry. The spectrophotometer measures the transmittance of light at a particular wavelength through the solution and then the transmittance of light can be read as an absorbance value on the instrument.

Since the above color reaction could only occur with inorganic phosphate, digestion must be employed to liberate P from all organic compounds. Traditionally two ashing methods, wet ashing and dry ashing, are used to digest the organic samples and convert any P-containing compounds such as phytic acid, phospholipids and nucleic acids, to Pi.

Wet ashing involves the use of strong acids such as sulfuric acid and nitric acid at a lower temperature than dry ashing (Gorsuch, 1970). Sulfuric acid mainly functions as an oxidant and dehydrating agent. The presence of H_2SO_4 in the digestion mixture containing nitric acid also serves to raise the boiling point of the mixture and so enhances the action of the other oxidant. Nitric acid is widely used as the primary oxidant for the destruction of organic matter. It boils at about 120°C, which assists in its removal after digestion. Sulfuric acid's high boiling point makes it difficult to remove and the difficulty

can be minimized by limiting the volume of sulfuric acid used in the digestion (Gorsuch, 1970). This is the reason why a small amount of H_2SO_4 compared to HNO_3 (ratio of 1:6) was used in this study. In addition, hydrogen peroxide is used in small amounts as a final treatment to remove small traces of color remaining after organic matter has been treated with sulfuric acid and nitric acid (Gorsuch, 1970).

In dry ashing organic matter is oxidized by reaction with gaseous oxygen, with the application of energy in some form (Gorsuch, 1970). Dry ashing of plant tissues is traditionally done in a muffle furnace at temperatures ranging from 400 to 600 ^{o}C (Ockenden and Lott, 1986b). An initial charring at lower temperatures is necessary to evaporate any volatile materials which otherwise would ignite at high temperature in the muffle furnace. The non-volatile residue is oxidized in a muffle furnace until all organic matter is destroyed. Gorsuch (1970) recommended using a post ashing treatment with diluted nitric acid and hydrochloric acid. The purpose of double acid treatment is to improve the recovery of the desired elements by converting them into more soluble forms (Gorsuch, 1970; Ockenden and Lott, 1986a).

The selection of ashing techniques depends on the needs of experiments. Studies by Smith and Schrenk (1972) showed that both ashing procedures gave identical results for their zinc and manganese measurements. In general the temperatures involved in wet ashing are much lower than in dry ashing and retention losses caused by reaction between the desired element and the containers are very much less likely. In terms of total P and PA-P analysis, wet ashing is used for the purpose of releasing phosphorus from the seed tissue samples. During the measurement of some metallic elements, such as Ca, Zn, Fe

and Mn, which are present at trace levels in the seed tissues, dry ashing is used because it allows preparation of a much larger sample size (i.e. 1.5g) as opposed to that (i.e. 0.1g) for wet ashing. Another reason to use dry ashing for metallic element measurements, lies in the finding in past work (personal communication with Dr. Ockenden) that wet ashing gave erroneous results for Ca and Fe, possibly due to binding of Ca or Fe with sulfuric acid remaining in the digest.

Once synthesized, most PA is deposited as a mixed "phytate" salt of potassium and magnesium or cations of other mineral elements such as calcium, zinc and iron (Lott, 1984). There are no specific reagents to react with phytate for colorimetric assay except Wade assay (Latta and Eskin, 1980), but many people suspect the accuracy of the Wade reaction. Trials in our laboratory generated too variable results compared to other procedures (personal communication with Dr. Ockenden). In addition, phytate does not have a characteristic ultra-violet (UV) or visible absorption spectrum (Oberleas and Harland, 1986). Many analytical methods are based on the extraction, purification and subsequent measurement of the phosphate component of PA. This study uses extraction of phytic acid by hydrochloric acid, purification by an anion-exchange resin column with final analysis by detection of phosphorus following ashing.

Ion-exchange resins consist of small beads, generally of polystyrene cross-linked with divinylbenzene (DVB) (Allen *et al.*, 1974; Korkisch, 1989). Ionizable functional groups are attached to the resin matrix and provide sites for exchange of ions of opposite charge. There is a considerable difference between the concentration of anions required to

elute Pi and that required to elute phytate, which makes separation possible (Oberleas and Harland, 1986).

Potassium, magnesium, calcium, zinc, iron and manganese are important mineral nutrients essential for plant physiology and growth (Taiz and Zeiger, 1998). In this study, measurement of these six mineral elements was carried out by using flame atomic absorption spectroscopy (FAAS). FAAS is a rapid and convenient method to determine the element concentration at the low level of μg/mL. It offers the advantage of high specificity, high sensitivity, and relatively fewer interferences over other techniques, such as colorimetric method (Isaac, 1980). The use of FAAS was first proposed and developed by Walsh (1955). Since then, FAAS has become a widely used analytical tool for metallic element measurement (Peters *et al.*, 1974). It has allowed researchers to measure a number of micronutrients essential for plant growth (Isaac, 1980). In FAAS, the absorption spectra of dissociated atoms are used to obtain information on the kind and number of atoms present in a sample solution and can therefore determine the element concentration of the sample (Peters *et al.*, 1974).

In FAAS, a sample solution is sprayed into a 1500-3000°C flame, which uses acetylene as a fuel and air as an oxidant. Inside the flame, the elements previously present as ions in the solution became atoms in the ground state (Allen *et al.*, 1974). Free atoms become excited after absorbing the energy at the characteristic wavelengths produced by the radiation sources. Atomic absorption spectra are thus formed (Allen *et al.*, 1974). The primary source of radiation is a hollow cathode lamp, whose cathode is made from the element being tested (Peters *et al.*, 1974). Radiation of a characteristic wavelength from a

hollow cathode lamp passes through the flame and the decrease in intensity is measured using a monochromator and detector-readout system. This decrease is related to the concentration of the element being analyzed in the solution and the concentration of the desired element is determined against a series of standards (Allen *et al.*, 1974).

There are 3 principal interferences during FAAS for element analysis, classified as chemical, ionization and matrix interferences (Isaac, 1980). A given element may be affected by one or more interferences.

Chemical interference is a severe problem associated with Ca and Mg measurement (Haswell, 1991; Rubeska and Moldan, 1969). It occurs due to formation of stable compounds by the element of interest and some anions, such as phosphates, sulfates and silicates. The compounds thus formed are not completely dissociated in the flame. This reduces the population of free atoms of the element being analyzed and therefore suppresses the degree of absorption, leading to erroneously lower concentrations for Ca and Mg (Isaac, 1980). This interference can be counteracted by adding an excess of a releasing agent, which acts as a competing cation which binds to the interfering anions leaving the element of interest in the ground state (Isaac, 1980). Lanthanum (La), strontium (Sr) and EDTA have been successfully used to overcome this kind of interference in Ca and Mg measurements by FAAS (Rubeska and Moldan, 1969).

Another interference occurring during FAAS is the ionization interference. This takes place when sufficient energy is present to overcome the ionization potential of the element being tested, thereby reducing the number of ground-state atoms and thus affecting the degree of absorption (Isaac, 1980). For some elements with low ionization

potentials, such as alkali metals, this is a pronounced problem. In this study, K was susceptible to ionization interference. Interference was overcome by adding an excess of a readily ionizable element, such as cesium (Cs), to both standards and samples (Haswell, 1991). Cesium in the solution is ionized thus increasing the concentration of free electrons in the flame, and thereby suppressing the ionization of potassium (Haswell, 1991).

A third interference is the matrix interference. The physical property of a sample solution, such as viscosity, may affect analytical results (Isaac, 1980). If a sample solution contains a large quantity of dissolved salts, its viscosity is higher than that of a simple aqueous solution. The increase in viscosity may cause reduced amounts of sample reaching the flame in a given time compared to standard solutions (Isaac, 1980). Thus the viscosity affects the aspiration rate. This problem can be overcome by additional dilution of samples, or by matching the concentration of the main sample components in the standard, if possible (Isaac, 1980).

Materials and Methods

Grain sources

This study was carried out on mature wild-type and *lpa*1-1 mutant corn grains. They were kindly provided by Dr. Victor Raboy (National Small Grains Germplasm Research Facility, USDA-ARS, Aberdeen, Idaho, USA). The wild-type grains were produced by two near-isogenic hybrids, A632×A619 wild type. *Low phytic acid* (*lpa*)1-1 grains were produced by A632×A619 *low phytic acid* 1-1, which was homozygous for the recessive *lpa*1-1 allele (personal communication with Dr. Raboy). Compared to the wild type, *lpa*1-1 mutant grains contained 55-65% reduced phytic acid-phosphorus (PA-P), accompanied by a corresponding increase in inorganic phosphorus (Raboy, 2000). The total phosphorus (total P) in this mutant grain was similar to that observed in the wild type (Raboy, 2000).

Sample preparation

(1) Dissection

Prior to dissection, WT and *lpa*1-1 mutant grains were put into separate vials and soaked in the 90% ethanol solution for 1.5 days. The whole grain was separated into 3 grain parts: root-shoot axis, scutellum and rest-of-grain fraction. This was achieved by using forceps to peel off the pericarp/seed coat above the embryo to expose the scutellum and root-shoot axis, then using a chisel to push apart the boundary of scutellum and root-shoot axis with care and finally scoop the tiny root-shoot axis out. After that, the

scutellum was removed by using a chisel to scoop it out of the rest of the grain. A total of 450 grains from each grain type were dissected for total P and PA-P analyses. The ethanol soaking solution was kept to measure the P, K, and Mg content.

(2) Grinding

For the total P and PA-P analyses of the whole grain, 50 WT and 50 *lpa*1-1 mutant grains were ground using a stainless steel grinder. The tissue was ground until most of it could pass through a 1mm screen. The final product had less than 5% of the material unable to pass through the 1mm screen.

The grinding method for the isolated grain parts differed according to the characteristics of the different tissues. The rest-of-grain portion which included the pericarp (fused with the seed coat), aleurone layer, and starchy endosperm, was ground by the same method as used for the whole grain. The scutellum was soft and oily and therefore was ground with a pestle and mortar. The root-shoot axis was very tiny and previous work showed that cutting it in half was adequate for good extraction or digestion. All samples were prepared in triplicate for total P and PA-P analyses.

Measurement of percent moisture

For each grain type, three samples of the prepared tissue (of the same sample size as used for chemical analyses of total P, PA-P measurement or FAAS) was used for percent moisture determination. They were weighed in aluminum weighing dishes, and placed into an oven at 130 °C for 2 h (Roberts and Roberts, 1972). The dishes were removed from the oven, cooled in a desiccator and weighed. The initial and final weights

of each sample were recorded. The percent moisture of each sample was calculated according to the formula of Allen (1974):

% moisture = [(initial weight - final weight) / initial weight] × 100%

Total phosphorus measurement

(1) Wet ashing

A wet-ashing procedure using concentrated HNO_3 and H_2SO_4 was employed to destroy all organic components and release phosphorus. The combination of 3 mL concentrated HNO_3 and 0.5 mL concentrated H_2SO_4 used here was adapted from Harland and Oberleas (1977). Three samples of prepared tissues (about 0.1g each) from each of the WT and *lpa*1-1 mutant were weighed onto weighing papers and transferred into three pre-labeled 100 mL digestion test tubes (7900 Tube, 25 mm × 200mm from VWR CANLAB) containing a glass bead each. The sides of the tubes were washed down with a few mL of water as needed. Three mL of concentrated HNO_3 and one-half mL of concentrated H_2SO_4 were added to each digestion tube. The tubes were placed in a Kjeldahl digestion unit (Gallenkamp, England) and heated. Initially the tubes were tapped gently with a plastic rod to avoid local overheating before spontaneous bubbling was established. Digestion was continued until only H_2SO_4 remained. The end point was indicated when a cloud of dense white fumes filled the tube. The white fumes were allowed to suspend above the digestion mixture for a few minutes and then the tubes were removed from the digestion unit and cooled to room temperature. After four drops of hydrogen peroxide were added to the cooled digests, the tubes were returned to the

digestion unit and heated to fuming. The digests were allowed to cool and then quantitatively transferred to separate volumetric flasks. The size of flasks differed depending on the anticipated amount of P for various grain parts (See Appendix A for Table 1). The quantitative transfer was achieved by using a small funnel which caught the glass bead and by using a small glass rod to avoid sample loss on the outside of the tube. The tube, rod and funnel were rinsed twice with the deionized water and the rinses were transferred to the flask. The flask was made up to volume with the deionized water and the contents were mixed thoroughly.

(2) Phosphorus assay

The molybdenum blue procedure used for P assay was based on the AOAC procedure (1990). Prior to spectrophotometric phosphorus measurement, separate solutions of ammonium molybdate, hydroquinone and sodium sulfite were prepared. Molybdate solution was made by preparing 5% ammonium molybdate in 2.75M H_2SO_4. A 0.5% hydroquinone solution was made by dissolving 0.5 g hydroquinone in 100 mL deionized water with one drop of H_2SO_4 to retard oxidation. A 20% sodium sulfite solution was made by dissolving 20 g Na_2SO_3 in 100 mL deionized water. A diluted standard P solution containing 0.0245 mg /mL P was prepared by diluting a 0.5 mg/mL PO_4 standard solution (Aldrich Chemical Company, Inc., Milwaukee, WI).

Two mL of each diluted digest was pipetted into separate 10 mL volumetric flasks. Standard P solutions (0.5, 1.0, 1.5, 2.0, 2.5, and 3.0 mL from the diluted P standard mentioned above) were pipetted into separate 10 mL volumetric flasks. A reagent blank was prepared using 2 mL of deionized water. One mL of each of the

ammonium molybdate, hydroquinone and sodium sulfite solutions was added in that sequence into each sample, each standard P solution and the blank. The flask was made up to volume with deionized water and the contents were mixed thoroughly. The absorbance was read at 650 nm on a Zeiss PMQ II spectrophotometer (Carl Zeiss, West Germany) about 1 hour after the reagents were added.

Using the absorbancy readings from the blank and the series of standard P solutions, a standard curve was generated. Since the standard curve was linear, a standard factor was calculated by dividing the amount of P that should be in the standard by the mean absorbance for the corresponding standard. The standard factor was used to calculate the mg of P in the experimental samples, which in turn gave the amount of P in the original samples by multiplying by the dilution factor. The amount of P was calculated on the basis of dry weight (DW), as mg/g, and on the basis of per grain (or per grain part), as mg/grain or mg/grain part. Two-sample T-test was used to determine whether there was a statistical difference at $P > 0.05$ (Zar, 1984) between WT and *lpa*1-1 samples.

Phytic acid-phosphorus measurement

(1) Extraction of samples

Based on the procedure in AOAC (1990), phytic acid along with other phosphorus-containing compounds were extracted from corn seed tissues by 2.4% HCl. Three samples from each of WT and *lpa*1-1 mutant grain (or grain part) were weighed into separate 125 mL Erlenmeyer flasks. The percent moisture was determined on

separate samples on the same day. Fifty mL of 2.4% HCl (w/v) was added to each flask and the flasks were placed on a shaker (Eberbach Corporation, Ann Arbor, Michigan) for 2.5 h. Every 20 minutes or so, the flasks were removed, swirled gently to loosen the tissues settled on the bottom of the flasks, and then returned to the shaker.

After 2.5 h, the extract was divided between two 50 mL plastic centrifuge tubes (Nalgene, round bottomed) and centrifuged for 15 min. at 10,000 rpm (12000 × g) at 5°C in a Sorvall Superspeed RC2-B Centrifuge (Ivan Sorvall Inc., Newtown, Connecticut). The supernatant was decanted into a funnel with Whatman No. 40 medium speed, ashless filter paper and collected in a new Erlenmeyer flask. The filtrates were then transferred to vials and stored in the refrigerator for column separation the next day.

(2) Column separation for phytic acid

The procedure for the isolation of PA was derived from AOAC (1990). Plastic columns (Econo Bio-Rad 0.7 x 15 cm) with about 5 cm of tygon tubing attached to the lower ends were clamped onto retort stands. A metal clamp that could control the flow rate of the column was attached to the tubing. For each column, about 0.5 g of Bio-Rad analytical grade anion exchange resin (AG 1-X8 200-400 mesh chloride form) was weighed and made into slurry with deionized water. The slurry was poured into the column after the metal clamp was fully closed. The resin was allowed to settle forming a resin bed about 1 cm high. The flow rate of each column was set at 10 drops per minute with additional water being added if necessary (Plaami and Kumpulainen, 1991). The flow rate was readjusted during the separation as necessary.

Once the rate had been set, the separation could be started with addition of 15 mL of deionized water to each column. Application of solutions to the columns was done slowly so as not to disturb the surface of the resin bed. When the water was just above the resin bed, 15 mL of 0.7 M NaCl was added to prime the column to bind with phytic acid and phosphate until the 0.7 M NaCl almost went through the column. After the column was washed with 15 mL of deionized water, the diluted extract was applied. A small amount (4-25 mL) of extract was diluted 10-fold with deionized water in a graduated cylinder. The volume of extract used in the column separation is summarized in Appendix A (Table 2). The dilution with water was done in order to decrease the acidity of the extract for better separation. Different volumes of extract were added to the column in order to bring the PA-P amount in the final eluate into the measurable levels for the color reaction in the spectrophotometer. To ensure all the extract was transferred to the column, the cylinder and pipette were rinsed twice with a small amount of deionized water and applied to the column. Again the resin was washed by running through it another 15 mL of water. Then, 15 mL of 0.1 M NaCl was applied to remove inorganic phosphate from the column. When the NaCl had almost gone through the column and the resin was nearly dry, the large beakers used for all previous collections were removed and replaced with new and clean beakers. Sixty mL of 2N HCl was added to each column to elute the phytic acid from the resin. Although the completion of the separation varied from 7 to10 hours, the column separation was done in an uninterrupted sequence.

The 60 mL of HCl containing phytic acid eluted from the column was evaporated at low temperature on a SYBRON thermolyne 2600 hot plate (Thermolyne Corporation,

Dubuque, Iowa) until about 2 or 3 mL remained. The residue was cooled and then transferred quantitatively to digestion tubes using a glass rod and funnel with two additional rinses of water each.

(3) Wet ashing

The wet ashing procedure was performed as previously described for total P measurement, except that no hydrogen peroxide was needed. After ashing, digests were diluted to bring the phosphorus concentrations within the measurable range of spectrophotometer (See Appendix A for Table 2). The dilution was made by quantitatively transferring each digest to a separate volumetric flask. Volumetric flasks of different sizes were used according to dilution volume needed for various grain parts (Appendix A- Table 2).

(4) Phosphorus assay

The molybdenum blue colorimetric procedure as previously described, was used for P measurement of the phosphorus that was bound originally as PA-P. As described earlier for the total P analysis, two-sample T-test was used to determine the statistical differences at $P > 0.05$ in the PA-P concentrations and the amounts of PA-P between WT and *lpa*1-1 mutant samples (Zar, 1984).

Measurements of K, Mg, Ca, Zn, Fe, and Mn using flame atomic absorption spectroscopy (FAAS)

(1) Matrix solution preparation for FAAS

There were two matrix solutions needed for K, Mg, Ca, Zn, Fe, and Mn measurements by FAAS. For Zn, Fe and Mn analyses, 2% HNO_3 (v/v) was prepared by diluting 20 mL concentrated HNO_3 with water to a final volume of 1L. The analyses of K, Mg, and Ca were carried out in 2% HNO_3 (v/v) to which 2000 ppm La^{3+} and 1000 ppm Cs^{+} were added to eliminate the interference effects during FAAS. The La/Cs/ HNO_3 solution was made by adding 3.6 mL concentrated HCl plus 2.346 g La_2O_3 plus 20 mL concentrated HNO_3 and finally 1.267 g CsCl to some water and diluting to volume in a 1L volumetric flask. The reason for adding 3.6 mL concentrated HCl to 2.346 g La_2O_3 is that such amounts of two compounds reacted to produce 3.532g $LaCl_3$, which contained 2g La^{3+}.

(2) Digestion and sample preparation for FAAS

Two ashing techniques, wet ashing and dry ashing, were used in this study to break down seed tissues to release any bound elements. The wet ashing procedure (Harland and Oberleas, 1977) was used to digest the samples for K and Mg measurements, as previously described for total P analysis. Three samples of ground tissues weighing about 0.2 g each from each of WT and *lpa*1-1, were digested for K and Mg analyses, respectively. After ashing, the digests were diluted to an estimated element concentration within the optimal range of FAAS absorbance. This was done by quantitatively transferring the digests to appropriate volumetric flasks and making up to

volume with 2000ppm La/1000ppm Cs/ 2% HNO_3. Some sequential dilution with the appropriate matrix solution was done as needed (See Appendix B).

The dry ashing procedure used for Ca, Zn, Fe and Mn samples was based on Ockenden and Lott (1986a). All samples were prepared in triplicate for Ca, Zn, and Fe analyses, respectively, unless otherwise cited. The ground tissues (about 1.0 g each) from each of WT and *lpa*1-1 corn grains were weighed into separate porcelain crucibles (Coors Porcelain, Golden, Co.). Since the expected Mn concentration in corn grain tissues was very low, a 1.5 g sample was weighed into each of two crucibles and then pooled after ashing. This was done in order to bring the expected Mn concentration in the final sample within the optimal working range of FAAS. For each set of ashed samples, a crucible blank was also prepared by letting an empty crucible go through the same treatment as the experimental samples, to test for any contamination.

Charring was done before dry ashing by putting the crucibles on a SYBRON thermolyne 2600 hot plate (Thermolyne Corporation, Dubuque, Iowa) set at 290°C until all smoking ceased. Initially the crucibles were placed on the cooler edge of the hot plate and then moved gradually towards the center. The crucibles were heated in the center until any smoking ceased. Finally, they were loosely covered with aluminum foil to complete charring.

After charring, the samples were ashed in a blue M Electric muffle furnace (Blue Island, Illinois) at 550°C for 4 h and removed to cool at room temperature. Following this, a double acid treatment was done to dissolve the salts in the ash (Gorsuch, 1970). About 1.5 mL HNO_3 : H_2O (1:2 v/v) was added to each crucible and evaporated to

dryness on the same hot plate at lowest setting. The crucibles were removed to cool at room temperature followed by another treatment of 1.5 mL HCl : H_2O (1:1 v/v). After all the acid evaporated and the crucibles cooled, about 5 mL of the appropriate matrix solution for each element (as described earlier) were added and the residue of each sample was quantitatively transferred to a 10 mL volumetric flask by using a glass rod and funnel with additional two rinses of the appropriate solution. The rinses were also transferred into the flask and the flask was brought to volume.

To remove insoluble ash residue, ten mL of the digested solutions were transferred to 15 mL centrifuge tubes and centrifuged for 8 min. at 3000 rpm (1470 × g) in an International Clinical Centrifuge (International Equipment Co., Needham, Mass.). After centrifuging, supernatants were filtered through Whatman No. 40 ashless filter papers. The filtrates were then diluted with the appropriate matrix solutions to element concentrations within the optimal working range of the FAAS as needed (see Appendix B). When the possible concentration range was very wide, a second dilution was done to ensure that at least one of the element concentrations was within the optimal working range of the instrument.

(3) Preparation of standards for FAAS

The K, Mg, Ca, Zn, Fe and Mn standards were prepared separately by diluting six VWR Scientific single element standards containing 1000ppm (1 ppm equals to 1 μg/ mL) each of six elements (VWR Scientific, West Chester, PA) on the same day as the analysis. Each standard was diluted with the appropriate solution for the element being

tested as previously described. A series of 5 diluted standards for each element were used at the concentrations as follows, since this concentration range for a given element generated the best standard curve (linear curve) to ensure the accurate experimental results, according to the Varian manual.

K: 0.2, 0.4, 0.8, 1.2, 1.6 ppm

Mg: 0.1, 0.2, 0.4, 0.6, 0.8ppm

Ca: 1.0, 2.0, 3.0, 4.0, 5.0 ppm

Zn: 0.1, 0.2, 0.3, 0.4, 0.5ppm

Fe: 1.0, 2.0, 3.0, 4.0, 5.0 ppm

Mn: 1.0, 2.0, 3.0, 4.0, 5.0 ppm

(4) Analytical procedures for K, Mg, Ca, Zn, Fe, and Mn measurement

The standards and samples were measured on a Varian SpectAA 220 FS atomic absorption spectrophotometer (Varian Techtron Pty. Limited, Springvale, Australia) using an air-acetylene flame. Single element Varian hollow cathode lamps were used. During FAAS, the lamps emitted radiation at the following wavelength according to guidelines in Varian Manual: K (766.5 nm), Mg (285.2 nm), Ca (422.7 nm), Zn (213.9 nm), Fe (248.3 nm) and Mn (279.5 nm), respectively. After each lamp was turned on, it needed to be optimized prior to the analysis. Then, aspiration rate was checked and, if needed, was adjusted to 5 ml per minute. Next, signal optimization was done by using the middle standard. The burner adjustment was made manually in the course of optimizing the signal. After all these were done, the standards and the samples could be analyzed. A

standard curve for each element was generated automatically by the instrument, which took triplicate readings of each standard concentration. For each sample, readings were also taken in triplicate by the spectrophotometer and the mean absorbancy reading was automatically converted to a concentration value in mg/L.

The concentrations in mg/L (1 mg/L = 1μg/mL) were converted to mg or μg per sample originally present by multiplying these concentrations by the dilution factor. Dividing these values of mg or μg per sample by the corresponding dry weight (DW) gave the amounts of element in mg or μg per g DW. The values of mg or μg element per grain or grain part were also calculated. Two sample T-test was performed using MINITAB to determine statistical differences between WT and *lpa*1-1 samples at $P>0.05$ (Zar, 1984).

Measurement of P, K and Mg leakage

(1) Sample preparation

The remaining 90% ethanol solutions that were used to soak the grains prior to dissection were allowed to dry. The number of grains soaked was noted. Deionized water was added, several rinses were used and the mixture was filtered through Whatman No. 40 ashless filter paper. The filtrates were pooled together to constitute leachate samples in duplicate for WT and *lpa*1-1 mutants respectively. Following that, the filtrates were transferred quantitatively to digestion tubes for wet ashing. The digests were analyzed for P, K and Mg content.

(2) Analytical procedure

Phosphorus leakage was measured using a P assay as previously described for total P analysis. Since phytate, including soluble Na-phytate, is virtually insoluble in 80-90% ethanol solution (Lott *et al.*, 1984), only the total P content leaking into the soaking solution was measured. Leakage of K and Mg was measured using FAAS as described earlier in this chapter.

Results

(1) Determination of percent moisture

The percent moisture data (Table 1) showed that whole grain had the highest moisture content among the various grain or grain parts tested, ranging from 8.60% to 9.35%. The root-shoot axis tissues had the lowest moisture content, ranging from 4.33% to 4.53%.

Table 1. Moisture content (%) of different grain parts and whole grain from WT and *lpa*1-1 mutant corn

Grain type	Whole grain	Embryo		Rest-of-grain
		Scutellum	Root-shoot axis	
WT	8.70-9.35	6.23-6.53	4.33	7.01-7.24
*lpa*1-1	8.60-9.25	5.79-6.07	4.53	6.61-7.48

(2) Measurements of total P, PA-P, K, Mg, Ca, Zn, Fe, and Mn

Quantitative measurements of P (total P and PA-P), K, Mg, Ca, Zn, Fe, and Mn were expressed in two ways: (1) on a dry weight basis (mg/g or μg/g) in the whole grain or a given grain part, (2) on a per grain or grain part basis (mg or μg/grain, or mg or μg/grain part). In the whole grain, total P concentration of *lpa*1-1 was similar to that of WT, while PA-P concentration of *lpa*1-1 was significantly different from that of WT, with a reduction of 58.2% on a dry weight basis (Table 2). Within the embryos, total P and PA-P concentrations in both scutella and root-shoot axes for *lpa*1-1 were significantly different from WT (Table 2). The concentrations of total P and PA-P in

*lpa*1-1 rest-of-grain fractions were significantly different from those in WT (Table 2). The scutellum total P concentration was slightly lower in *lpa*1-1 mutant grains than WT grains, while the reverse pattern occurred in root-shoot axes and rest-of-grain fractions (Table 2). In terms of PA-P concentration, *lpa*1-1 scutella, root-shoot axes and rest-of-grain fractions had a reduction of 63.8%, 56.4% and 38.5% respectively, as compared to WT (Table 2).

In wild-type corn, the rest-of-grain fraction made up the bulk of the grain, forming 86.8% of the total grain dry weight, while the rest-of-grain fraction in the *lpa*1-1 mutant grains accounted for 89.4% of the total grain dry weight (derived from Table 2). The mean rest-of-grain dry weight for *lpa*1-1 was lower than WT and this was the cause of a decrease in whole grain dry weight for *lpa*1-1 as compared to WT (Table 2).

When expressed on a per grain basis, grain total P level was not different between *lpa*1-1 and WT, while the grain PA-P level of *lpa*1-1 was reduced by 61.6% as compared to WT (Table 2). For the two embryo parts, on a per grain part basis *lpa*1-1 had a reduction of 6.9% in the scutellum total P and an increase of 29.2% in the root-shoot axis total P as compared to WT (derived from Table 2). However, the reduction of PA-P levels per scutellum and per root-shoot axis in *lpa*1-1 mutants *versus* WT were 62.6% and 57.1% respectively (Table 2). Taken together, the *lpa*1-1 PA-P level per embryo was reduced by 62.4% while total P level of *lpa*1-1 per embryo dropped by 4.8% compared to WT (derived from Table 2). In *lpa*1-1 rest-of-grain fractions, the total P per rest-of-grain fraction increased by 31.8% (derived from Table 2) while PA-P level per rest-of-grain fraction decreased by 42.3% as compared to WT (Table 2).

It was found that as a percentage of whole-grain total P, the scutellum, root-shoot axis and the rest-of-grain fractions were 80.2%, 4.9%, and 11.3% respectively in WT corn grains. For *lpa*1-1 mutant grains, as a percentage of whole-grain total P were 77.6% in the scutellum, 6.6% in the root-shoot axis, and 15.5% in the rest-of-grain (derived from Table 2). In relation to whole-grain values, % of PA-P in the WT scutellum, root-shoot axis and the rest-of-grain were 91.6%, 3.6%, and 3.3%, respectively, while % of PA-P in the *lpa*1-1 scutellum, root-shoot axis and the rest-of-grain were 89.3%, 4.0%, and 5.0%, respectively (Table 2).

On a dry weight basis, whole-grain Mg, Ca, Fe and Mn concentrations of *lpa*1-1 were significantly different from those of WT, while whole grain concentrations of K and Zn were not different (Table 3). The concentrations of Mg, Fe and Mn were higher in *lpa*1-1 grains than in WT grains, and Ca was lower (Table 3). Furthermore, the K, Ca and Fe concentrations for *lpa*1-1 embryos were significantly different from WT embryos, whereas Mg, Zn and Mn concentrations were not different (Table 3). The embryo K and Ca concentrations were lower but embryo Fe concentration was higher in *lpa*1-1 than those in WT. It was noted that *lpa*1-1 Fe concentrations were markedly increased in whole grain and embryo, by 33.2% and 33.1% respectively, as compared to WT (derived from Table 3). In the rest-of-grain fractions, *lpa*1-1 had an increase in K, Mg, Fe and Mn concentrations while their Ca and Zn concentrations remained unchanged as compared to WT (Table 3).

When expressed on a per grain basis, the amounts of Mg, Fe, and Mn in *lpa*1-1 grains were significantly higher than in WT grains and Ca was significantly lower, while

the amounts of K and Zn were not different (Table 4). On a per embryo basis, *lpa*1-1 had a decrease in K and Ca levels and an increase in Fe level as compared to WT. However, Mg, Zn, and Mn levels were not different between *lpa*1-1 embryo and WT embryo (Table 4). It was noted that the amounts of Fe per grain and per embryo in *lpa*1-1 were increased by nearly one-third when compared to WT (derived from Table 4). On a per rest-of-grain part basis, *lpa*1-1 had increased K, Mg, Fe, and Mn levels as compared to WT, but similar Ca and Zn levels to WT (Table 4).

Table 2. Concentrations (mg/g ± SD, N=3) and amounts (mg/grain or grain part ± SD, N=3) of total P and PA-P in the whole grain, scutellum, root-shoot axis and rest-of-grain fractions of wild-type and *lpa*1-1 mutant corn

		Whole grain	Scutellum	Root-shoot axis	Rest-of-grain
Total P (mg/g)	**WT**	3.439±0.098a[1]	23.983±0.212a	11.859±0.122a	0.439±0.005a
	***lpa*1-1**	3.607±0.062a	21.773±0.295b	14.687±0.136b	0.652±0.006b
PA-P (mg/g)	**WT**	2.753±0.071a	22.010±0.233a	7.057±0.294a	0.104±0.002a
	***lpa*1-1**	1.152±0.002b	7.970±0.077b	3.080±0.035b	0.064±0.001b
	% Reduction	58.2	63.8	56.4	38.5
PA-P as % of total P	**WT**	80.1	91.8	59.5	23.7
	***lpa*1-1**	31.9	36.6	21.0	9.8
Dry weight per grain or grain part (mg)	**WT**	288.30±11.6a	32.49±0.057a	4.04±0.081a	250.38±0.329a
	***lpa*1-1**	260.50±0.99b	33.41±0.054b	4.14±0.31a	232.82±1.19b
Total P (mg/grain or grain part)	**WT**	0.972±0.028a	0.780±0.007a (80.2%[2])	0.048±0.0004a (4.9%)	0.110±0.001a (11.3%)
	***lpa*1-1**	0.936±0.016a	0.726±0.010b (77.6%)	0.062±0.0035b (6.6%)	0.145±0.001b (15.5%)
PA-P (mg/grain or grain part)	**WT**	0.779±0.020a	0.714±0.008a (91.6%[3])	0.028±0.002a (3.6%)	0.026±0.0005a (3.3%)
	***lpa*1-1**	0.299±0.001b	0.267±0.003b (89.3%)	0.012±0.001b (4.0%)	0.015±0.0003b (5.0%)
	% Reduction	61.6	62.6	57.1	42.3

1. Values in the same column followed by the same letter are not statistically different at P >0.05.
2. Percentage of total P in the grain part to the whole grain total P.
3. Percentage of PA-P in the grain part to the whole grain PA-P.

Table 3. Element concentrations (mg/g or µg/g ± SD, N=3) of K, Mg, Ca, Zn, Fe and Mn in the whole grain, embryo and rest-of-grain fractions of wild-type and *lpa*1-1 mutant corn

Element		Whole grain	Embryo	Rest-of-grain
K	WT	3.313±0.053a[1]	20.689±0.085a	0.864±0.01a
(mg/g)	*lpa*1-1	3.249±0.480a	18.420±0.908b	0.993±0.005b
Mg	WT	1.255±0.018a	9.891±0.044a	0.084±0.002a
(mg/g)	*lpa*1-1	1.429±0.056b	10.267±0.256a	0.100±0.002b
Ca	WT	46.51±3.53a	54.31±2.87a	39.12±1.01a
(µg/g)	*lpa*1-1	37.94±2.42b	47.32±2.21b	39.99±2.14a
Zn	WT	24.62±2.10a	106.90±1.70a	7.452±0.229a
(µg/g)	*lpa*1-1	26.82±1.02a	106.38±3.39a	7.548±0.367a
Fe	WT	17.96±0.96a	56.82±1.18a	7.501±0.19a
(µg/g)	*lpa*1-1	23.93±0.84b	74.59±2.39b	9.109±0.31b
Mn	WT	5.607±0.044a	19.774±0.211a	2.296±0.026a
(µg/g)	*lpa*1-1	6.864±0.040b	20.076±0.252a	2.829±0.052b

1. Values in the same column followed by the same letter are not statistically different at $P > 0.05$.

Table 4. Amounts (µg/grain or grain part ± SD, N=3) of K, Mg, Ca, Zn, Fe and Mn in the whole grain, embryo and rest-of-grain fractions of wild-type and *lpa*1-1 mutant corn

Element		Whole grain	Embryo	Rest-of-grain
K (µg /grain or grain part)	WT	943.49±15.0a[1]	769.63±3.16a	202.96±4.23a
	*lpa*1-1	880.50±130.2a	670.50±33.0b	219.38±1.99b
Mg (µg/grain or grain part)	WT	359.78±5.03a	354.09±1.57a	20.14±0.52a
	*lpa*1-1	380.85±14.90b	362.41±9.05a	22.53±0.51b
Ca (µg/grain or grain part)	WT	13.25±1.01a	2.18±0.12a	9.35±0.24a
	*lpa*1-1	9.77±0.62b	1.88±0.09b	9.03±0.48a
Zn (µg/grain or grain part)	WT	6.964±0.595a	4.29±0.068a	1.78±0.05a
	*lpa*1-1	6.963±0.265a	4.23±0.135a	1.71±0.08a
Fe (µg/grain or grain part)	WT	5.08±0.27a	2.28±0.05a	1.79±0.05a
	*lpa*1-1	6.21±0.22b	3.06±0.10b	2.06±0.07b
Mn (µg/grain or grain part)	WT	1.59±0.01a	0.79±0.01a	0.55±0.01a
	*lpa*1-1	1.78±0.01b	0.80±0.01a	0.64±0.01b

1. Values in the same column followed by the same letter are not statistically different at $P > 0.05$.

(3) Phosphorus, K and Mg leakage into grain soaking solutions

The amounts of phosphorus, potassium and magnesium leaked into 90% ethanol solutions during grain soaking are shown in Table 5. When expressed as a percentage of the amount originally present in the grains before soaking, leakage of P, K and Mg was very low, less than 1%. Among the three elements measured, K was leaked the most, followed by P and Mg.

Table 5. Leakage of P, K and Mg into 90% ethanol solutions during grain soaking prior to separation of grain parts

Element	Grain type	Element leaked per grain (μg)	Total amount of element per grain (μg)	% of element leaked per grain
P	**WT**	1.763	972.00	0.18
	***lpa*1-1**	1.695	936.00	0.18
K	**WT**	8.482	943.49	0.90
	***lpa*1-1**	6.517	880.50	0.74
Mg	**WT**	0.166	359.78	0.05
	***lpa*1-1**	0.145	380.85	0.04

Discussion

The concentrations of elements and PA-P expressed on a dry weight basis, as mg /g or μg /g, facilitate the comparison and evaluation of wild-type and *lpa*1-1 corn grains in animal and human nutrition. The amounts of elements and PA-P presented on a per grain or per grain part basis aid in the comparison and assessment of mineral nutrient and PA-P distribution within the corn grain in a plant biology context.

The measurements of total P, PA-P, K, Mg, Ca, Zn, Fe, and Mn were made of the whole-grain samples, and rest-of-grain fractions. Total P and PA-P measurements were made of two embryo components, namely the scutellum and root-shoot axis, while measurements of metallic elements were made of the embryo. The reasons were: (1) distribution and quantitation of total P and PA-P among different grain parts in *lpa*1-1 mutant grains was of special interest since the *lpa*1-1 mutant used in this study was genetically modified for a PA reduction. (2) if the tiny root-shoot axis sample was analyzed for Ca, Zn, Fe and Mn, their concentrations would be below the detectable limit of FAAS unless great labor was spent isolating root-shoot axes from thousands of grains.

The *lpa*1-1 grain total P level was similar to WT while PA-P was reduced by 61.6% as compared to WT. This is in agreement with the reduction reported by Raboy (2000), whose value ranged from 55 to 65%. However, I extended my studies to include the investigation of the total P and PA-P differences in distribution and amounts within different grain parts in *lpa*1-1 grains.

My data showed that in WT corn grains, 91.6%, 3.6%, and 3.3% of PA-P was stored in the scutellum, root-shoot axis, and rest-of-grain fractions, respectively, and in *lpa*1-1 mutant grains, 89.3%, 4.0%, and 5.0% of PA-P was in the scutellum, root-shoot axis, and rest-of-grain fractions, respectively. This leads to two conclusions: (1) that the *lpa*1-1 mutation did not alter the relative partitioning of PA-P between the scutellum and root-shoot axis within the embryo, and (2) that 95.2% of PA-P was stored in the embryo (the sum of scutellum and root-shoot axis) in WT corn grains. O'Dell *et al.* (1972) reported that 88.0% of PA-P in the normal, non-mutant mature corn grains was found in the embryo. My value for percentage of PA-P in the embryo was higher. This could be due to a different corn cultivar, fertilizer application, soil conditions and other environmental conditions. However, from O'Dell *et al.* (1972) the sum of the percentages of the PA-P in the embryo (88.0%), endosperm (3.2%), and hull (0.4%) was 91.6%. The sum of percentages of PA-P in the scutellum (91.6%), root-shoot axis (3.6%) and rest-of-grain (3.3%) from my data was 98.5%, which is very close to the theoretical value 100%. A few reasons maybe account for this difference: (a) the preparation procedure used. O'Dell *et al.* (1972) used distilled water soaking before grain parts separation. It is very likely some water-soluble phytate, such as K-phytate, was lost in the water, contributing to the lower value of embryo PA-P. My procedure used 90% ethanol soaking solution before separation, where water-soluble phytate was thought to be virtually insoluble (Lott *et al.*, 1984). (b) the sample size used. O'Dell *et al.* (1972) used 5-25 mg samples from a total of 12 embryos for PA-P analysis. Studies of squash seeds reported that the embryo-to-embryo variation could be minimized when 20-25 embryos were pooled (Ockenden,

1987). The very small samples used by O'Dell *et al.* may also have introduced imprecise measurements. In contrast, for PA-P analysis I used 0.9 g samples containing 30 scutella each. Since the preparation procedure used in this study allowed the better recovery than O'Dell *et al.* and a large sample minimized the experimental errors, the data reported here are more accurate. Although the preparation procedure was time-consuming, it was necessary to obtain results with good precision.

Within the embryo, the total P and PA-P concentrations in the scutellum were markedly higher than those in the root-shoot axis for both grain types. When expressed on a dry weight basis, the scutellum total P and PA-P concentrations were 1.5-2 times and 2-3 times higher than the root-shoot axis respectively. Given the bigger weight of a scutellum than that of a root-shoot axis (~ 8 fold), in both grain types it was not surprising that the amounts of total P and PA-P per scutellum were far higher than those per root-shoot axis.

Deposition of PA, mainly sequestered as globoids inside the protein bodies, in the scutellum was more than that in the root-shoot axis. Previous studies of seeds of some conifers and dicots, like *Pinus* and *Arabidopsis thaliana*, indicated that the protoderm and procambium globoids contained less P than their counterparts in the ground meristem of both cotyledon and root-shoot axis (West and Lott, 1993; Lott and West, 2001). Wada and Lott (1997) demonstrated that in rice scutellum and root-shoot axis, the provascular (procambium) and protoderm tissues had smaller globoids than the ground meristem. In wheat grains the protoderm tissues in scutellum, radicle and shoot apex contained smaller globoids than the ground meristem tissue (Lott and Spitzer, 1980). Electron microscopic

observation in this study revealed that the protoderm and provascular globoids were, on average, smaller in size than their counterparts in the ground meristem of scutella from both WT and *lpa*1-1 corn grains. It is likely that the ratio of protoderm plus provascular tissue to the ground meristem tissue is higher within the root-shoot axis than within the scutellum on a per unit volume, since the root-shoot axis has a lot of protoderm covering the root, stem, coleoptile, plumule, and coleorhiza, and many provascular strands in those structures. One reason that corn root-shoot axes contained less phytate than scutella was that they had a higher proportion of protoderm and provascular tissues where the globoids tended to be smaller and a lower proportion of ground meristem tissue where the globoids were larger and more numerous.

Recent studies by Yoshida *et al.* (1999) demonstrated the Ins(3)P_1 synthase gene expression was related to the formation of globoids in the developing rice seeds. By testing the transcript levels of the Ins(3)P_1 synthase gene, Yoshida and coworkers found that its expression was highest in the aleurone layer and scutellum, and the signals of transcript lasted there longest, coinciding with the appearance of globoids (Yoshida *et al.*, 1999). The enzyme, Ins(3)P_1 synthase, which catalyzes the conversion of glucose 6-P to Ins(3)P_1, is key to the synthesis of both inositol and phytic acid (Loewus and Murthy, 2000). Ins(3)P_1 may be used to synthesize $InsP_6$ (PA) via stepwise phosphorylation or may be used to produce inositol, which in turn lead to $InsP_6$ (PA) synthesis via the intermediate of phosphatidyl inositol (Loewus and Murthy, 2000). Yoshida *et al.* (1999) also showed that the signals were detected in the root-shoot axis for a shorter time than in the scutellum, suggesting that less PA was synthesized in the root-shoot axis than in the

scutellum. My quantitative data showing a lower PA-P level in the root-shoot axis than in the scutellum support their hypothesis.

When *lpa*1-1 samples were compared, on a per part basis, to WT counterparts, it appeared that a slight decrease of total P level in the scutella was offset by increases of total P levels in both the root-shoot axes and rest-of-grain fractions. As a result, the total P level remained unchanged in *lpa*1-1 *versus* WT whole grain. This suggests that the *lpa*1-1 mutation altered the distribution of P among the different grain parts. The possibility that the *lpa*1-1 mutation in rice altered the distribution of P was proposed by Liu *et al.* (2004).

Compared to their WT counterparts, the PA-P level of *lpa*1-1 scutella dropped to a greater degree than the root-shoot axes and rest-of-grain fractions. This indicated that: (1) *lpa*1-1 mutation didn't affect PA-P accumulation within different grain parts uniformly, and (2) the scutellum contributed more to the whole grain PA-P reduction than any other grain part in the *lpa*1-1 corn grains.

There could be several factors that affect PA accumulation within different parts of the corn grain:

(1) One factor could be the supply of nutrients, such as P and inositol, to different grain parts and/or nutrient uptake by the different grain parts. Since the scutellum total P level dropped slightly in *lpa*1-1 as compared to WT, one could speculate that P supply to and/or uptake by the scutellum were probably reduced by the *lpa*1-1 mutation. However, the root-shoot axis P supply and/or uptake didn't seem to be reduced by the *lpa*1-1 mutation since the root-shoot axis total P level in *lpa*1-1 was slightly elevated compared

to WT. Two possible explanations follow. (a) Possibly the *lpa*1-1 mutation influences the uptake of P by the scutellum. Since there is no vascular connection between the scutella (or root-shoot axes) and the maternal plant (Bewley and Black, 1978), phosphate has to move apoplastically. The path of P flux could be from the pericarp/testa to endosperm to scutella to root-shoot axes. It is shown that there is no shortage of P supply to root-shoot axes, thus the scutella should have an adequate supply of P. Probably the *lpa*1-1 mutation has effects on the ability of scutella to take up P. (b) It is possible that inositol synthesis, supply and/or uptake influences the PA synthesis in the embryo. Inositol may be translocated from other grain parts (i.e. endosperm) into the embryo or synthesized *in situ* in the embryo itself using the transported materials such as glucose. The timing of nutrient (e.g. phosphorus and inositol) accumulation in the root-shoot axis and scutellum during seed maturation are incompletely understood, but they could differ to some degree.

(2) Secondly, the PA synthetic pathways could be perturbed by the *lpa*1-1 mutation at any step. As described earlier in Chapter 1, the PA synthesis may proceed via stepwise phosphorylation (Stephens and Irvine, 1990; Brearley and Hanke, 1996), phosphatidyl-inositol intermediate (York *et al.*, 1999) or multiple pathways (Shi *et al.*, 2003). One may assume that any enzyme block in these complicated and branched pathways could result in a decrease of PA synthesis.

(3) Thirdly, the reduced PA level could be due to an increased rate of PA degradation, mainly caused by increased phytase activity. The studies by Raboy *et al.* (2000) eliminated this possibility for corn. An increased phytase activity would be a gain-of-function mutation, which commonly is dominant. But in *lpa*1-1 and *lpa*2-1 maize

grains both mutations appear to be recessive (Raboy *et al.*, 2000). The mutation rate for gain-of-function is 10^{-5} whereas Raboy *et al.* (2000) observed a mutation rate of 10^{-3} in the selection of *lpa*1-1 and *lpa*2-1, which is typical of loss-of-function mutations.

The *lpa*1-1 mutant grain had a dry weight reduction of ~10% compared to WT grain, a reduction that occurred in the rest-of-grain fraction. One could speculate whether this is related to the higher Pi level commonly found in the *lpa*1-1 mutant grains than the WT grains. Starchy endosperm makes up the bulk of the rest-of-grain fraction. The rate-limiting step of starch synthesis in plants is the conversion of glucose 1-P to ADP-glucose by ADP-glucose pyrophosphorylase, an enzyme which is inhibited by Pi (Dennis and Blakeley, 2000; Plaxton and Preiss, 1987). This enzyme has both plastid and cytosolic forms. In maize and barley starchy endosperm, ADP-glucose appeared to be synthesized in the cytosol at the later stage of grain development and then transported into plastids (Dennis and Blakeley, 2000). However, in *lpa*1-1, the higher level of Pi than the normal wild-type cytoplasmic Pi level is thought to be mainly sequestered inside the certain compartments, such as vacuoles (or protein bodies in the case of mature grain), so as not to disrupt the cellular metabolic processes (Raboy, 1998). One possible factor which could cause the dry weight reduction in the *lpa*1-1 rest-of-grain fractions is that a small change in Pi concentration within the starchy endosperm cell cytoplasm could occur during grain development. Since there are no vascular or plasmodesmatal connections between the testa and the aleurone layer, and the starchy endosperm and the embryo, P movement is at least partially via the apoplastic pathway. At the later stage of grain development when starch is synthesized, the *lpa*1-1 mutation could influence the P

uptake by starchy endosperm cells. For example, a slightly higher Pi in *lpa*1-1 than WT could enter the starchy endosperm cells when an influx of P passes there from the aleurone layer to the embryo, thereby affecting the starch synthesis in the *lpa*1-1. The lower dry weight of *lpa*1-1 than WT in corn grains, may also be caused by other factors. Dorsch *et al.* (2003) proposed that inositol deficiency could be the possible reason for seed dry weight loss in barley *lpa* mutants. The *lpa*1-1 mutation has impacts on the chemistry of phosphate and inositol, which are two important compounds in cells. Probably the downstream effects on seed physiology, gene expression and/or regulation of genes in the pathways requiring P or inositol could occur (Dorsch *et al.*, 2003). Hitz *et al.* (2002) reported that a mutation in Ins(3)P_1 synthase gene resulted in both reduced PA and reduced raffinosaccharides in soybean seeds.

The embryos were richer in five metallic elements (K, Mg, Zn, Fe, and Mn) than the rest-of-grain fractions on a grain part basis for both grain types, ranging from 1.25 times to 17.6 times higher. Other work on non-mutant corn grains demonstrated a similar pattern (O'Dell *et al.*, 1972). It is known that calcium may be deposited in the cell walls as calcium pectate (Mengel and Kirkby, 1982). Since the testa (seed coat) and aleurone layer consist of thick-walled cells, it is likely that Ca deposition was greater in the cells of seed coat and aleurone layer than the embryo cells. On the other hand, it was found that the proportion of element level per embryo to that per rest-of-grain portion for a given metallic element was relatively similar in both grain types, suggesting that the partitioning of nutrients between the embryo and rest-of-grain portion was not affected by the *lpa*1-1 mutation.

When given on a weight basis (μg/g), all the six mineral nutrients were concentrated in the embryo for both grain types. This might be attributed to: 1) more active metabolic roles that the embryo has during seed development, and 2) provision of reserves needed for germination and seedling growth. The embryo undergoes cell division and expansion to give rise to a new seedling plant. It is living and dynamic throughout seed maturation and germination, whereas the bulk of rest-of-grain, namely starchy endosperm, is dead at maturity (Bewley and Black, 1978). The element concentrations per gram of embryo were much higher than those of rest-of-grain, ranging from 1.2 times higher for Ca level to 117.8 times higher for Mg level. However, high element concentration in the embryo was diluted by the bulk weight of the rest-of-grain fraction, rendering element concentration for the whole grain not much higher than that for the rest-of-grain fraction.

It was found that the *lpa*1-1 mutation resulted in an elevated Fe concentration among all the three morphological components measured. Iron concentrations in *lpa*1-1 were increased by one-third for both the whole grains and embryos, and increased by 21.4% for rest-of-grain fractions, as compared to WT. The increases in Fe are in the greatest magnitude among the metallic elements tested in this study. In the whole grain and the rest-of-grain fractions, *lpa*1-1 Mn concentration rose by 22.4% and 23.2% respectively, when compared to WT. This would benefit the mineral nutrition in humans and animals if *lpa*1-1 corn grains are consumed as foods or feeds. As reviewed by Tucker (2003), deficiency of iron and zinc, together with vitamin A, affects more than 40% of the world's human population. Phytic acid may be among the most important compounds

associated with Fe and Zn deficiency (Brinch-Pedersen *et al.*, 2002), since it binds cations and thus reduces their uptake and bioavailability (Lott *et al.*, 2000). Given both the reduced PA-P and the increased Fe concentrations in *lpa*1-1 mutant grains, *lpa*1-1 mutant corn grains are of positive nutritional value as human foods and animal feeds.

It is almost impossible to separate the corn grain parts precisely in the dry state. If cut dry, some starchy endosperm remains attached to the embryo or some embryo fragments remain with the endosperm, thus making the data on element concentration inaccurate. I believe that the error introduced by dry sample preparations was more than 5%. Pre-soaking in 90% ethanol solutions allowed the hard and dry corn grains to soften a little for much more accurate separation of grain parts. Measurement of P, K, and Mg leakage into 90% ethanol revealed that less than 1% of the initial amount of K escaped into the soaking solutions, and P and Mg leaked less than 0.2% of the initial amount. Taken together, it turned out that the pre-soaking procedure was justifiable for sample preparation since the much improved precision during dissection outweighed the very little element loss into the soaking solutions. Studies on element leakage from cabbage seeds on element leakage into water showed that K was leaked much more than Mg, Ca, Mn and Cl (Loomis and Smith, 1980). A later leakage study on 11 monocot and dicot seeds supported these results (Lott *et al.*, 1991). Since elements like Ca, Zn, Fe and Mn are present in more bound forms than K, they are relatively insoluble inside seed tissues (Loomis and Smith, 1980; Lott *et al.*, 1991), and are lost less during soaking. The comparison of P leakage into 90% ethanol solution in this study and P leakage into water in West *et al.* (1994) for non-mutant corn grains, showed that the latter was 5 times

higher than the former. Since measurement of elements known to be most readily leaked by imbibed seeds revealed very little loss into 90% ethanol, it is very unlikely that much, if any, of the other elements of interest would be have been leaked.

Chapter 3
Ultrastructural examination and measurement of various elements in globoids of corn scutellum and aleurone layer cells using electron microscopy techniques

Introduction

The electron microscopy techniques used in this study were environmental scanning electron microscopy (ESEM), transmission electron microscopy (TEM), scanning transmission electron microscopy (STEM) and energy dispersive X-ray (EDX) analysis. ESEM provided surface images in the subcellular regions of interest, while TEM was used to examine the ultrastructure of protein bodies within a section of corn seed tissue. EDX analysis was used to obtain data on the element composition of cell contents (clusters of protein bodies) in bulk specimens viewed with ESEM, and the element composition of electron-dense inclusions called globoids was obtained from sections viewed in the STEM mode.

All electron microscopies make use of the interaction of an electron beam with the specimen. As shown in Figure 3, the interactions between the electron beam and the specimen may produce: back-scattered primary electrons, secondary electrons which emit from or near the specimen surface, absorbed electrons which transfer the energy to heat and light, transmitted electrons which may penetrate the specimen without direction

change or be scattered at varied angles, and X-rays. The release of characteristic X-rays is the basis of X-ray microanalysis (Chandler, 1977).

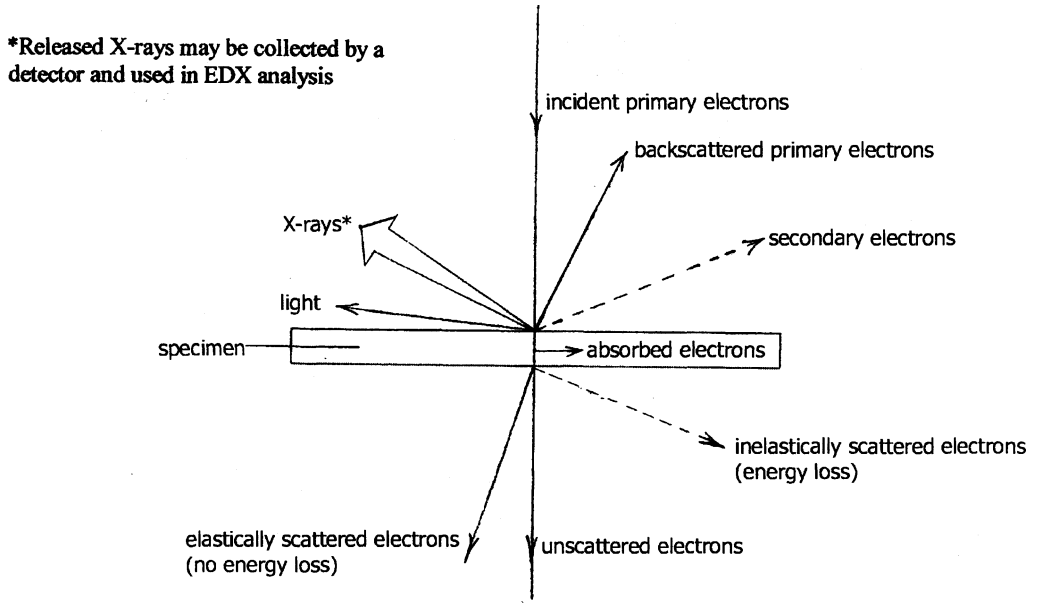

Figure 3. The electron-specimen interaction (Adapted from Chandler, 1977)

Environmental scanning electron microscopy (ESEM)

The scanning electron microscopy (SEM), which came into commercial use in the mid-1960's (Robert Johnson Associates, 1996), can produce a three-dimensional image of the sample surface (Meek, 1976). Conventional SEM (CSEM), has some advantages over many other microscopies, namely good resolution and immense depth of field. It also allows study of relatively large-sized specimens and may have a short sample preparation time, compared to specimen preparation for transmission electron microscopy (TEM) (Meek, 1976).

All SEM's include: (1) an electron gun and an electron column, which produces the electron beam, (2) a sample chamber where the electron beam interacts with the sample, (3) detectors which collect various signals coming from the interaction between the electron beam and the sample, (4) and a viewing system to build up an image from the signals (Robert Johnson Associates, 1996). When the electron beam scans the specimen surface repeatedly and continuously in a raster pattern, as is seen in a television set, a picture of the surface is produced on the face of the display tube (Hayat, 1978).

In SEM, secondary electrons are generally used rather than back-scattered primary electrons. The back-scattered primary electrons have high energy. Secondary electrons, which are generated by ionization of the specimen atoms by the incident primary electrons, have low energy (Meek, 1976). Because they have low energy they are only released at or very close to the surface and thus provide an excellent signal for surface imaging. When the electron beam strikes the sample surface, any variations in the specimen, such as surface topography, sample density, and sample thickness, determine the signal reaching the detector. Thus, a picture of the specimen surface is built up (Hayat, 1978). Although SEM offers good performance, its use is limited by the requirements of needing specimens that can tolerate a high vacuum and the need to have electrically conductive samples. However, biological samples are poorly vacuum tolerant and non-conductive. Since most biological samples routinely are dehydrated and coated with a thin layer of metal prior to CSEM examination, a question as to what the sample looks like in its natural state arises.

ESEM differs from all CSEM's in that ESEM uses multiple pressure limiting apertures, which allow the use of a relatively low vacuum sample chamber (Robert Johnson Associates, 1996). This aperture and vacuum pumping system maintains a high vacuum in the electron column while allowing pressure up to 50 Torr in the sample chamber. Wet, dirty and oily samples can be examined without sample preparation. Since most biological specimens are non-conductive and hydrated, ESEM offers the opportunity of observing them in their natural states, thereby eliminating the possibility of artifacts due to fixation, dehydration and coating (Robert Johnson Associates, 1996).

Transmission electron microscopy (TEM) and scanning transmission electron microscopy (STEM)

The TEM makes use of transmitted electrons from the interaction of electrons and the specimen to form a magnified image on the screen or photographic films (Meek, 1976). STEM combines the features of both the SEM and the TEM. The STEM is same as the TEM in that electrons are transmitted through a very thin section. It is similar to the SEM in that a small electron probe is rastered over an area of the specimen (Hayat, 1978). In the STEM, an electron probe spot of fine size is scanned across a specimen section. The transmitted electrons are captured by a detector beneath the specimen (Meek, 1976). As the fine probe scans across the specimen, the signal reaching the detector reflects the variation of the mass and thickness of the specimen. Then, the electrical current coming from the detector is amplified and modulates the brightness of a display spot on a cathode ray tube (CRT). The display spot is scanned synchronously with the probe spot. In this

way, STEM image is produced (Hayat, 1978). In this study TEM images were recorded on film whereas STEM images were used to locate sample areas for EDX analysis.

Energy dispersive X-ray (EDX) analysis

With X-ray microanalysis, it is possible to determine the presence and relative amounts of elements in selected areas of tissues. The principle behind X-ray microanalysis is stated as follows. An atom of each element has a certain number of electrons. X-ray analysis is based on the fact that atoms in the specimen, when hit by high-energy electrons from an external source, produce X-rays characteristic of those atoms (Chandler, 1977). Therefore, emitted X-rays carry useful information about the element composition of the sample under investigation (Chandler, 1977).

When the atoms in a specimen are bombarded by a high-energy electron beam, the energy carried by these electrons is partly transferred to the atoms of specimen, potentially ejecting inner shell electrons from the atoms (Chandler, 1977). Such an atom is in an excited state and is unstable until an electron from an outer shell with a higher energy fills in the vacancy of the missing inner shell electron. This occurs very quickly, in less than

10^{-15} seconds (Russ, 1972). The X-ray given off during this inter-orbital transition has the energy difference between the two shells (Chandler, 1977). An electron from a more outer shell with an even higher energy may fall to fill this new vacancy, thereby creating several possible electron transitions, each giving rise to a characteristic X-ray emission (Chandler, 1977).

EDX analysis system utilizes a solid state detector, which enables detection and display of the energies of X-rays leaving the specimen, thereby allowing the simultaneous analysis of all measurable elements present in the specimen (Chandler, 1977). Traditionally, a silicon semi-conductor partly diffused with a lithium layer is used. When using a beryllium window on the detector, EDX analysis is limited to detecting elements of atomic number 11 (Na) and heavier (Chandler, 1977). With window-less or thin-window detectors, elements with even lower atomic number can be detected (Lott, 1984). EDX analysis can identify the kinds of elements present and their relative abundances within the sample. It thus allows the examiner to make assumption as to probable types of compound in the sample, but it cannot be used to directly identify the compounds.

When an X-ray system is combined with an ESEM, it is called ESEM-EDX analysis. Since ESEM samples are not fixed, ESEM-EDX analysis provides a control against the possible loss of elements from samples prepared by other procedures. When an X-ray system is combined with a STEM, it is called STEM-EDX analysis. A fine beam of high energy electron is directed at a small region of a sample, thereby allowing high precision in EDX analysis (Chandler, 1977). STEM-EDX analysis provides a powerful and convenient tool for analyzing the elemental composition in a semi-thin specimen (i. e. ~1.5 μm thick section in this study). Since globoids are naturally electron dense under STEM, they are good subjects for EDX analysis due to their density and also since they are easy to locate (Lott, 1984). Previous EDX studies (Lott, 1981; Lott *et al.*, 1995) indicate that P, K, and Mg are generally present in globoids and occasionally other elements such as Ca, Mn, Zn, Fe and Ba are found. The composition of elements in

globoids varies with species, organ, tissue type, cell type and location within one cell type as well (Lott *et al.*, 1995).

The number of X-ray counts in any given peak is proportional to the mass of atoms for that element in the area of the specimen bombarded by electrons. The total number of counts in a peak includes a background coming from white-radiation (continuum). The background is not uniform for all X-ray energies. The white-radiation occurs when the primary electron beam interacts with the nucleus of an atom (Chandler, 1977). It is not characteristic for individual elements (Chandler, 1977). In order to get the net counts for a given element, background X-ray counts are subtracted from the total counts in the peak plus background corresponding to that element. Previous studies indicated that using peak-to-background (P/B) ratios, instead of the gross peak values, may produce more useful results since it helps to compensate for variations of sample thickness and density as well as helping to minimize the effects of uneven specimen surface topography on X-ray collection (Lott *et al.*, 1978; Ockenden and Lott, 1991). P/B ratios are defined as the number of counts above the background for a peak divided by the number of background counts (Ockenden and Lott, 1991).

Several factors should be taken into account when P/B ratios are used to determine the element composition. (1) Element P/B ratios are more useful and convenient for comparing globoid composition than visual peak heights of elements, since data from numerous spectra can be consolidated and differences can be evaluated statistically. (2) In EDX analysis Mg is underestimated and K is overestimated compared to P (Russ, 1972). These P/B ratios are also dependent on the electron microscope used,

the operating conditions and the method used to calculate peak and background numbers, and thus dependent on the entire system used to collect X-rays. For a given microscope, operating conditions such as accelerating voltage, aperture, spot size, tilt and detector distance were kept constant for all analyzes used in this study. Thus, P/B ratios should not be considered to be quantitative measures of element concentrations inside a globoid. (3) P/B ratios may be used to provide information about the element composition of the sample, but cannot tell the examiner exactly what kind of compound is present in that sample. (4) Since a background modeling procedure was used for background subtraction, very small positive or negative values occurred when there was no element present.

The low-water-content procedure

Conventional aqueous TEM preparation procedures have been shown to cause major loss of soluble phytate in plant tissue samples (Lott *et al.*, 1984). The low-water-content procedure used in this study was designed to retain phytate in place and minimize the element loss due to extraction (Lott *et al.*, 1984). It involves the application of 85% ethanol solution in the initial step, which allows the dry seed tissues to swell a little. This swelling facilitates resin infiltration in a later step. The previous studies (Lott *et al.*, 1984) showed that phytate, including water-soluble Na-phytate, was virtually insoluble in 80-90% ethanol. Although it may result in some loss of other compounds due to solubilization, it greatly reduces the extraction of phytate compared to aqueous fixation procedures.

Light microscopy of monitor sections

In order to monitor section quality for STEM-EDX analysis, light microscopy was used to provide useful low magnification information. It allows a quick quality check so that poorly processed sections (such as the ones with deep knife marks or chatter) may be discarded. Under the light microscope, it is also easier and faster to locate the specific areas of interest in the section. Before the sections are put on the grids, a monitor section was produced by cutting a 1.5 μm section with a microtome, mounting it on a glass slide and staining it with Toluidine Blue O (Spence, 2001). Toluidine Blue O is a metachromatic stain, due to the fact that it imparts different colors to different cellular structures (Spence, 2001). Toluidine Blue O stains phytate-rich globoids a red color while the rest of the protein body is stained blue (Fulcher *et al.*, 1981). In this way, globoids may be distinguished.

Objectives

--To examine the possible differences in the ultrastructure between protein bodies of wild-type and *lpa*1-1 mutant corn grain tissues by using ESEM image technology.

--To illustrate possible element composition differences of rastered areas of cell contents between unfixed wild-type and *lpa*1-1 mutant samples by using ESEM-EDX analysis.

--To test whether the low-water-content specimen preparation procedure caused major element extraction in the case of *lpa*1-1 mutant corn grain tissues by comparing ESEM-EDX spectra from unfixed samples with STEM-EDX spectra from fixed and embedded samples within a given selected region.

--To illustrate whether there was any element shift to starchy endosperm cells in

*lpa*1-1 mutant grains by using ESEM-EDX analysis.

--To study the element composition of the phytate-containing inclusions at the subcellular level by using STEM-EDX analysis, and to provide the semi-quantitative P/B ratio data for P, K, Mg, Ca, Zn and Fe within the scutellum and aleurone layer globoids.

--To examine by TEM whether the *lpa*1-1 mutations have altered structure and distribution of globoids within the scutellum and aleurone layer cells.

Materials and Methods

Environmental scanning electron microscopy (ESEM)

(1) Sample preparation

Normal appearing and undamaged grains were selected and six grains from both WT and *lpa*1-1 mutants were cut longitudinally through the center of embryo so that mid-grain scutellum, aleurone layer and starchy endosperm were exposed for ESEM examination. A file was used to flatten the other side of the grain so that the specimen could be mounted parallel to the surface of specimen stubs. The specimens were attached to aluminum stubs via double-sided sticky tape with the cut surface up.

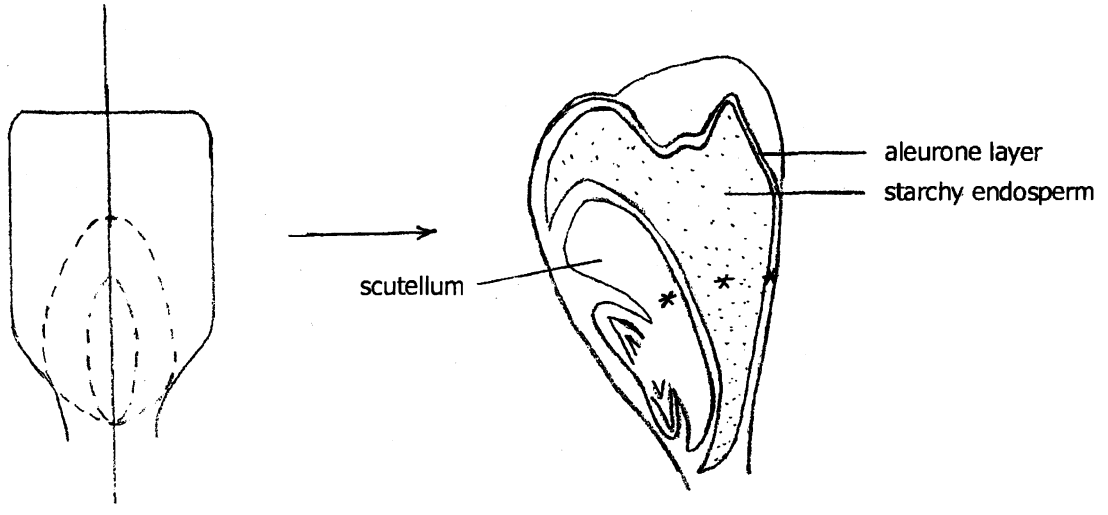

Figure 4. Diagram showing a median longitudinal section of a corn grain. Stars represent the locations where the ESEM images and ESEM-EDX spectra were collected.

(2) ESEM examination

The samples mounted on aluminum stubs were put into the sample chamber and viewed in an ElectroScan 2020 (ElectroScan Corporation, Wilmington, MA) using an accelerating voltage of 20kV. Four samples from each grain type were examined in the scutellum, aleurone layer, and starchy endosperm. The operating conditions of ESEM, such as working distance, pressure etc., were kept constant for all the samples. Micrographs were taken at set magnifications (i.e. 2000 ×, 3500 ×) to facilitate the structural comparisons.

Scanning transmission electron microscopy (STEM) and transmission electron microscopy (TEM)

(1) Sample preparation

(i) Dissection

For each of wild type and *lpa*1-1 mutant, 12 normal appearing and undamaged grains were soaked in 90% ethanol overnight. With the help of stainless steel chisel and forceps, each grain was separated into embryo and the rest-of-grain fractions. Then, the scutellum was dissected from the embryonic axis with care. The aleurone layer with its adhering testa and pericarp was cut away from the rest-of-grain portion using a razor blade. As much starchy endosperm as possible was removed from the aleurone layer and adhering testa and pericarp.

(ii) The low-water-content specimen preparation procedure

After dissected grain parts were obtained, the middle portions of scutellum and the aleurone-testa-pericarp layer were selected and cut into $1mm^3$ pieces, respectively,

and then put into separate labeled plastic vials. All samples then were prepared using the low-water-content procedure of Lott *et al.* (1984).

The low-water-content procedure was carried out as follows:

(a) fixed in 85% ethanol for 24 h at room temperature

(b) dehydrated in 100% ethanol for 24 h at room temperature

(c) dehydrated in propylene oxide for another 12-24 h at room temperature

(d) infiltrated with Spurr's resin using the following series:

propylene oxide: resin---3:1 24 h on rotator

propylene oxide: resin---2:1 24 h on rotator

propylene oxide: resin---1:1 24 h on rotator

propylene oxide: resin---1:2 24 h on rotator

propylene oxide: resin---1:3 24 h on rotator

propylene oxide: resin---0:1 24 h on rotator (100% Spurr's)

propylene oxide: resin---0:1 24 h on rotator (100% Spurr's)

(e) embedded in 100% Spurr's resin and polymerized at 70°C for 8 h

For each grain type, eight moulds were used to embed each kind of grain part from 8 individual grains. The total blocks embedded were 32 for both WT and *lpa*1-1 mutant samples.

(iii) Sectioning

All sections, about 1.5 μm thick, were cut dry using a glass knife and a Reichet OmU2 ultramicrotome. A monitor section was produced by mounting a section on a glass slide and staining it with Toluidine Blue O. The monitor section was viewed under the

light microscope prior to STEM and TEM examination. The sections were picked up from the edge of glass knife with an eyelash and transferred to Formvar-carbon-coated 100 mesh copper grids. A drop of 100% ethanol was used to flatten the sections on the grids.

(2) STEM and TEM examination

The grids with sections were placed in the carbon holder and inserted into a TEM. Sections were studied for ultrastructural features using a JEOL-1200 EX-II TEMSCAN microscope (JEOL, Tokyo) operating at 80kV. STEM images were used to locate specific areas within the sections for EDX analysis. To obtain TEM micrographs of relatively thick sections, an accelerating voltage of 120 kV was used. Micrographs were taken to illustrate the nature of the globoids in the scutellum and aleurone layer cells of each grain type. TEM micrographs were taken at the same magnification (4000 ×) to facilitate comparisons between WT and *lpa*1-1 mutant samples.

Energy Dispersive X-ray (EDX) Analysis

(1) ESEM-EDX analysis

Elements present in a selected cellular structure were measured with a PGT IMIX energy dispersive X-ray analysis system (Princeton Gamma Tech., Princeton, New Jersey) attached to an ElectroScan 2020 ESEM operating at 20 kV. The operating conditions such as detector distance, tilt, aperture, 60s count time, accelerating voltage etc., remained constant for all analyzes. Mid-grain region scutellum ground meristem (parenchyma) cells, starchy endosperm cells and aleurone layer cells were studied using ESEM-EDX analysis. ESEM-EDX analyses may provide an unfixed control for

comparison with STEM-EDX data obtained from the fixed samples. The same batch of samples and the same number of samples as were used for ESEM structural examination were used for X-ray analysis. For each of the 4 grains studied, three analyses, each using a ½ raster area at 1000× magnification, were carried out over cell content regions of each of scutellum, aleurone layer and starchy endosperm.

(2) STEM-EDX analysis

Naturally electron-dense inclusions (globoids) were spot analyzed with a PGT IMIX EDX analysis systems (Princeton Gamma Tech., Princeton, New Jersey) attached to a JEOL 1200 EX-II TEMSCAN operating at 80kV. For each grain, 15-17 spectra were collected from different globoids in different cells within both the scutellum and the aleurone layer. Globoids of various size and type (discrete or clustered) were included in the analyses. More than 80 spectra were collected in either of scutellum and aleurone layer cells, from each of wild type and *lpa*1-1 mutants. A total of at least 320 spectra were collected and saved in the computer.

X-ray counts for all the spectra were collected by integrating peaks at the window widths: Mg, 1153.7-1354.3 eV; P, 1905.3-2120.7 eV; K, 3193.7-3432.3 eV; Ca, 3568.6-3813.4 eV; Mn, 5758.5-6037.5 eV; Fe, 6259.9-6546.1 eV; Cu, 7891.7-8200.3 eV and Zn, 8478.9-8795.1 eV (Beecroft and Lott, 1996). In order to produce the best fit background line for all elements, points were connected at the following eV values: 510, 660, 814, 1453, 1730, 2500, 2800, 3020, 4200, 5400, 8400, 9400, and 11000 eV. Background subtraction was carried out for each element in each spectrum by subtracting the number of counts in the background from the total number of counts in the peak plus background

for each element. A useful format to express elemental composition is in the form of peak-to-background (P/B) ratios, which have been defined as the number of counts above the background for a peak divided by the number of background counts under that peak (Ockenden and Lott, 1991).

Due to peak overlaps, correction factors were used to calculate the actual Ca, Fe and Zn counts in each spectrum (West and Lott, 1993). Correction factors were used after background subtraction. The K_β peak of K overlaps the K_α peak of Ca and therefore a correction factor of 8.80% of the total X-ray counts for the K K_α peak was subtracted from the total counts in the Ca window to give the actual counts for Ca. Similarly, the K_β peak of Mn overlaps the K_α peak of Fe and thus a correction factor of 11.60% of the total X-ray counts for Mn K_α peak was subtracted from the total counts in the Fe window to give a corrected Fe value. Finally, the K_β peak of Cu overlaps the K_α peak of Zn and thus 2.00% of the net Cu K_α counts was subtracted from the total Zn counts to give a corrected Zn value.

(3) Statistical analysis

The mean P/B ratios were calculated for each element from wild type and *lpa*1-1 samples respectively. By using MINITAB's two-sample T-test, the statistical significance was determined at $P>0.05$ between wild type and *lpa*1-1 samples (Zar, 1984).

Results

(1) ESEM and TEM images

(i) ESEM images

The scutellum ground meristem cells of corn grains contained protein bodies with globoids inside. In both wild-type and *lpa*1-1 mutant samples, globoids within scutellum cells were spherical inclusions that appeared light colored when viewed with ESEM (Fig. 5a to 5d). The globoids in the *lpa*1-1 mutants usually were smaller in diameter and more numerous than in the WT (Fig. 5b and 5d compared to Fig. 5a and 5c), and in most cases they formed clusters inside the protein bodies while WT scutellum globoids tended to be larger and more discrete (Fig. 5d compared to Fig. 5c). Globoids at least 1.5 μm in diameter were common in the WT scutella (Fig. 5c) and infrequent in the *lpa*1-1 scutella (Fig. 5d). Both WT and *lpa*1-1 mutants had globoids of variable sizes in their scutella.

The aleurone layer of WT corn grains was generally one cell thick and had thick cell walls. Both WT and *lpa*1-1 mutant corn aleurone layer cells contained many protein bodies with globoids. The diameter of aleurone globoids in WT samples, on average, was larger than that in *lpa*1-1 samples (Fig. 5e compared to Fig. 5f). Globoids that were not spherical were found in the *lpa*1-1 aleurone layer (Fig. 5f). Moreover, when compared to scutellum globoids, aleurone globoids of WT had a reduced size (Fig. 5e compared to Fig. 5a).

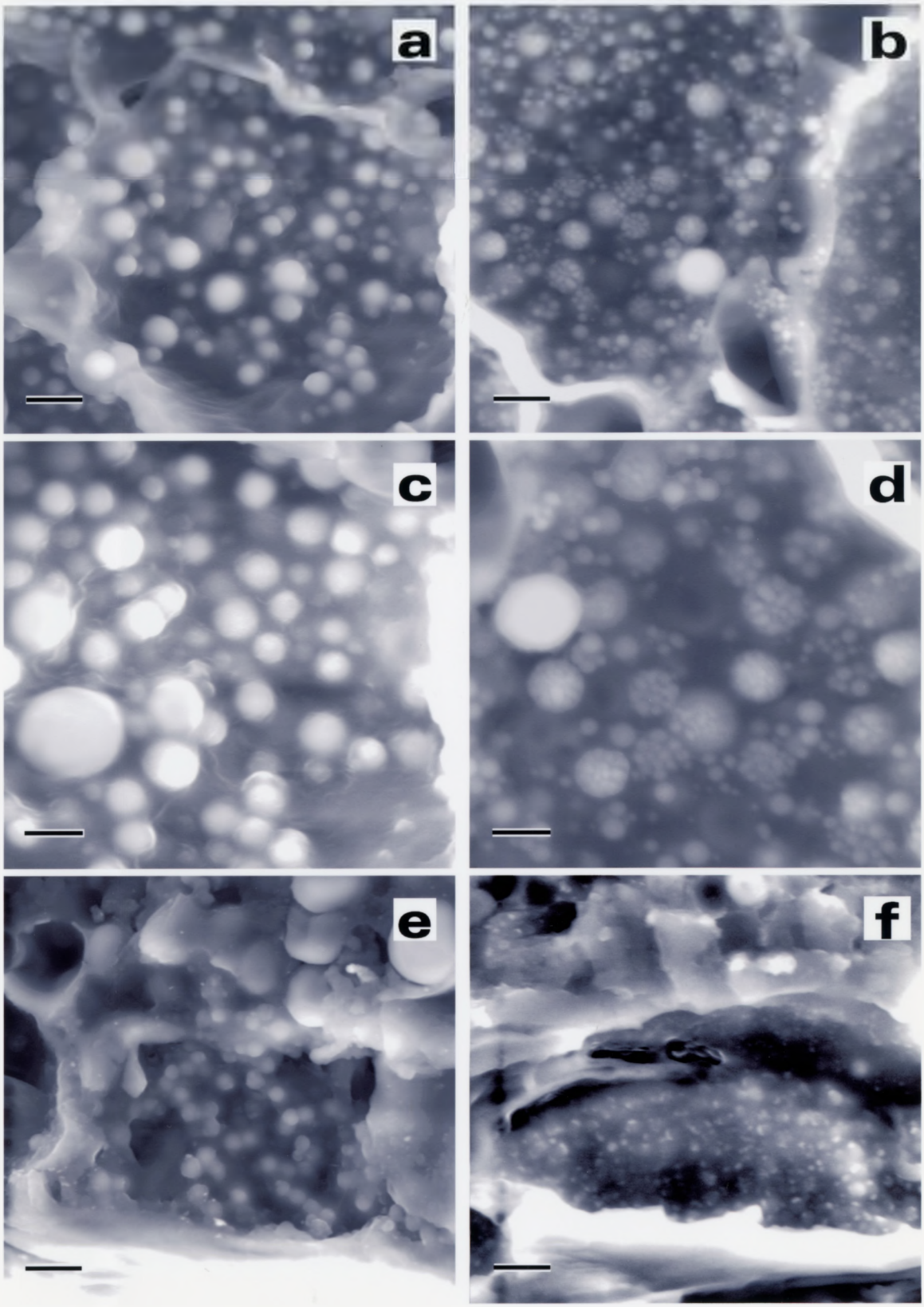
a
b
c
d
e
f

Figure 5. ESEM images of cut surfaces of mid-grain scutellum and aleurone layer from WT (Figs. 5a, 5c and 5e on the left side) and *lpa*1-1 (Figs. 5b, 5d and 5f on the right side) mature corn grains, showing globoids inside cells. Figs. 5a-5d are from scutellum cells; Figs. 5e-5f are from aleurone layer cells. In Figs. 5a and 5b and 5e and 5f, scale bars = 5 μm; In Figs. 5c and 5d, scale bars = 3μm.

(ii) TEM micrographs using semi-thin sections

WT scutellum cells had globoids of variable sizes but often they were 1.5-2 μm in diameter (Fig. 6a). In contrast, *lpa*1-1 scutellum cells had more numerous and smaller (usually < 0.8 μm) globoids, which tended to aggregate in clusters inside protein bodies (Fig. 6b). TEM micrographs of scutellum globoids matched the ESEM images in that the electron-dense globoids seen with TEM were similar to the white intracellular particles seen with ESEM. WT aleurone cells generally contained globoids with smaller size than WT scutellum globoids, but both were present as discrete, spherical particles (Fig. 6c compared to 6a). However, compared to WT aleurone cells, *lpa*1-1 aleurone cells contained smaller globoids, many with atypical, non-spherical shape (Fig. 6d compared to 6c).

(2) EDX analysis

(i) ESEM-EDX spectra

Square raster areas of cell contents from scutellum ground meristem (Figs. 7a and 7b), aleurone layer (Figs. 7c and 7d) and starchy endosperm (Figs. 7e and 7f) were analyzed with ESEM-EDX to study the element composition without any chemical treatment (i.e. fixation, dehydration or embedding). Carbon and oxygen peaks were found in all three regions in both WT and *lpa*1-1 mutants.

In the scutellum and aleurone layer cells of both the WT and the *lpa*1-1 mutant, in addition to C and O, the main nutrients detectable were P, K, Mg and S. Of these four elements, P peak was highest followed by K, Mg and lastly S. In both the scutellum and

aleurone layer cells, about 15% and 20% spectra revealed trace amounts of Ca and Fe, respectively. Traces of Cl were more frequent in the cell contents of aleurone layer cells than those of scutellum cells. The scutellum and aleurone layer cells contained similar kinds of elements for both WT and *lpa*1-1 mutant, but the concentration of the elements present in the *lpa*1-1 mutant samples was lower than WT samples. At a standardized vertical scale of 1600 for scutellum samples (Fig. 7a compared to 7b) and 800 for aleurone layer samples (Fig. 7c compared to 7d), respectively, element peak heights in the *lpa*1-1 samples were lower than those in the WT counterparts.

EDX spectra of starchy endosperm samples revealed high peaks of C and O and sometimes a very small peak of S. In most cases P, K, Mg, Ca, and Cl were undetectable in the cell contents of starchy endosperm cells.

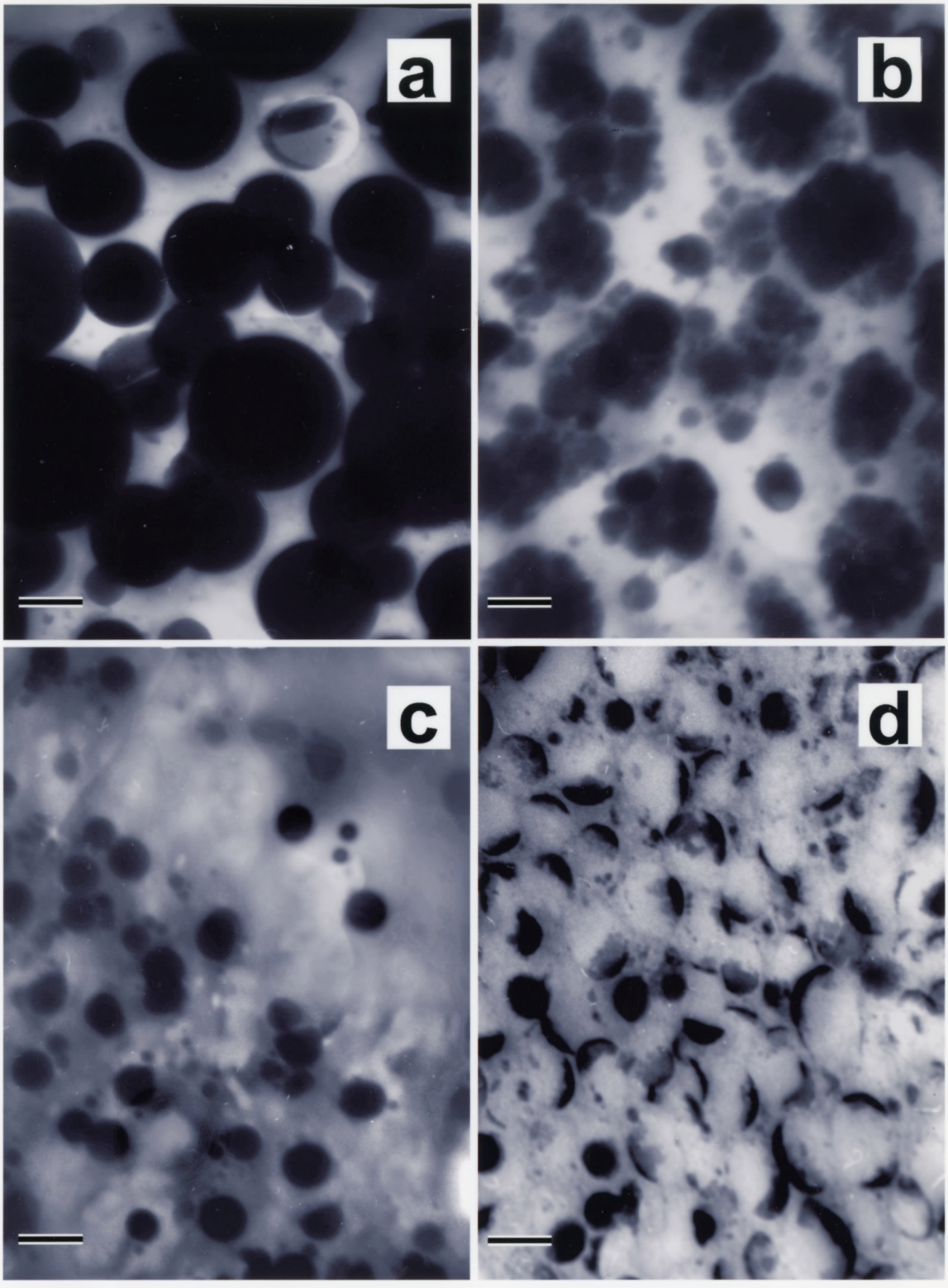
a
b
c
d

Figure 6. TEM micrographs of about 1-1.5 μm thick sections of scutellum cells and aleurone layer cells from WT and *lpa*1-1 corn grains. All dark areas are due to natural electron density since no electron-dense stains were added during the low-water-content sample preparation procedure. Dark particles seen with TEM are globoids. Fig. 6a, WT scutellum; Fig. 6b, *lpa*1-1 scutellum; Fig. 6c, WT aleurone layer; Fig. 6d, *lpa*1-1 aleurone layer. Scale bar = 1 μm.

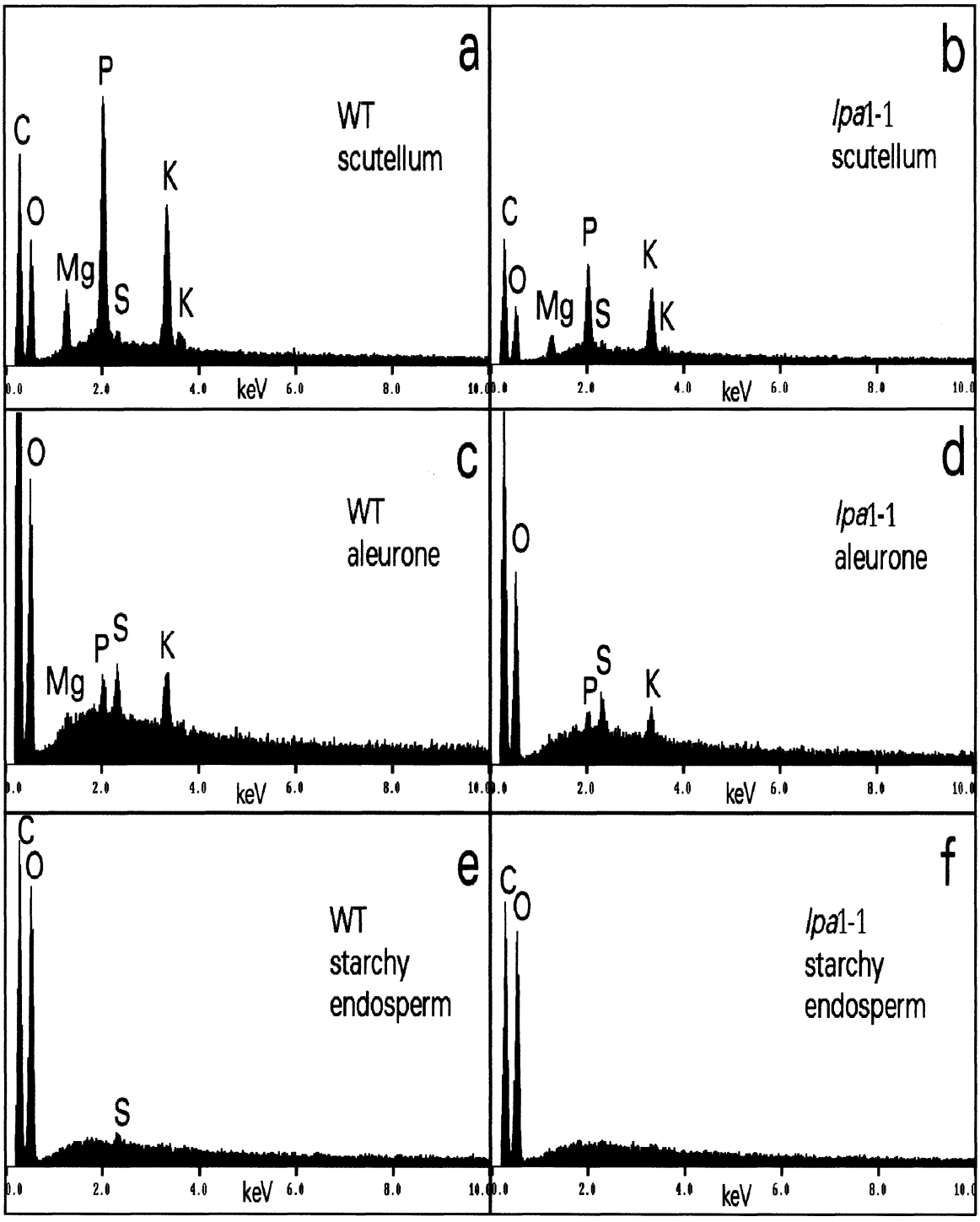
a
WT
scutellum
C
O
Mg
P
S
K
K
keV
b
lpa1-1
scutellum
C
O
Mg
P
S
K
K
keV
c
WT
aleurone
O
Mg
P
S
K
keV
d
lpa1-1
aleurone
O
P
S
K
keV
e
WT
starchy
endosperm
C
O
S
keV
f
lpa1-1
starchy
endosperm
C
O
keV

Figure 7. Typical ESEM-EDX analysis spectra on square rastered areas of cell contents from cut WT and *lpa*1-1 dry corn grains. Spectra on the left side (Figs. 7a, 7c and 7e) are from WT and spectra on the right side (Figs. 7b, 7d and 7f) are from *lpa*1-1 corn grains. Figs. 7a and 7b are from the cell content areas of scutella; Figs.7c and 7d are from the cell content areas of aleurone layers; Figs. 7e and 7f are from the cell content areas of starchy endosperms. Carbon and O peaks were present due to the use of a thin film EDX detector. Markers on the horizontal axes are the X-ray energy values (0.0, 2.0, 4.0, 6.0, 8.0 and 10.0 keV). The vertical scales were set at a fixed level for a given group, i.e. 1600 for 7a and 7b, 7e and 7f, and 800 for 7c and 7d. The energy lines for each element present are as follows: C (K_α =0.28 keV); O (K_α =0.52 keV); Mg (K_α =1.25 keV); P (K_α =2.02 keV); S (K_α =2.31 keV); K (K_α =3.31 keV, K_β = 3.59 keV); Ca (K_α =3.69 keV, K_β = 4.01 keV); Fe (K_α =6.40 keV, K_β = 7.10 keV); Zn (K_α =8.63 keV, K_β = 9.57 keV).

(ii) STEM-EDX spectra

Naturally electron-dense inclusions, namely globoids, were spot-analyzed with an EDX analysis system under STEM mode. STEM-EDX analysis showed that for both WT and *lpa*1-1, globoids within scutellum and aleurone layer cells contained P, K, and Mg in major amounts. Of these three elements, the P peak was highest, followed by the K peak, and the Mg peak. In aleurone layer globoids, Ca was frequently found and in some cases traces of Fe and Zn were present. The Cl present in the STEM-EDX spectra of sectioned samples likely originated from chlorine in the Spurr's resin used for embedding. S was absent in the STEM-EDX spectra of both scutellum and aleurone globoids.

From the STEM-EDX spectra (standardized vertical scale =7000), it was obvious that the peak heights of P, K and Mg in WT scutellum globoids were taller than those in *lpa*1-1 counterparts, respectively (compare Fig. 8a to 8b). Each of the peaks of P, K, and Mg, was higher in the scutellum globoids than in the aleurone globoids, respectively, for both WT and *lpa*1-1 (compare Fig. 8a to 8c; compare Fig. 8b to 8d). Furthermore, representative STEM-EDX spectra illustrated that major elements P, K, and Mg were in approximately similar peak height proportions to those studied with ESEM-EDX.

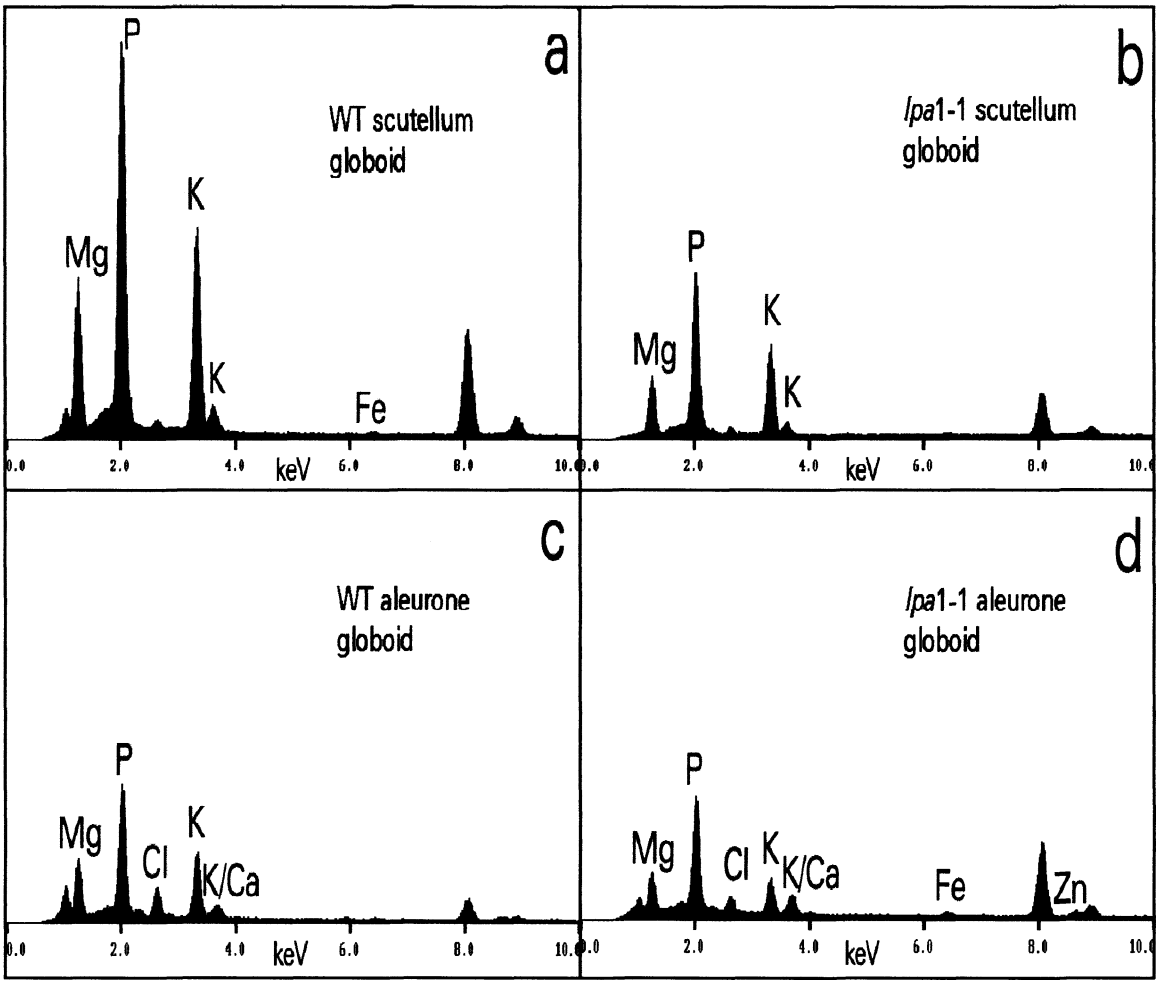
a
WT scutellum
globoid
P
K
Mg
K
Fe
keV
b
*Ipa*1-1 scutellum
globoid
P
K
Mg
K
keV
c
WT aleurone
globoid
P
Mg
K
Cl
K/Ca
keV
d
*Ipa*1-1 aleurone
globoid
P
Mg
Cl
K
K/Ca
Fe
Zn
keV

Figure 8. Typical STEM-EDX analysis spectra of electron-dense globoids in thick sections from scutellum (Figs. 8a and 8b) and aleurone layer (Figs. 8c and 8d) of WT (Figs. 8a and 8c on the left side) and *lpa*1-1 (Figs. 8b and 8d on the right side) corn grains. The beryllium window used in the STEM-EDX system eliminates the C and O peaks in the spectra which are seen in ESEM-EDX spectra. Markers on the horizontal axes are the X-ray energy values (0.0, 2.0, 4.0, 6.0, 8.0 and 10.0 keV). The vertical scales were set at a standardized level of 7000. Note that the peaks at 8.04 and 8.91 keV in the spectra are the Cu K_α and K_β peaks, respectively, from the copper grids used for holding the sections. Chlorine peaks in the spectra likely originated from the Cl in Spurr's resin used for specimen preparation. The energy lines for each element illustrated are as follows: Mg (K_α =1.25 keV); P (K_α =2.02 keV); Cl (K_α =2.62 keV); K (K_α =3.31 keV, K_β = 3.59 keV); Ca (K_α =3.69 keV, K_β = 4.01 keV); Fe (K_α =6.40 keV, K_β = 7.10 keV); Zn (K_α =8.63 keV, K_β = 9.57 keV).

(iii) Peak-to-background (P/B) ratios of various elements in globoids within scutellum and aleurone layer cells

Semi-quantitative data for globoids within the scutellum and aleurone layer cell sections from both grain types were presented as peak-to-background (P/B) ratios in Tables 6 and 7. Data showed that P, K, and Mg were present in major amounts in globoids, while Ca, Fe, and Zn were found in low to trace amounts in globoids. Elements Mn and S were not detectable. In scutellum globoids, P and K levels were lower in *lpa*1-1 than WT whereas the Fe level was higher. No significant differences were found in Mg, Ca and Zn levels between *lpa*1-1 and WT scutellum globoids. In aleurone layer globoids, P and Mg levels were lower in *lpa*1-1 than WT while Ca and Fe levels were higher. Potassium and Zn levels were not significantly different between *lpa*1-1 and WT aleurone globoids.

Table 8 compared the P/B ratios of globoids within the two selected regions examined (scutellum and aleurone layer) and demonstrated whether aleurone globoids were significantly different from scutellum globoids for a given element in the same grain type. It was found that for both WT and *lpa*1-1, aleurone globoids contained lower levels of major elements P, K, and Mg, and higher levels of minor elements Ca, Fe, and Zn, than scutellum globoids. Significant differences at $P>0.05$ were found throughout the comparison of element levels between the scutellum and aleurone globoids for a given grain type (WT or *lpa*1-1). Among various elements, the biggest difference was found in Ca level when the comparison was made, where aleurone globoids contained

12 and 15 times higher Ca level than scutellum globoids for WT and *lpa*1-1, respectively.

Table 6. Mean (±SD) peak-to-background (P/B) ratios of elements in globoids within scutellum cells of the wild-type and *lpa*1-1 mutant corn grains*

Grain type	P	K	Mg	Ca	Fe	Zn
WT	10.10 ±1.72a	14.44 ±2.94a	7.29 ±1.56a	0.15 ±0.28a	0.14 ±0.12a	0.10 ±0.16a
***lpa*1-1**	9.30 ±1.62b	12.82 ±2.81b	7.28 ±1.79a	0.16 ±0.31a	0.29 ±0.16b	0.11 ±0.13a

* Values in the same column followed by the same letter are not significantly different at P>0.05. Each mean (±SD) was calculated using 82 values.

Table 7. Mean (±SD) peak-to-background (P/B) ratios of elements in globoids within aleurone layer cells of the wild-type and *lpa*1-1 mutant corn grains*

Grain type	P	K	Mg	Ca	Fe	Zn
WT	5.96 ±2.31a	4.83 ±2.65a	4.85 ±3.21a	1.99 ±2.09a	0.43 ±0.34a	0.54 ±0.67a
***lpa*1-1**	5.37 ±2.01b	4.98 ±2.82a	2.76 ±1.80b	2.68 ±2.10b	0.99 ±0.89b	0.39 ±0.34a

* Values in the same column followed by the same letter are not significantly different at P>0.05. Each mean (±SD) was calculated using 82 values.

Table 8. Element P/B ratios in aleurone globoids compared to the P/B ratios in scutellum globoids from the same grain type

Grain Type	P	K	Mg	Ca	Fe	Zn
WT	L[1] (41.0%)	L (66.6%)	L (33.5%)	H[2] (1226.7%)	H (207.1%)	H (440.0%)
***lpa*1-1**	L (42.3%)	L (61.2%)	L (62.1%)	H (1575.0%)	H (241.4%)	H (254.5%)

1. L means that P/B ratios in the aleurone globoids were lower than those in the scutellum globoids, where significant differences at P>0.05 were found.

2. H means that P/B ratios in the aleurone globoids were higher than those in the scutellum globoids, where significant differences at P>0.05 were found.

Discussion

The low-water-content preparation procedure was designed to retain water-soluble phytate in tissue (Lott *et al.*, 1984). The first step in the low-water-content preparation procedure involved immersion of the tissue in 85% ethanol, in which water-soluble phytates such as Na-phytate, are known to be insoluble (Lott *et al.*, 1984). The 15% water content introduced in this step allowed the tissue to expand and thus facilitated the infiltration of resin in a later step. The improved infiltration is critical to the quality of sectioning. Thin sectioning on a water-filled microtome boat was not used here due to its extraction problems (Skilnyk and Lott, 1992). Instead, semi-thin sections (1.5μm thick) were cut dry on glass knives to minimize the extraction of water-soluble elements. Compared to ultrathin sections, semi-thin sections have the advantage of preventing the shattering of globoids. This is important because globoid shattering may leave holes in the section or electron-dense debris on the section surface and also cause scratches in sections (Lott and Buttrose, 1978). In addition, the semi-thin sectioning may help to keep more globoids intact in sections than the ultrathin sectioning, thus facilitating understanding the structure and arrangement of globoids.

The previous studies with seeds from a number of species indicated that the low-water-content fixation procedure was a suitable procedure prior to STEM-EDX examination (Lott *et al.*, 1984). No evidence to date shows whether it would hold true for *lpa*1-1 mutant corn grains where PA was greatly reduced and Pi was increased. The ESEM-EDX and STEM-EDX studies, which were conducted in parallel, allowed us to

make comparisons of element composition between unfixed *lpa*1-1 samples and the *lpa*1-1 samples which underwent the low-water-content procedure. The fact that STEM-EDX spectra revealed a similar element composition to ESEM-EDX spectra for a given selected region (e. g. scutellum, aleurone layer) of *lpa*1-1, provided evidence that the low-water-content preparation procedure also was satisfactory in treating *lpa*1-1 corn seed tissues since it didn't cause major element extraction or relocalization.

ESEM images gave useful information as to what the protein bodies and globoids looked like in the natural state and TEM provided a means of determining natural electron density. The white spherical inclusions seen under ESEM matched the electron-dense globoids seen with TEM.

In terms of structure, both ESEM and TEM images showed that *lpa*1-1 scutellum globoids were different from WT scutellum globoids in that the former were mostly present in clusters of small ones, whereas the latter were present as discrete and large ones. It was also found that most of the *lpa*1-1 aleurone globoids were of non-spherical shape, whereas WT aleurone globoids were spherical. Given the changes in the structure of both scutellum and aleurone layer globoids in *lpa*1-1 compared to WT, it is clear that the *lpa*1-1 mutation which caused a reduced PA concentration, had an impact on the formation of globoids. A first possible reason for these differences could be the influence on PA biosynthesis, which resulted in fewer PA molecules available for globoid assembly. Greenwood and Bewley (1984) showed that cytoplasmic phytate-containing particles moved to the developing protein bodies for storage. Materials deposited into protein bodies may self-assemble into distinct structural units called globoids. Lott *et al.*

(1994) hypothesized that divalent or trivalent cations like Mg^{++}, Ca^{++}, and/or Fe^{+++}, are able to bind with the negatively charged phosphate groups of neighboring PA molecules. Such cross-linking of PA molecules likely is the key to globoid formation (Lott *et al.* 1994). There are fewer PA molecules present in *lpa*1-1 mutant grains, thus there are fewer negatively-charged sites provided by PA molecules for cations to bind with and fewer linkages between PA molecules and cations. However, in *lpa*1-1 grain tissues the reduction in PA was matched by "molar-equivalent" increases in Pi. Raboy (1998) speculated that higher Pi in *lpa*1-1 corn grains than wild-type corn grains would be mainly sequesterd within protein storage vacuoles (protein bodies) so as not to disturb the normal cellular metabolism. I speculate that Pi may provide negatively-charged sites for cation chelation, thereby contributing, in part, to the globoid formation. Since there are much fewer negatively-charged sites per molecule present in Pi than PA (2:12), it is likely that globoid self-assembly could proceed differently. For example, most *lpa*1-1 aleurone layer globoids appeared crescent shape. TEM micrographs showed that they aggregated along the edge of protein body as curved bits. This phenomenon could be explained if some Pi present within protein bodies was used to form electron-dense regions. A second possible reason for these structural differences could be associated with changing the protein storage vacuole microenvironment such as pH or ion concentration, thus changing globoid packaging. The factors causing globoids to form as spheres in developing seeds are not understood to date. The effects of the *lpa*1-1 mutation on globoid formation may involve more than one factor.

The size of globoids inside cells from a given grain part reflected the PA-P concentration of that grain part on a dry weight basis. I hypothesized that the reduction in PA, which occurred in *lpa*1-1 mutants, would cause either smaller diameter globoids, fewer globoids than WT, or both. My electron microscopic studies illustrated that *lpa*1-1 mutant grains contained more numerous but much smaller diameter globoids in both scutellum and aleurone layer cells than WT. Size is a very important consideration. For example, large globoids with a diameter of 1.0 μm have a volume of 0.524 μm^3 whereas globoids with a diameter of 0.1 μm have a volume of 0.000524 μm^3. It would take a thousand globoids with diameters of 0.1 μm to equal the volume of one particle with a diameter of 1.0 μm (Lott *et al.*, 1995). Thus, the change in globoid diameter is more significant than the change in number of globoids in reflecting the difference in PA-P level.

STEM-EDX analyses of proteinaceous regions lacking globoids showed the presence of S which was likely from certain amino acids in protein inside protein bodies. It seems likely that ESEM-EDX analyses detected P, K, and Mg from globoids and S from the cell contents other than globoids.

No visible peaks of P, K, Mg were present in either the WT or the *lpa*1-1 starchy endosperm. This allowed me to conclude that: (1) the *lpa*1-1 mutation didn't cause any major element shift to the starchy endosperm, and (2) the starchy endosperm was not a site of PA deposition in either WT or *lpa*1-1 mutant corn grains. The results on WT grains was in agreement with the results reported by Yoshida *et al.* (1999) in rice grains. They found that expression of the Ins(3)P_1 synthase gene, which encoded an enzyme

critical to the pathway of $InsP_6$ (PA) synthesis, was absent in rice starchy endosperm. Earlier work suggested that PA synthesis was restricted to the cells where PA was accumulated and stored (Greenwood and Bewley, 1984).

STEM-EDX analysis revealed a higher globoid P level in WT than in *lpa*1-1 for both scutellum and aleurone layer. This is consistent with higher PA-P concentrations in WT than in *lpa*1-1 in both scutellum and the rest-of-grain portions. Two possible reasons account for this consistency: (1) previous studies (O' Dell *et al.*, 1972; Lott, 1980) showed that 80% of grain P was found as PA-P in mature corn grains and that most PA-P was located in the globoids within protein bodies. Studies of the chemical composition of the isolated globoids from dry grains/seeds provided evidence that phytate, the salt of PA, was the major compound in globoids (Lui and Altschul, 1967; Suvorov *et al.*, 1970; Ogawa *et al.*, 1975). Lui and Altschul (1967) reported that about 97.5% of the total P inside cottonseed globoids was organic P, and PA was identified as the only organic phosphorus compound present. Cottonseed globoids contained 60% PA and a total of about 10% of K, Mg and Ca. Studies of castor bean globoids showed that phytate made up 70-80% of their dry weight (Suvorov *et al.*, 1970). PA, together with K and Mg, makes up over 90% of the compounds inside the isolated rice globoids, while other metallic elements like Ca, Fe, Mn were present in small to trace amounts (Ogawa *et al.*, 1975). (2) The comparison of aleurone layer globoid phosphorus P/B ratios between the WT and *lpa*1-1, showed a similar trend to that of the rest-of-grain PA-P concentrations derived from chemical analysis. I conclude that for the *lpa*1-1 corn grain, the aleurone layer is where PA-P was stored in the rest-of-grain portion. This was confirmed by

ESEM-EDX studies, which demonstrated a lack of P within the starchy endosperm of *lpa*1-1.

P/B ratios derived from STEM-EDX analysis, showed that *lpa*1-1 scutellum globoids contained lower K and higher Fe than WT, while Mg, Ca, and Zn remained unchanged. FAAS data showed that embryo K and Ca concentrations were lower and embryo Fe concentration was higher in *lpa*1-1 than in WT, whereas embryo Mg and Zn concentrations of *lpa*1-1 were not significantly different from those of WT. Thus a similar pattern of K decreasing, Fe increasing, and Mg and Zn being constant was found when *lpa*1-1 samples were compared to WT with two different methods. This indicated that the great majority of embryo K, Fe, Mg and Zn is located in scutellum globoids. However, a different pattern was shown in Ca distribution, where scutellum globoid Ca level was constant while embryo Ca concentration dropped in *lpa*1-1 compared to WT. Ca likely was in cellular compartments other than globoids (cytoplasm, cell walls, and nuclei), or located in the embryonic regions other than scutellum ground meristem, for example root-shoot axes. Ca was reported to be stored in globoids in regions where growth occurred first, such as root-shoot axes in squash embryos (Lott *et al.*, 1978). It is believed that more Ca is required for the cells that undergo rapid division and wall formation (Taiz and Zeiger, 1998).

STEM-EDX analysis demonstrated that for both WT and *lpa*1-1 corn grains, the aleurone layer globoids contained lower P/B ratios of P, K, Mg and higher P/B ratios of Ca, Fe, Zn than scutellum globoids. Several factors could account for this phenomenon:

(1) In the context of mineral ion uptake, maybe the aleurone layer cells and/or vacuoles (a cellular compartment to sequester high concentrations of ions) took up more Ca, Fe and Zn and less K and Mg than the scutellum cells and/or vacuoles. It is known that some transporters (located on plasma membrane and/or tonoplast), and pumps (i.e. plasma membrane H^+-ATPase, vacuolar H^+-ATPase) may be involved in the energy-mediated ion transport processes across the plasma membrane and/or tonoplast (Bray *et al.*, 2000). In the case of mature grains, most of the cations (K^+, Mg^{++}, Ca^{++}, Fe^{+++}, Zn^{++}) transported into the protein storage vacuoles may be stored within globoids.

(2) From the aspect of ion counterbalance, the levels of Ca, Zn and Fe rose at the expense of K and Mg. The cations of Ca, Zn and Fe may partly occupy the negatively-charged sites of PA in place of K and Mg.

(3) It is believed that some Ca is required for the production and secretion of α-amylase in the aleurone layer cells during seed germination (Raboy, 1997). The α-amylase enzyme is a Ca-metaloenzyme which binds one mole of Ca per mole of enzyme (Jones *et al.*, 1993). It is possible that a relatively higher Ca level was stored within globoids in the aleurone layer cells of mature corn grains, to ensure sufficient Ca for production of α-amylase during germination and seedling growth. In addition, the smaller sized but more numerous globoids inside aleurone layer cells could promote the release of Ca, P and other cations, as their larger surface areas facilitate access for phytase upon imbibition and germination.

(4) Recent research shows that Zn is a structural component of numerous transcription factors, which affect RNA synthesis and have subsequent influence on protein synthesis (Kochian, 2000). It is known that the aleurone layer is the site specialized to synthesize and secrete hydrolases (i.e. amylase, protease etc.) for degradation of storage starch, protein and other compounds during seedling growth (Ritchie *et al.*, 2000). Possibly more Zn present in the aleurone globoids than scutellum globoids is to ensure sufficient Zn for enzyme protein synthesis upon imbibition.

(5) Since there is no vascular strands between the maternal plant and the endosperm or the embryo, the mineral ions have to move via apoplastic pathways: from the testa to the aleurone layer and from the starchy endosperm to the scutellum. This study showed that scutellum cells got enough K and Mg ions. Since the flux of K^+ and Mg^{++} passed the aleurone layer and then entered the scutellum, the aleurone layer should not be short of a supply of K^+ and Mg^{++}. The possible explanation is that for some reason, the ion uptake mechanisms of corn aleurone layer cells don't favor the absorption of K^+ and Mg^{++}.

It is impossible to isolate the intact aleurone layer from the rest-of-grain fraction in the dry state since a mature corn grain contains only a single layer of aleurone layer cells located between the pericarp/seed coat and starchy endosperm. Even if the procedure of pre-soaking in 90% ethanol solutions is used, it is still almost impossible to get intact aleurone layers. However, the mean dry weight of aleurone layer may be estimated, based on the chemical analysis data previously presented in chapter 2 and electron

microscopical studies in this chapter. I used the amounts of PA-P (mg/grain part) as markers because it is believed that PA represented the majority (>90%) of the compounds inside globoids (Lui and Altschul, 1967; Suvorov *et al.*, 1970; Ogawa *et al.*, 1975). For the wild-type corn grain, the amount of PA-P per scutellum was 0.714 mg while that per rest-of-grain was 0.026 mg. Therefore, the ratio of PA-P amount per rest-of-grain to that per scutellum is 1:27. If all PA-P within the rest-of-grain fractions was stored in the aleurone layer, the ratio of PA-P amount per aleurone layer to that per scutellum is approximately 1:27. Based on electron microscopical structural studies, for example ESEM images, I estimated that the ratio of globoids in an area of aleurone layer cell cytoplasm to that in a similar sized area of scutellum cell cytoplasm to be approximately 1:8. Since the mean scutellum dry weight is known to be 32.50mg for wild-type corn, if aleurone layer and scutellum cell areas had same density of globoids, the calculated aleurone layer weight would be

$(1/27)\times 32.50 = 1.20$ mg. However, aleurone cytoplasm areas have 1/8 of the globoid density of scutellum cytoplasm, the effective aleurone weight would be 8 times greater, which equals to $1.20\times 8 = 9.6$ mg. In addition, I measured the mean dry weight of the rest-of-grain fraction to be 250.4 mg. Therefore, I estimate that, as % of rest-of-grain fraction weight, the aleurone layer occupies 3.8%.

In summary, the electron microscopic studies indicated that the low-water-content preparation procedure is acceptable for preparing *lpa*1-1 corn grain tissues for microscopy. Both scutellum and aleurone layer globoids differed in structure and element composition between WT and *lpa*1-1 samples, which led me to conclude that the *lpa*1-1

mutation had an impact on the formation of globoids. The lower P/B ratios of P, K, and Mg and higher P/B ratios of Ca, Fe, and Zn present in the aleurone globoids than scutellum globoids, may be associated with the different physiological roles that the aleurone layers and scutella have during the grain development and seedling growth. The aleurone layer is speculated to form less than 5% of the rest-of-grain fraction on the weight basis.

Chapter 4
Key findings and future research

Previous research studied element and PA-P concentrations in the wild-type mature corn grains (O'Dell *et al.* 1972). Recent studies have documented whole-grain P and PA-P concentrations in maize *lpa*1-1 and WT grains (Raboy *et al.*, 2000), in rice *lpa*1-1 and WT grains (Larson *et al.*, 2000), and in several barley *lpa* mutants with different PA-P reductions and WT grains (Dorsch *et al.*, 2003). Liu *et al.* (2004) have investigated the distribution of seven mineral elements (P, K, Mg, Ca, Zn, Fe, Mn) and PA-P within different parts of *lpa*1-1 rice grain in comparison to WT.

Key findings

The research reported in this thesis was the first comprehensive research about nutritionally important elements and PA-P concentrations within separated grain parts (the scutellum, root-shoot axis and rest-of-grain fractions) of wild-type and *lpa*1-1 corn grains. It also reported the first studies of the ultrastructure and element composition of phosphorus-rich globoids within *lpa*1-1 scutellum and aleurone layers as compared to closely matching WT counterparts.

The key findings presented here are as follows:

(i) PA-P, located in the WT scutellum, root-shoot axis, and rest-of-grain fractions, as a percentage of whole-grain amounts, were 91.6%, 3.6% and 3.3%, respectively, while % of PA-P in the *lpa*1-1 scutellum, root-shoot axis,

and rest-of-grain fractions were 89.3%, 4.0% and 5.0%, respectively. Although the *lpa*1-1 mutation caused a greatly reduced level of PA-P, it was found that relative partitioning of PA-P between the two embryo parts, the scutellum and root-shoot axis, was not altered in *lpa*1-1 corn grains as compared to WT grains.

(ii) For both WT and *lpa*1-1 corn grains, the scutellum was the main site for PA accumulation in the embryo. As a percentage of whole embryo amounts, PA-P in the scutellum was 96.2% for WT, and 95.7% for *lpa*1-1 grains.

(iii) When expressed as a percentage of whole-grain amounts, the WT embryo PA-P was 95.2%, which is higher than the 88.0% previously reported by O'Dell *et al.* (1972). The improved sample preparation procedure and the larger sample used in my studies resulted in more accurate data about the PA-P distribution among various grain parts of WT grains. As reported here, the sum of the % of PA-P located in various WT corn grain parts was 98.5%, which was closer to the theoretical value of 100% than the 91.6% reported by O'Dell *et al.* (1972).

(iv) The distribution of the total P among various grain parts was somewhat altered by the *lpa*1-1 mutation. The amount of scutellum total P was slightly lower in *lpa*1-1 grains than WT grains, which was offset by slight increases in total P located in both the root-shoot axis and rest-of-grain fractions. Overall, the amount of total P in *lpa*1-1 whole grains remained constant in comparison to WT.

(v) On a whole grain basis, the amounts of Mg, Fe, and Mn were higher in *lpa*1-1 grains than WT grains; K and Zn were similar; and Ca was lower. It was found that *lpa*1-1 mutation resulted in redistribution of K, Mg, Ca, Zn, Fe, and Mn. Among these six nutritionally important elements measured in whole grains, embryos, and rest-of-grain fractions, the increases in Fe were in the greatest magnitude (by ~ 1/3) when *lpa*1-1 was compared to WT. A "double-benefit" of *lpa*1-1 corn grains used as human food or animal feed, would be high iron and improved bioavailability due to the reduced PA-P concentration.

(vi) For both WT and *lpa*1-1, all measured metallic elements, except Ca, were richer in the embryos than in the rest-of-grain fractions. This is the first report of these elements for grains of an *lpa* corn mutant.

(vii) For both WT and *lpa*1-1 corn grains, the procedure of 90% ethanol soaking prior to separation of various grain parts was advantageous over water-soaking for grain part isolation in that there was little loss of P, K and Mg into the 90% ethanol solution.

(viii) Even though the *lpa*1-1 grain tissue contained more Pi than WT, the low-water-content sample preparation procedure was acceptable for preparing sections of *lpa*1-1 mutant corn grain tissue for microscopy.

(ix) The globoids in WT and *lpa*1-1 corn grains differed both in structure and element composition. For both scutellum and aleurone layer cells, the *lpa*1-1 globoids were smaller and more numerous than WT globoids. This indicates that globoid diameter is more significant factor than globoid number in PA

storage. Most of the *lpa*1-1 scutellum globoids tended to aggregate in clusters and most of *lpa*1-1 aleurone globoids were unusual in that they were of non-spherical shape. The *lpa*1-1 mutation thus had an impact on the formation of globoids.

(x) P/B ratios derived from STEM-EDX analysis demonstrated that WT globoids contained higher P than *lpa*1-1 globoids for both scutellum and aleurone layer. This is consistent with the reduced PA-P level in the *lpa*1-1 mutant grains. In addition, Fe P/B ratios in *lpa*1-1 globoids were higher than in WT globoids for both scutellum and aleurone layer, consistent with the changes in Fe concentration measured by FAAS.

Future research

Several possible future research projects into corn *lpa* mutants are listed below:

(i) Further research should include the measurement of metallic element (K, Mg, Ca, Zn, Fe, and Mn) concentrations in the scutellum and root-shoot axis, the two parts constituting the embryo. This will give information on the distribution of nutritionally important elements within *lpa*1-1 mutant embryos. It should be noted that the separation process would be extremely laborious, especially for those elements present in trace amounts. Future research should also include the ESEM and TEM examination of the root-shoot axis for globoid structure, as well as EDX analysis in the same region for element composition. The comparison of data obtained for the root-shoot axis and data

obtained for the scutellum, should be useful for determining whether element redistribution occurred within the embryo, the main site for PA accumulation in *lpa*1-1 mutant corn grains. In addition, the question as to whether phosphorus-rich globoids in *lpa*1-1 root-shoot axis had altered their structure in response to a reduced PA level should be answered by further experimental work.

(ii) Future studies should include the measurement of element loss of imbibing *lpa*1-1 mutant corn grains that contained a higher Pi and a lower PA-P concentration than WT. This will allow the comparison of element leakage from *lpa*1-1 mutant corn grains and that from WT grains during the imbibition, a feature that could be important for pathogen attack during seedling growth.

(iii) Future studies should also involve other types of corn *lpa* mutants, such as *lpa*2-1, which has a different reduction of PA-P. In *lpa*2-1, the reduction in PA-P level is paired with both increases in Pi and lower inositol phosphates. Such research would provide a clear picture regarding how the *lpa*2-1 mutation alters both mineral nutrient distribution and globoid structure of mature corn grains.

(iv) It is hypothesized that the *lpa* mutation influenced globoid formation and subsequent utilization. The mechanism underlying the globoid assembly is poorly understood and needs to be elucidated by future research. Further research on WT, *lpa*1-1 and *lpa*2-1 may address such questions as: (1) what is the globoid formation process during the *lpa* mutant corn grain development in comparison to WT grains? (2) what happens during the seedling growth of *lpa* corn as compared to WT? Given the increased

Pi in *lpa* grains and altered globoid size, the timing of globoid usage and the manner in which globoids would be enzymatically attacked is not clear.

(iv) To test the hypothesis that Pi and lower inositol phosphates other than IP_6 could help to form globoids in *lpa* mutant corn grains, future research should be carried out on the isolation and characterization of *lpa* globoids. This would provide direct evidence as to whether Pi and lower inositol phosphates other than IP_6 are also involved in the assembly of globoids in *lpa* mutant corn grains. Previous studies (Lui and Altschul, 1967; Suvorov et al., 1970; Ogawa et al., 1975) used certain aqueous isolation procedures and non-aqueous procedures to purify the globoids. For studies of *lpa* globoids non-aqueous methods must be used and the contamination by other cellular components should be minimized. To assist with purification of globoids only isolated embryos should be used since embryos contained most of globoids in corn grains. Perhaps even corn seedlings at an early growth stage could be used as the starting subjects.

Literature cited

Abelson, P. H. 1999. A potential phosphate crisis. Sci. 283: 2015

ADM Foods Look Where Our Corn Goes. Archer Daniels Midland Company, Cedar Rapids, IA, USA

Allen, S. E., Grimshaw, H. M., Parkinson, J. A. and Quarmby, C. 1974. Instrumental techniques. In: Allen, S. E. (Ed.), Chemical Analysis of Ecological Materials, John Wiley and Sons, Inc., New York, NY, USA, pp 375-463

AOAC Official Methods of Analysis 1990. 15th edition, Association of Official Analytical Chemists, Arlington, VA, USA, pp 56, 800-801

Batten, G. D. 1992. A review of phosphorus efficiency in wheat. Plant Soil 146: 163-168

Beecroft, P. and Lott, J. N. A. 1996. Changes in the element composition of globoids from *Cucurbita maxima* and *Cucurbita andreana* cotyledons during early seedling growth. Can. J. Bot. 74: 838-847

Bewley, J. D. and Black, M. 1978. The legacy of seed maturation. In: Bewley, J. D. and Black, M. (Ed.), Physiology and Biochemistry of Seeds. Springer-Verlag, Berlin Heidelberg, Germany, Vol. 1, pp 40-105

Bewley, J. D. and Black, M. 1985. Seeds: Physiology of Development and Germination. Plenum Publishing Co., New York, NY, USA, pp1-28

Bray, E. A., Bailey-Serres, J. and Weretilnyk, E. 2000. Response to abiotic stresses. In: Buchanan, B. B., Gruissem, W. and Jones, R. L. (Ed.), Biochemistry and Molecular Biology of Plants. American Society of Plant Physiologists, Rockville, MD, USA, pp 1158-1203

Brearley, C. A. and Hanke, D. E. 1996. Inositol phosphates in the duckweed *Spirodela polyrhiza* L. Biochem. J. 314: 215-225

Briggs, A. P. 1924. Some applications of the colorimetric phosphate method. J. Biol. Chem. 59: 255-264

Brinch-Pedersen, H., Sorensen, L. D. and Holm, P. B. 2002. Engineering crop plants: getting a handle on phosphate. Trends Plant Sci. 7: 118-125

Chandler, J. A. 1977. X-ray microanalysis in the electron microscope. In: Glauert, A. M. (Ed.), Practical Methods in Electron Microscopy, Elsevier/North-Holland Publishing Company, Amsterdam, The Netherlands

Chen, P. and Lott, J. N. A. 1992. Studies of *Capsicum annuum* seeds: structure, storage reserves, and mineral nutrients. Can. J. Bot. 70: 518-529

Chen, L. H. and Pan, S. H. 1977. Decrease of phytates during germination of pea seeds (*Pisum sativa*). Nutr. Rep. Intl. 16: 125-131

Cosgrove, D. J. 1980. Inositol hexakisphosphates. In: Cosgrove, D. J. (Ed.), Inositol Phosphates: Their Chemistry, Biochemistry and Physiology, Elsevier Scientific Publishing Company, Amsterdam, The Netherlands, pp 26-43

Dennis, D. T. and Blakeley, S. D. 2000. Carbohydrate metabolism. In: Buchanan, B. B., Gruissem, W. and Jones, R. L. (Ed.), Biochemistry and Molecular Biology of Plants. American Society of Plant Physiologists, Rockville, MD, USA, pp 630-675

Dorsch, J. A., Cook, A., Young, K. A., Anderson, J. M., Banman, A. T., Volkmann C. J., Murthy, P. P. N. and Raboy, V. 2003. Seed phosphorus and inositol phosphate phenotype of barley *low phytic acid* genotypes. Phytochem. 62: 691-706

Duffus, C. and Slaughter, C. 1980. Seed plants. In: Duffus, C. and Slaughter, C. (Ed.), Seeds and Their Uses, John Wiley and Sons Ltd., UK, pp1-34,

Eubanks, M. W. 2001. The mysterious origin of maize. Econ. Bot. 55: 492-514

FAO Yearbook on Production 1998. 1999. Food and Agriculture Organization of the United Nations. Vol. 52, Rome, Italy

Fulcher, R. G., O'Brien, T. P. and Wong, S. I. 1981. Microchemical detection of niacin, aromatic amine, and phytin reserves in cereal bran. Cereal Chem. 58: 130-135

Gorsuch, T. T. 1970. The Destruction of Organic Matter. Pergamon Press, Oxford

Graf, E. 1986. Chemistry and applications of phytic acid: an overview. In: Graf, E. (Ed.), Phytic Acid: Chemistry and Applications, Pilatus Press, Minneapolis, MN, USA, pp1-21.

Graf, E. and Eaton, J. W. 1990. Antioxidant functions of phytic acid. Free Rad. Biol. Med. 8: 61-69

Graf, E., Empson, K. L. and Eaton, J. W. 1987. Phytic acid: a natural antioxidant. J. Biol. Chem. 262: 11647-11650

Greenwood, J. S. and Bewley, J. D. 1984. Subcellular distribution of phytin in the endosperm of developing castor bean: a possibility for its synthesis in the cytoplasm prior to deposition within protein bodies. Planta 160:113-120

Harland, B. F. and Oberleas, D. 1977. A modified method for phytate analysis using an ion-exchange procedure: application to textured vegetable proteins. Cereal Chem. 54: 827-832

Haswell, S. J. 1991. Atomic Absorption Spectrometry: Theory, Design and Applications. Elsevier Scientific Publishing Company, Amsterdam, The Netherlands, pp 353-368.

Hayat, M. A. 1978. Introduction to Biological Scanning Electron Microscopy. University Park Press, Baltimore, MD, USA.

Heiser, C. B., Jr. 1973. The origin of agriculture. In: Heiser, C. B., Jr. (Ed.), Seed to Civilization: The Story of Man's Food, W.H. Freeman and Company, San Francisco, CA, USA, pp 1-14

Hitz, W. Z., Carlson, T. J., Kerr, P. S. and Sebastian S. A. 2002. Biochemical and molecular characterization of a mutation that confers a decreased raffinosaccharide and phytic acid phenotype on soybean seeds. Plant Physiol. 128: 650-660

Hoseney, R. C. 1986. Structure of cereals. In: Hosensy, R. C. (Ed.), Principles of Cereal Science and Technology, American Association of Cereal Chemists, Inc., St. Paul, MN, USA

Isaac, R. A. 1980. Atomic absorption methods for analysis of soil extracts and plant tissue digests. J. Assoc. Off. Anal. Chem. 63: 788-796

IUPAC and IUPAC-IUB 1968. The nomenclature of cyclitols. Europ. J. Biochem. 5: 1-12

Jones, R. L., Gilroy, S. and Hillmer, S. 1993. The role of calcium in the hormonal regulation of enzyme synthesis and secretion in barley aleurone. J. Exp. Bot. 44. Supplement: 207-212

Kochian, L. V. 2000. Molecular physiology of mineral nutrient acquisition, transport, and utilization. In: Buchanan, B. B., Gruissem, W. and Jones, R. L. (Ed.), Biochemistry

and Molecular Biology of Plants, American Society of Plant Physiologists, Rockville, MD, USA, pp 1204-1249

Korkisch, J. 1989. Handbook of Ion-exchange Resins: Their Applications to Inorganic Analytical Chemistry, Vol. I, CRC Press Inc., Boca Raton, FL, USA, pp 3-16

Larson, S. R., Rutger, J. N., Young, K. A., and Raboy, V. 2000. Isolation and genetic mapping of a non-lethal rice (Oryza sativa L.) *low phytic acid 1* mutation. Crop Sci. 40: 1397-1405

Larson, S. R., Young, K. A., Cook, A., Blake, T. K. and Raboy, V. 1998. Linkage mapping of two mutations that reduce phytic acid content of barley grain. Theor. Appl. Genet. 97: 141-146

Latta, M. and Eskin, M. 1980. A simple and rapid colorimetric method for phytate determination. J. Agric. Food Chem. 28: 1313-1315

Lee, E. J., Kenkel, N. C., and Booth, T. 1996. Pollen deposition in the boreal forest of west central Canada. Can. J. Bot. 74: 1265-1272

Liu, J., Ockenden, I., Truax, M. and Lott, J. N. A. 2004. Phytic acid-phosphorus and other nutritionally important mineral elements in grains of wild-type and *low phytic acid* (*lpa*1-1) rice. Seed Sci. Res. (In press)

Loewus, F. A. and Murthy, P. P. N. 2000. Myo-inositol metabolism in plants. Plant Sci. 150: 1-19

Lonnerdal, B. 2002. Phytic acid-trace element (Zn, Cu, Mn) interactions. Intl. J. Food Sci. Tech. 37: 749-758

Loomis, E. L. and Smith, O. E. 1980. The effect of artificial aging on the concentration of Ca, Mg, Mn, K, and Cl in imbibing cabbage seed. J. Amer. Soc. Hort. Sci. 105: 647-650

Lopez, H. W., Leenhardt, F., Coudray, C. and Remesy, C. 2002. Minerals and phytic acid interactions: is it a real problem for human nutrition? Intl. J. Food Sci. Tech. 37: 727-739

Lott, J. N. A. 1980. Protein bodies. In: Tolbert, N. E. (Ed.), The Biochemistry of Plants, Vol. 1, Academic Press, Inc., New York, NY, USA, pp 589-623.

Lott, J. N. A. 1981. Protein bodies in seeds. Nor. J. Bot. 1: 421-432

Lott, J. N. A. 1984. Accumulation of seed reserves of phosphrus and other minerals. In: Murray, D. R. (Ed.), Seed Physiology, Vol. 1, Academic Press, Sydney, Australia, pp 139-166.

Lott, J. N. A. and Buttrose, M. S. 1978. Thin sectioning, freeze fracturing, energy dispersive X-ray analysis, and chemical analysis in the study of inclusions in seed protein bodies: almond, Brazil nut, and quandong. Can. J. Bot. 56: 2050-2061

Lott, J. N. A., Cavdek, V. and Carson, J. 1991. Leakage of K, Mg, Cl, Ca and Mn from imbibing seeds, grains and isolated seed parts. Seed Sci. Res. 1: 229-233

Lott, J. N. A., Goodchild, J. S. and Craig, S. 1984. Studies of mineral reserves in pea (*Pisum sativum*) cotyledons using low-water-content procedures. Aust. J. Plant Physiol. 11: 459-469

Lott, J. N. A., Greenwood, J. S. and Vollmer, C. M. 1978. Energy dispersive X-ray analysis of phosphorus, potassium, magnesium and calcium in globoid crystals in protein bodies from different regions of *Cucurbita maxima* embryos. Plant Physiol. 61: 984-988

Lott, J. N. A., Greenwood, J. S. and Batten, G. D. 1995. Mechanism and regulation of mineral nutrient storage during seed development. In: Kigel J. and Galili G. (Ed.), Seed Development and Germination, Marcel Dekker, Inc., New York, NY, USA, pp 215-235

Lott, J. N. A., Ockenden, I., Kerr, P., West, M., Leech, T. and Skilnyk, H. 1994. The influence of experimentally induced changes in the (Mg+Ca): K balance on protein bodies formed in developing *Cucurbita* seeds. Can. J. Bot. 72: 364-369

Lott, J. N. A., Ockenden, I., Raboy, V. and Batten, G. D. 2000. Phytic acid and phosphorus in crop seeds and fruits: a global estimate. Seed Sci. Res. 10: 11-33

Lott, J. N. A., Ockenden, I., Raboy, V. and Batten, G. D. 2002. A global estimate of phytic acid and phosphorus in crop grains, seeds and fruits. In: Reddy, N. R. and Sathe, S. K. (Ed.), Food Phytate, CRC Press, Boca Raton, FL, USA, pp 7-24

Lott, J. N. A. and Spitzer, E. 1980. X-ray analysis studies of elements stored in protein body globoid crystals of *Triticum* grains. Plant Physiol. 66: 494-499

Lott, J. N. A. and West, M. M. 2001. Elements present in mineral nutrient reserves in dry *Arabidopsis thaliana* seeds of wild type and *pho*1, *pho*2, and *man*1 mutants. Can. J. Bot. 79: 1292-1296

Lui, N. S. T. and Altschul, A. M. 1967. Isolation of globoids from cottonseed aleurone grain. Arch. Biochem. Biophy. 121: 678-684

Marie Minihane, A. and Rimbach, G. 2002. Iron absorption and the iron binding and anti-oxidant properties of phytic acid. Intl. J. Food Sci. Tech. 37: 741-748

Matheson, N. K. and Strother, S. 1969. The utilization of phytate by germinating wheat. Phytochem. 8: 1349-1356

Meek, G. A. 1976. Practical Electron Microscopy for Biologists. 2nd edition, John Wiley and Sons Ltd., London, UK

Mengel, K. and Kirkby, E. A. 1982. Principles of Plant Nutrition. 3rd edition, International Potash Institute, Bern, Switzerland, pp 437-459

National Research Council 1988. Quality-protein Maize. National Academy Press, Washington D.C., USA

Oberleas, D. and Harland, B. F. 1986. Analytical methods for phytate. In: Graf, E. (Ed.), Phytic Acid: Chemistry & Application, Pilatus Press, MN, USA, pp 77-100

Ockenden, I. 1987. Studies of calcium and other storage minerals in embryos of *Cucurbita maxima*, *Cucurbita andreana* and their reciprocal hybrids. PhD thesis, McMaster University, Hamilton, Ontario, Canada

Ockenden, I. and Lott, J. N. A. 1986a. A possible enhancement of measured calcium in small samples of dry-ashed *Cucurbita* embryos as determined by atomic absorption analysis. Commun. Soil Sci. Plant Anal. 17: 601-626

Ockenden, I. and Lott, J. N. A. 1986b. Ease of extraction of calcium from ash of *Cucurbita maxima* and *Cucurbita andreana* embryos following dry ashing at different temperatures. Commun. Soil Sci. Plant Anal. 17: 645-666

Ockenden, I. and Lott, J. N. A. 1991. Beam sensitivity of globoid crystals within seed protein bodies and commercially prepared phytates during X-ray microanalysis. Scanning Microsc. 5: 767-778

O'Dell, B. L., de Boland, A. R. and Koirtyohann, S. R. 1972. Distribution of phytate and nutritionally important elements among the morphological components of cereal grains. J. Agr. Food Chem. 20: 718-721

Ogawa, M., Tanaka, K. and Kasai, Z. 1975. Isolation of high phytin containing particles from rice grains using an aqueous polymer two phase system. Agr. Biol. Chem. 39: 695-700

Peters, D. G., Hayes, J. M. and Hieftje, G. M. 1974. Atomic absorption spectroscopy. In: Peters, D. G., Hayes, J. M. and Hieftje, G. M. (Ed.), Chemical Separations and Measurements: Theory and Practice of Analytical Chemistry, W. B. Saunders Co., Philadelphia, PA, USA, pp 688-695

Pilu, R., Panzeri, D., Gavazzi, G., Rasmussen, S. K., Consonni, G. and Nielsen, E. 2003. Phenotypic, genetic and molecular characterization of a maize low phytic acid mutant (*lpa241*). Theor. Appl. Genet. 107: 980-987

Plaami, S. and Kumpulainen, J. 1991. Determination of phytic acid in cereals using ICP-AES to determine phosphorus. J. Assoc. Off. Anal. Chem. 74: 32-36

Plaxton, W. C. and Preiss, J. 1987. Purification and properties of nonproteolytic degraded ADP glucose pyrophosphorylase from maize endosperm. Plant Physiol. 83: 105-112

Raboy, V. 1997. Accumulation and storage of phosphate and minerals. In: Larkins, B. A. and Vasil, I. K. (Ed.), Cellular and Molecular Biology of Plant Seed Development, Kluwer Academic Publishers, Dordrecht, The Netherlands, pp 441-477.

Raboy, V. 1998. The genetics of seed storage phosphorus pathways. In: Lynch, J. P. and Deikman, J. (Ed.), Phosphorus in Plant Biology: Regulatory Roles in Molecular, Cellular, Organismic, and Ecosystem Processes. Vol. 19, American Society of Plant Physiologists, Rockville, MD, USA, pp 192-203.

Raboy, V. 2000. Low-phytic acid grains. Food Nutr. Bull. 21: 423-427

Raboy, V. 2002. Progress in breeding low phytate crops. J. Nutr. 132: 503S-505S

Raboy, V., Gerbasi, P. F., Young, K. A., Stoneberg, S. D., Pickett, S. G., Bauman, A. T., Murthy, P. P. N., Sheridan, W. F. and Ertl, D. S. 2000. Origin and seed phenotype of maize *low phytic acid* 1-1 and *low phytic acid* 2-1. Plant Physiol. 124: 355-368

Raboy, V., Young, K. A. and Ertl, D. S. 1997. Breeding corn for improved nutritional value and reduced environmental impact. Dec. 10-11, 52nd Annual Corn & Sorghum Research Conference, Chicago, IL, USA

Raboy, V., Young, K. A., Larson, S. R. and Cook, A. 2002. Genetics of phytic acid synthesis and accumulation. In: Reddy, N. R. and Sathe, S. K. (Ed.), Food Phytate, CRC Press, Boca Raton, FL, USA, pp 63-83.

Rasmussen, S. K. and Hatzack, F. 1998. Identification of two low-phytate barley (*Hordeum vulgare* L.) grain mutants by TLC and genetic analysis. Hereditas 129: 107-112

Ritchie, S., Swanson, S. J. and Gilroy, S. 2000. Physiology of the aleurone layer and starchy endosperm during grain development and early seedling growth: new insights from cell and molecular biology. Seed Sci. Res. 10: 193-212

Roberts, E. H. and Roberts, D. L. 1972. Moisture contents of seeds. In: Roberts, E. H. (Ed.), Viability of Seeds, Syracuse University Press, Syracuse, pp 424-429

Robert Johnson Associates 1996. Environmental Scanning Electron Microscopy: an Introduction to ESEM, Wilmington, MA, USA

Rooney, L. W., Faubion, J. M. and Earp, C. F. 1983. Scanning electron microscopy of cereal grains. In: Bechtel, D. B.(Ed.), New Frontiers in Food Microstructure, American Association of Cereal Chemists, Inc., St. Paul, MN, USA, pp 201-240

Rubeska, L. and Moldan, B. 1969. Atomic Absorption Spectrophotometry, Iliffe Book Ltd., London, UK, pp 122-125

Russ, J. C. 1972. Elemental Xray Analysis of Materials: EXAM methods, EDAX International Inc., IL, USA, pp 2-10

Sandstead, H. H. 1992. Fiber, phytates, and mineral nutrition. Nutr. Rev. 50(1): 30-31

Schachtman, D. P., Reid, R. J. and Ayling, S. M. 1998. Phosphorus uptake by plants: from soil to cell. Plant Physiol. 116: 447-453

Shen, B., Li, C., Min, Z., Meeley, R., Tarczynski, M. and Olsen, O. 2003. *Superal*1 determines the number of aleurone cell layers in maize endosperm and encodes a CHMP family member of the class E vacuolar sorting proteins. Plant Biology 2003 Conference, July 25-30, Honolulu, Hawaii, USA

Shi, J., Wang, H., Wu, Y., Hazebroek, J. and Meeley, R. B. 2003. A *myo*-inositol phosphate kinase involved in phytic acid biosynthesis in developing maize seeds. Plant Biology 2003 Conference, July 25-30, Honolulu, Hawaii, USA

Skilnyk, H. R. and Lott, J. N. A. 1992. Mineral analyses of storage reserves of *Cucurbita maxima* and *Cucurbita andreana* pollen. Can. J. Bot. 70: 491-495

Smith, D. L. and Schrenk, W. G. 1972. Application of atomic absorption spectroscopy to plant analysis. I. Comparison of zinc and manganese analysis with official colorimetric methods. J. Assoc. Off. Agric. Chem. 55: 669-675

Souza, E., Guttieri, M. J., Dorsch, J. A. and Raboy, V. 2003. A low phytic acid mutant of bread wheat. Plant and Animal Genomes XI Conference 2003, Jan. 11-15, San Diego, CA, USA

Spence, J. 2001. Plant histology. In: Hawes, C. and Satiat-Jeunemaitre, B. (Ed.), Plant Cell Biology, 2nd edition, Oxford University Press Inc., New York, NY, USA, pp189-206

Stephens, L. R. and Irvine, R. F. 1990. Stepwise phosphorylation of *myo*-inositol leading to *myo*-inositol hexakisphosphate in *Dictyostelium*. Nature 346: 580-583

Strother, S. 1980. Homeostasis in germinating seeds. Ann. Bot. 45: 217-218

Suvorov, V. I., Buzulukova, N. P., Sobolev, A. M. and Sveshnikova, I. N. 1970. Structure and chemical composition of globoids from aleurone grains of castor seeds. Plant Physiol. *U.S.S.R* 17:1020-1027, translated from *Fiziologiya Rastenii* 17: 1223-1231

Taiz, L. and Zeiger, E. 1998. Plant Physiology. 2nd edition, Sinauer Associates, Inc., Publishers, Sunderland, MA, USA

Thompson, L. U. 1993. Potential health benefits and problems associated with anti-nutrients in foods. Food Res. Intl. 26: 131-149

Thompson, L. U. and Zhang, L. 1991. Phytic acid and minerals: effect on early markers of risk for mammary and colon carcinogenesis. Carcinogenesis 12: 2041-2045

Tucker, G. 2003. Nutritional enhancement of plants. Cur. Opin. Biotech. 14: 221-225

Wada, T. and Lott, J. N. A. 1997. Light and electron microscopic and energy dispersive X-ray microanalysis studies of globoids in protein bodies of embryo tissues and the aleurone layer of rice (*Oryza sativa* L.) grains. Can. J. Bot. 75: 1137-1147

Walsh, A. 1955. The application of atomic absorption spectra to chemical analysis. Spectrochim. Acta 7: 108-117

West, M. M. and Lott, J. N. A. 1993. Studies of mature seeds of eleven *Pinus* species differing in seed weight. II. Subcellular structure and localization of elements. Can. J. Bot. 71: 577-585

West, M. M., Ockenden, I. and Lott, J. N. A. 1994. Leakage of phosphorus and phytic acid from imbibing seeds and grains. Seed Sci. Res. 4: 97-102

Wilcox, J. R., Premachandra, G. S., Young, K. A. and Raboy, V. 2000. Isolation of high seed inorganic P, low-phytate soybean mutants. Crop Sci. 40:1601-1605

York, J. D., Odom, A. R., Murphy, R., Ives E. B. and Wente, S. R. 1999. A phospholipase C-dependent inositol polyphosphate kinase pathway required for efficient messenger RNA export. Sci. 285: 96-100

Yoshida, K. T., Wada, T., Koyama, H., Mizobuchi-Fukuoka, R. and Naito, S. 1999. Temporal and spatial patterns of accumulation of the transcript of myo-inositol-1-phosphate synthase and phytin-containing particles during seed development in rice. Plant Physiol. 119: 65-72

Zar, J. H. 1984. Biostatistical Analysis, Prentice-Hall, Englewood Cliffs, NJ, USA

Appendix A. Dilution volumes for total P and PA-P analyses in the whole grains and grain parts from WT and *lpa*1-1 mutant corn

Table 1. Dilution of digests for total P analysis in the whole grain, scutellum, root-shoot axis and rest-of-grain fractions from WT and *lpa*1-1 mutant corn

Grain or grain part		Final dilution volume (mL)
Whole grain	WT (n=3)	25
	*lpa*1-1(n=3)	25
Scutellum	WT (n=3)	100
	*lpa*1-1(n=3)	100
Root-shoot axis	WT (n=3)	50
	*lpa*1-1(n=3)	50
Rest-of-grain	WT (n=3)	25
	*lpa*1-1(n=3)	25

Table 2. The extract volume for column separation of PA and digest dilution volume for PA-P analysis in the whole grain, scutellum, root-shoot axis and rest-of-grain fractions from WT and *lpa*1-1 mutant corn

Grain or grain part		Volume of extract used for column separation (mL)	Digest dilution volume for PA-P analysis (mL)
Whole grain	WT (n=3)	4	25
	*lpa*1-1(n=3)	12	25
Scutellum	WT (n=3)	4	50
	*lpa*1-1(n=3)	12	50
Root-shoot axis	WT (n=3)	16	25
	*lpa*1-1(n=3)	25	25
Rest-of-grain	WT (n=3)	12	10
	*lpa*1-1(n=3)	25	10

Appendix B. Sample and mineral element standard dilutions for FAAS in WT and *lpa*1-1 mutant corn grains and grain parts

Sample dilution for FAAS in WT and lpa1-1 mutant corn whole grains

1) Potassium
0.2 g digest into 50mL 2000ppmLa/1000ppmCs/2%HNO_3
5mL→ 100mL
Total dilution: 1000mL (calculated by 50mL×100/5=1000mL)

2) Magnesium
0.2 g digest into 50mL 2000ppmLa/1000ppmCs /2%HNO_3
2mL→ 25mL
Total dilution: 625mL (calculated by 50mL×25/2=625mL)

3) Calcium
1.0 g digest into 10mL 2000ppmLa/1000ppmCs /2%HNO_3
2mL→ 10mL
Total dilution: 50mL

4) Zinc
1.0 g digest into 50mL 2% HNO_3

5) Iron
1.0 g digest into 10mL 2% HNO_3

6) Manganese
1.5 g × 2 (crucibles) digests pooled together into 10mL 2% HNO_3

Sample dilution for FAAS in WT and lpa1-1 mutant corn embryos

1) Potassium
0.1 g digest into 50mL 2000ppmLa/1000ppmCs/2%HNO_3
5mL → 100mL
5mL → 10mL
Total dilution: 2000mL (calculated by 50mL×100/5 ×10/5=2000mL)

2) Magnesium
0.1 g digest into 50mL 2000ppmLa/1000ppmCs/2%HNO_3
5mL → 100mL
5mL → 10mL
Total dilution: 2000mL (calculated by 50mL×100/5 ×10/5=2000mL)

3) Calcium
1.0g digest into 50mL 2000ppmLa/1000ppmCs/2%HNO_3

4) Zinc
0.1 g digest into 50mL 2% HNO_3

5) Iron
1.0 g digest into 50mL 2% HNO_3

6) Manganese
1.0 g digest into 10mL 2% HNO_3

Sample dilution for FAAS in the rest-of-grain fractions of WT and lpa1-1 mutant corn

1) Potassium
0.1 g digest into 100mL 2000ppmLa/1000ppmCs/2%HNO_3

2) Magnesium
0.1 g digest into 100mL 2000ppmLa/1000ppmCs/2%HNO_3

3) Calcium
1.5g digest into 25mL 2000ppmLa/1000ppmCs/2%HNO_3

4) Zinc
1.5 g digest into 10mL 2% HNO_3
2mL →10mL
Total dilution: 10 mL×10/2 =50mL

5) Iron
1.5 g digest into 10mL 2% HNO_3

6) Manganese
1.5 g × 2 (crucibles) digest pooled together into 10mL 2% HNO_3

The dilutions of mineral element standards for FAAS

1) Potassium
   1000ppm K stock (VWR purchased)
   5mL → 50mL = 100ppm (in 2000ppmLa/1000ppmCs/2% HNO_3)
   10mL → 50mL = 20ppm
   20mL → 100mL = 4ppm

   Serial dilutions:
   2.5mL → 50mL = 0.2ppm
   5mL → 50mL =0.4ppm
   20mL → 100mL =0.8ppm
   15mL → 50mL = 1.2ppm
   20mL → 50mL = 1.6ppm

2) Magnesium
   1000ppm Mg stock (VWR purchased)
   5mL → 50mL = 100ppm (in 2000ppmLa/1000ppmCs/2% HNO_3)
   10mL → 50mL = 20ppm
   10mL → 100mL = 2ppm

   Serial dilutions:
   2.5mL → 50mL = 0.1ppm
   5mL → 50mL =0.2ppm
   20mL → 100mL =0.4ppm
   15mL → 50mL = 0.6ppm
   20mL → 50mL = 0.8ppm

3) Calcium
   1000ppm Ca stock (VWR purchased)
   5mL → 100mL = 50ppm (in 2000ppmLa/1000ppmCs/2% HNO_3)

   Serial dilutions:
   1mL → 50mL = 1ppm
   2mL → 50mL = 2ppm
   3mL → 50mL = 3ppm
   4mL → 50mL = 4ppm
   5mL → 50mL = 5ppm

4) Zinc
   1000ppm Zn stock (VWR purchased)

10mL → 100mL = 100ppm (in 2% HNO_3)
5mL → 100mL = 5ppm

Serial dilutions:
1mL → 50mL = 0.1ppm
2mL → 50mL = 0.2ppm
3mL → 50mL = 0.3ppm
4mL → 50mL = 0.4ppm
5mL → 50mL = 0.5ppm

5) Iron
1000ppm Fe stock (VWR purchased)
5mL → 100mL = 50ppm (in 2% HNO_3)

Serial dilutions:
1mL → 50mL = 1ppm
2mL → 50mL = 2ppm
3mL → 50mL = 3ppm
4mL → 50mL = 4ppm
5mL → 50mL = 5ppm

6) Manganese
1000ppm Mn stock (VWR purchased)
5mL → 100mL = 50ppm (in 2% HNO_3)

Serial dilutions:
1mL → 50mL = 1ppm
2mL → 50mL = 2ppm
3mL → 50mL = 3ppm
4mL → 50mL = 4ppm
5mL → 50mL = 5ppm

Appendix C. Bar graphics for distribution of mineral elements, PA-P and mean dry weights in WT and *lpa*1-1 mutant corn grains

Total P

(mg/grain or grain part)

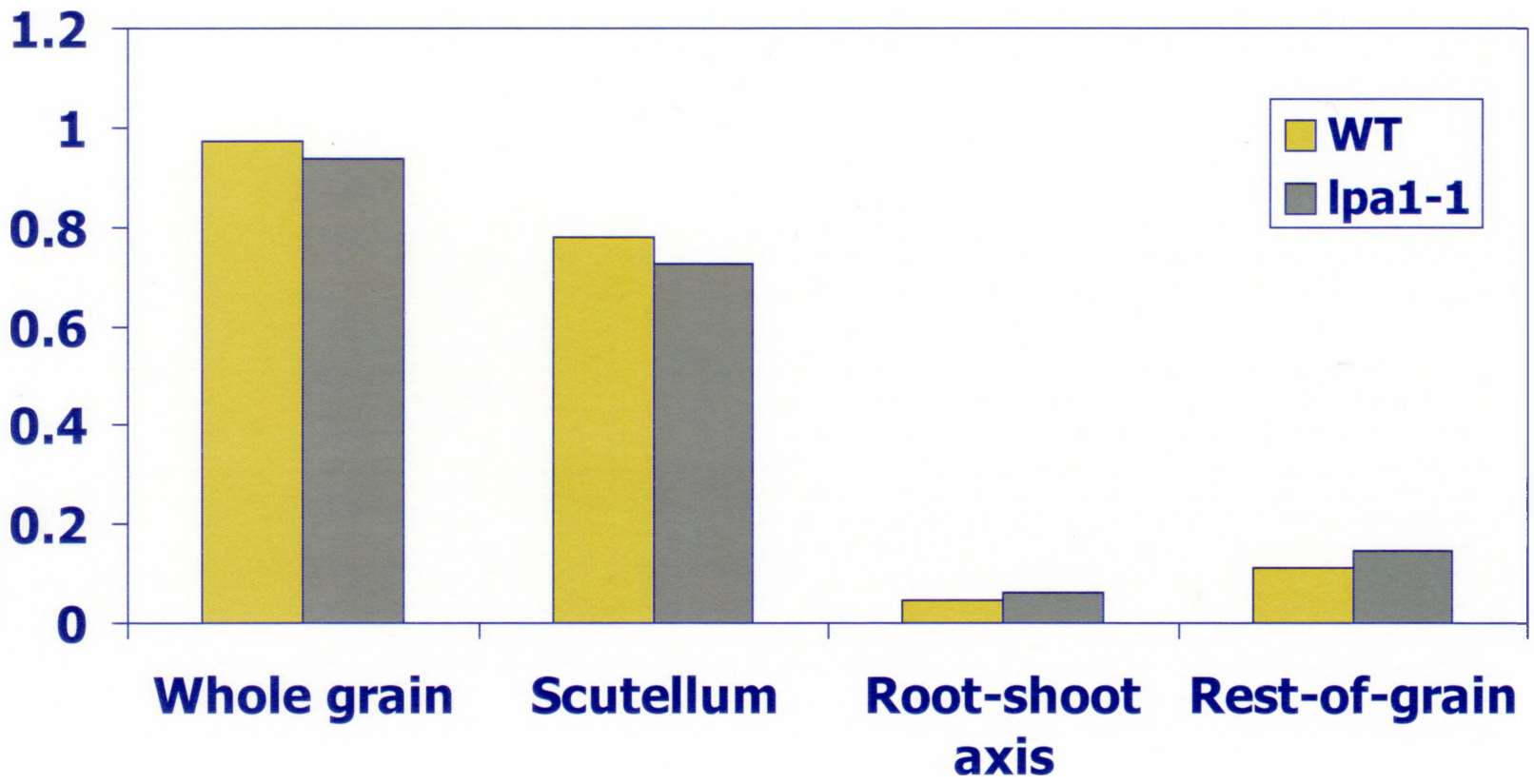

PA-P

(mg/grain or grain part)

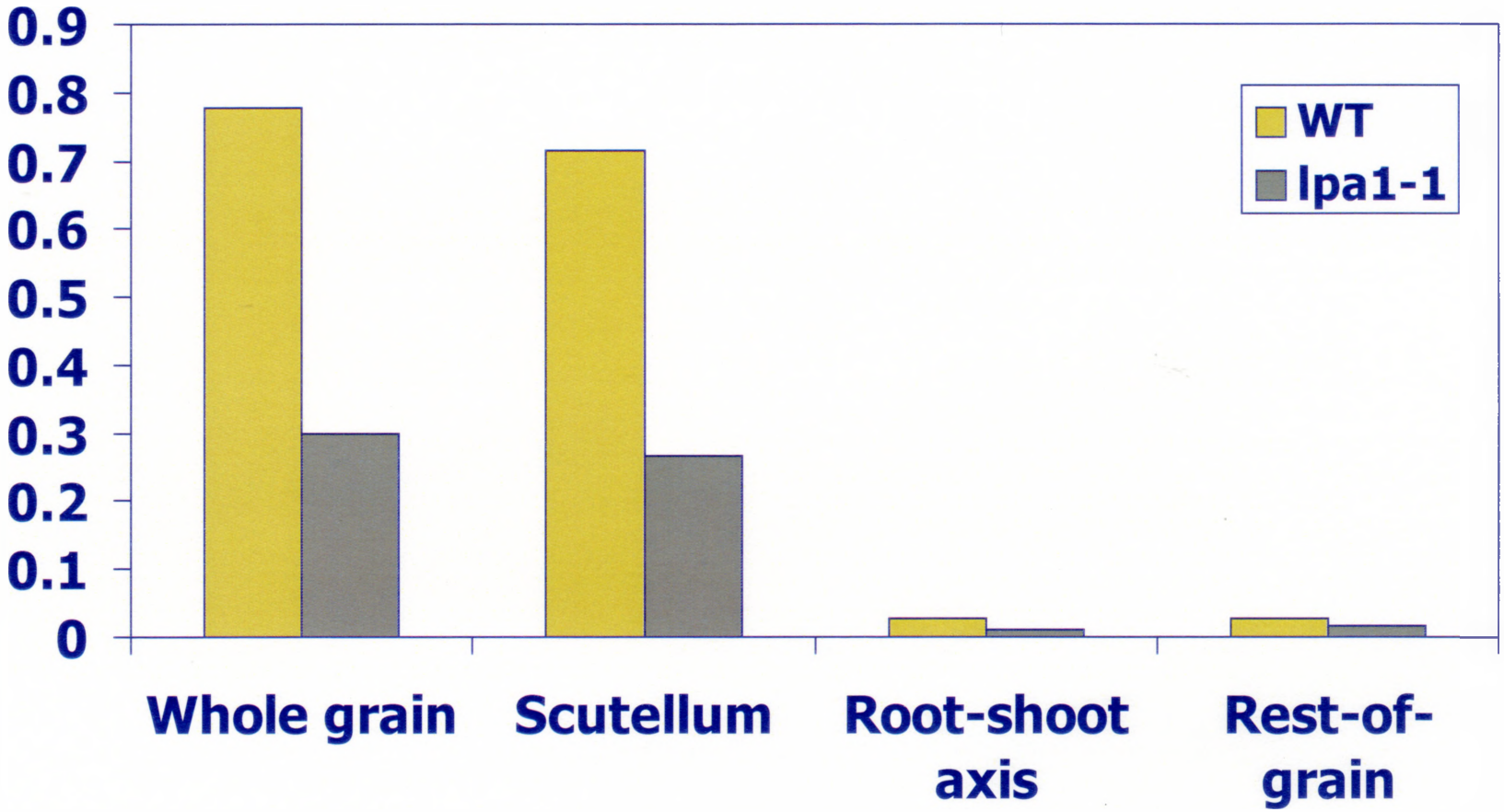

K (μg/grain or grain part)

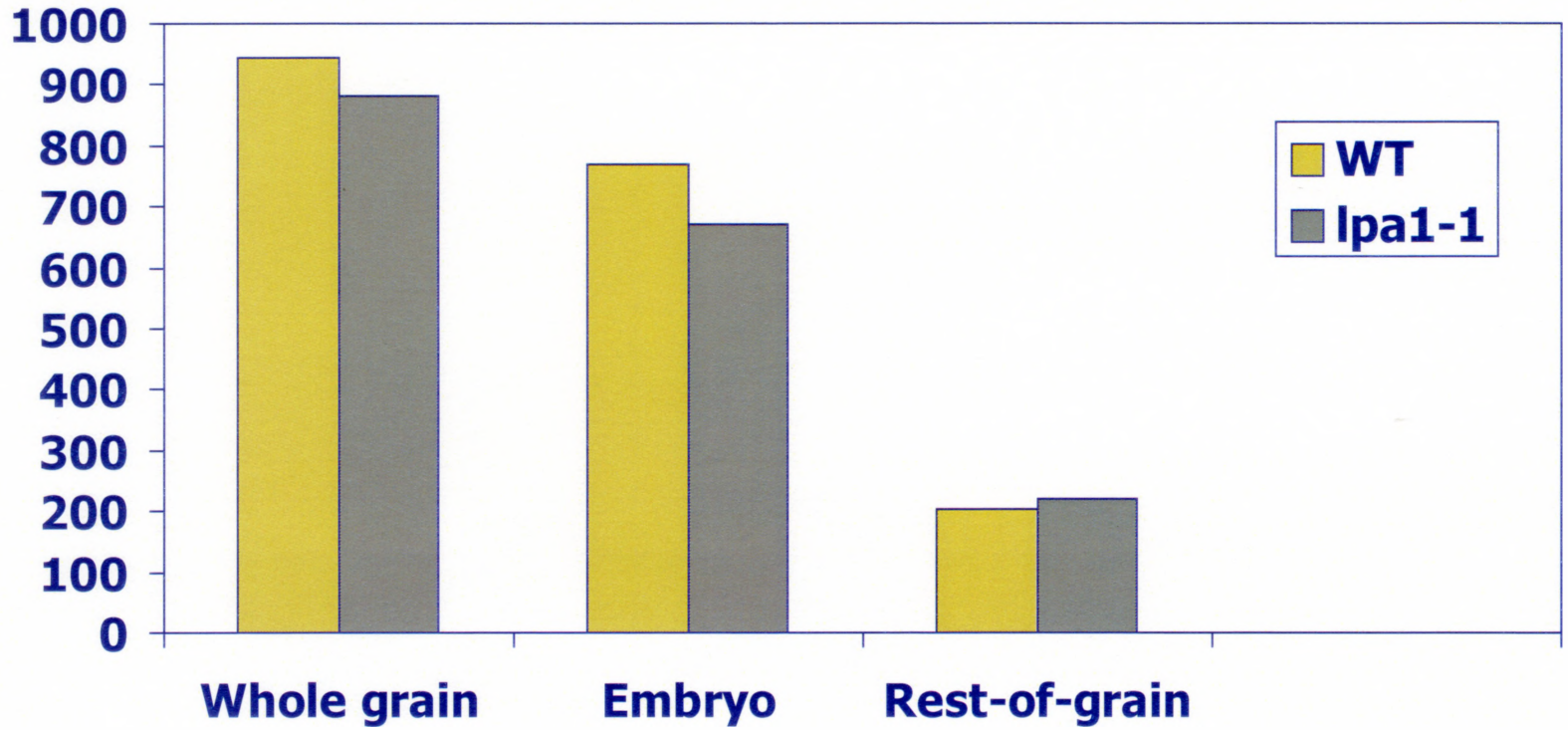

Mg (μg/grain or grain part)

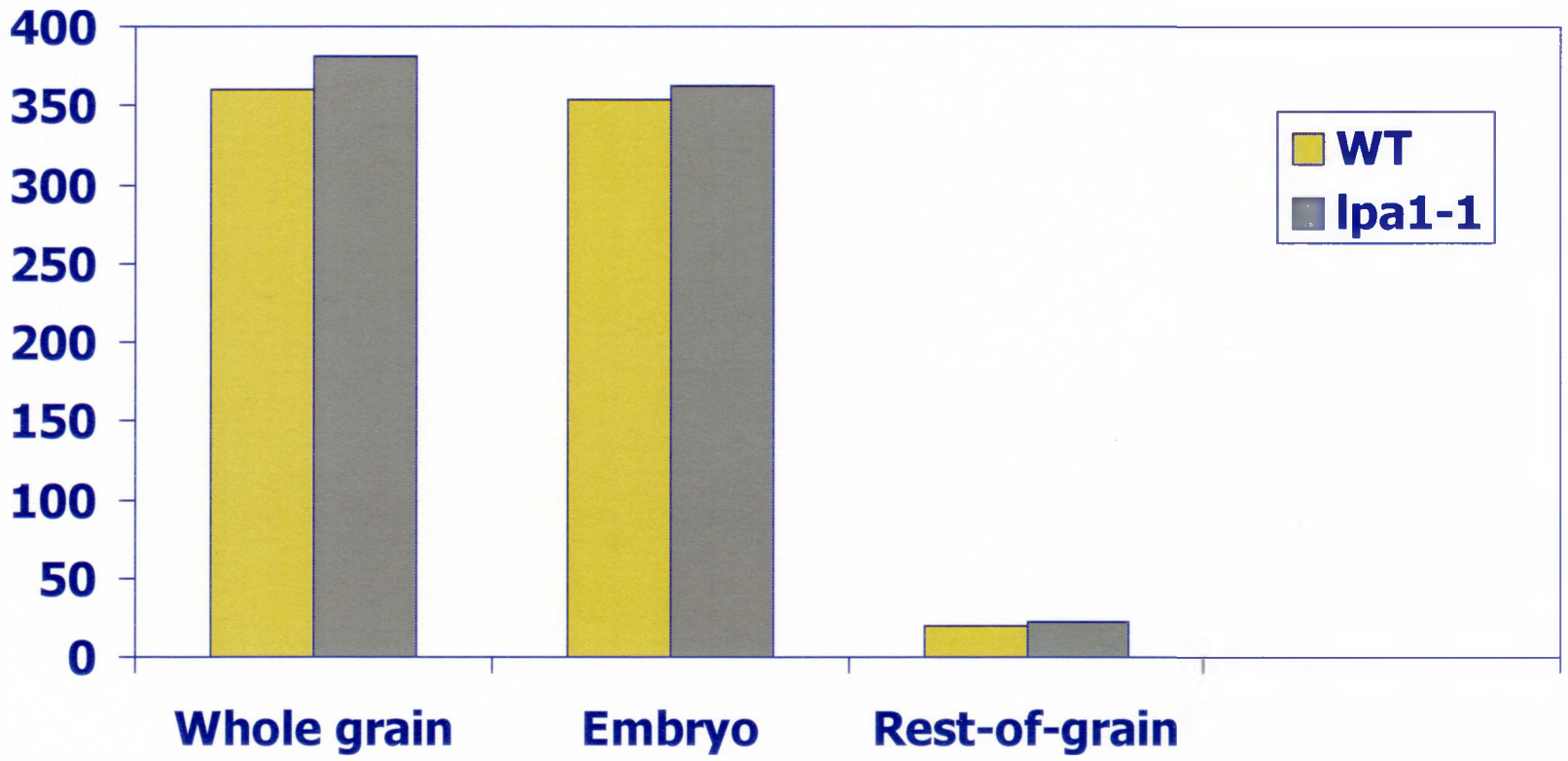

Ca (μg/grain or grain part)

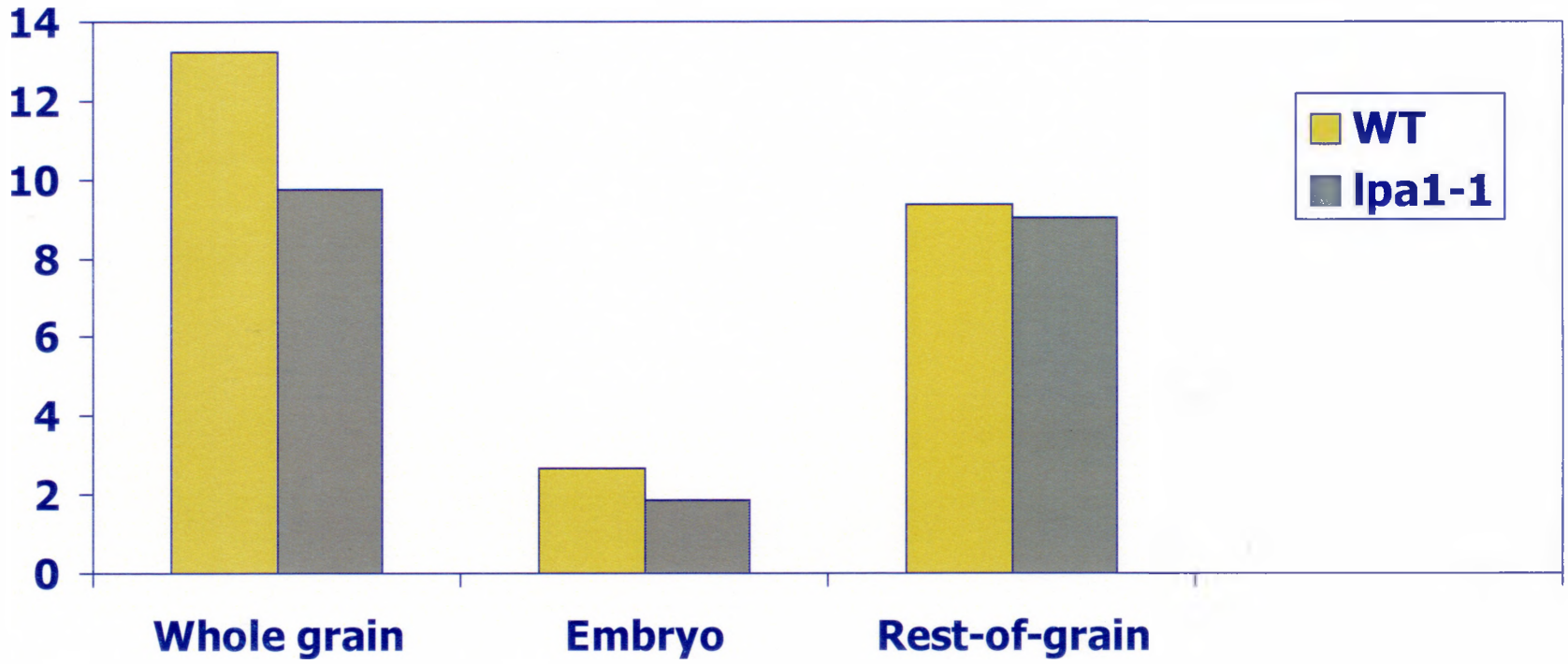

Zn (μg/grain or grain part)

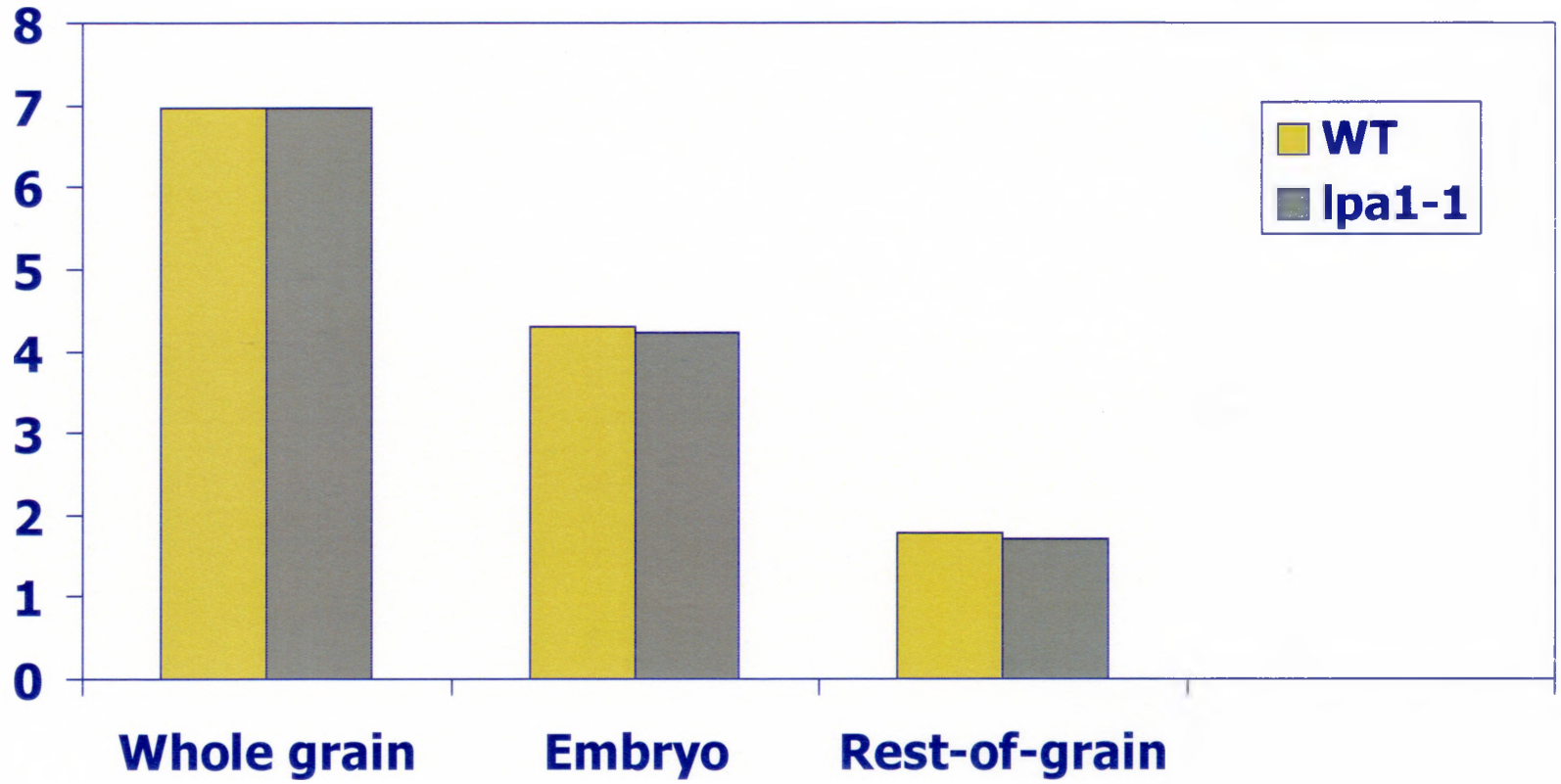

Fe (μg/grain or grain part)

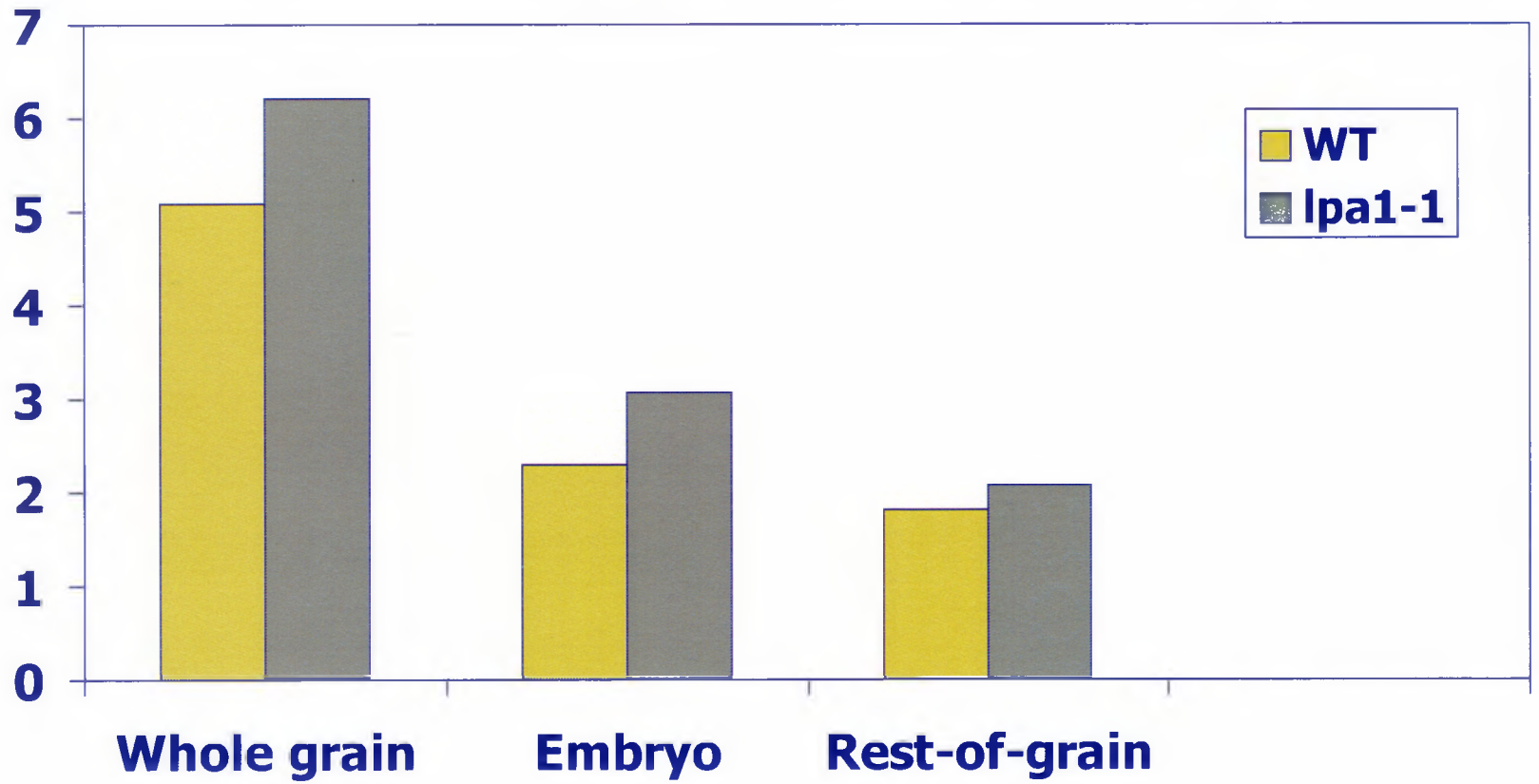

Mn (μg/grain or grain part)

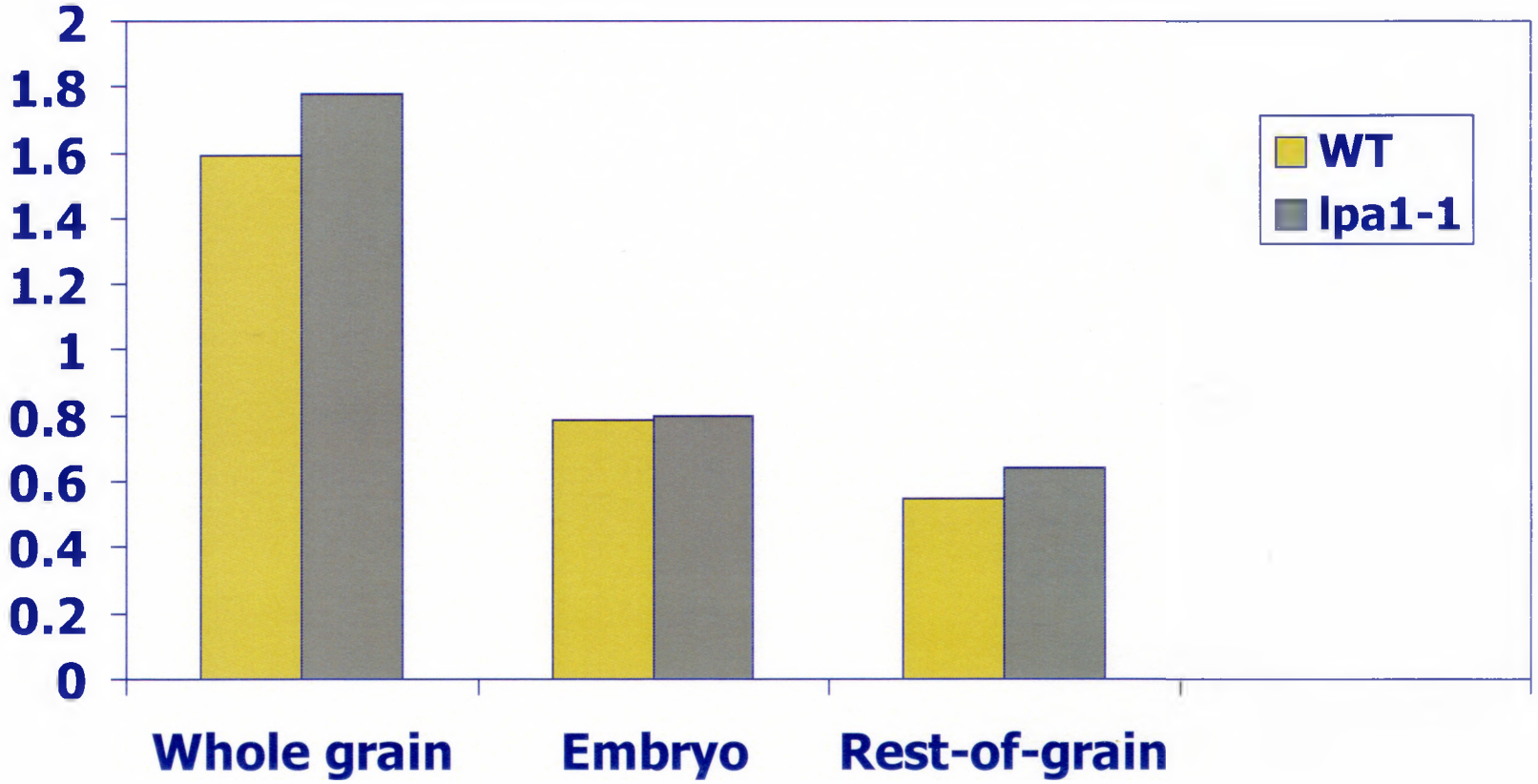

Mean dry weight (mg/grain or grain part)